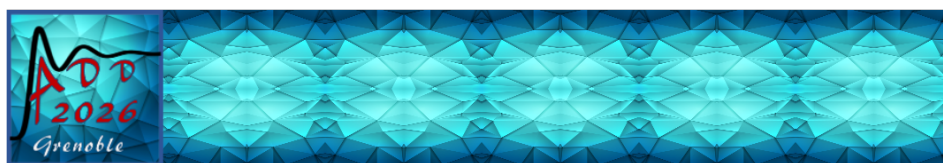


School and Conference on Analysis of Diffraction Data in Real Space

Sunday, 11 January 2026 - Saturday, 17 January 2026

The EPN Campus



Book of Abstracts

Contents

Short-range atomic ordering in PbZrxTi1-xO3 single crystal revealed by diffuse scattering and 3D- Δ PDF modeling 147	1
Short-range atomic ordering in PbZrxTi1-xO3 single crystal revealed by diffuse scattering and 3D- Δ PDF modeling 31	1
School welcome and opening 114	1
Amorphous Pharmaceuticals 131	1
Amorphous Pharmaceuticals 26	2
Recent and future developments in PDF-land 117	2
DiffPy-CMI - a software toolbox for real-space structure analysis and Complex Modeling 120	2
CO-induced dynamic behaviour of Al2O3-supported Pd nanoparticles at room temperature 145	3
The new Debye beamline at SLS2.0: a versatile operando platform for X-ray scattering and X-ray absorption spectroscopy 82	3
PDFgui – a small box modelling platform for nanoscale structure analysis 119	3
PDFgui – a small box modelling platform for nanoscale structure analysis 14	4
Using mPDF to probe magnetic exchange interactions 72	4
X-ray PDF-analysis applied to energy materials, including in operando studies 136	5
Topas 122	5
Introduction and information 130	5
ToScaNA: A Python Module for the Treatment of Total Neutron Scattering Data 90 . . .	5
Investigating preferential adsorption of N2 from the air in Zeolite 13X using total neutron scattering 148	5
Introduction and information 115	6
Information on tutorials 125	6

diffpy.mpdf - Investigating short-range magnetic correlations in real space with magnetic pair distribution function analysis 121	6
Real-time observation of rapid densification and degradation in flash sintered multilayer systems for battery materials 144	6
Liquid-liquid phase transition in covalent materials 100	6
Total scattering as a tool to understand the incomplete phase transition in sodium-ion battery materials 22	7
Structural origin of magnetic softening of annealed 3D-printed and as-cast Co-free Fe-Si-B-based metallic glasses 61	7
Mechanistic Insights into Solvent-Guided Growth of MoO ₂ Nanoparticles from in situ Total Scattering Studies 137	8
Mechanistic Insights into Solvent-Guided Growth of MoO ₂ Nanoparticles from in situ Total Scattering Studies 39	8
Understanding local structure and dynamics in Prussian blue analogues 151	9
In-Situ Observation of an Isosymmetric Superionic Phase Transition in Li ₇ P ₃ S ₁₁ 78 . . .	9
Grazing Incidence Total Scattering at PETRA III: Extending Local Structure Analysis to Ultrathin Films on Single-Crystal Substrates 152	9
Grazing Incidence Total Scattering at PETRA III: Extending Local Structure Analysis to Ultrathin Films on Single-Crystal Substrates 42	10
3D-DeltaPDF: From synchrotron to in-house sources 146	10
Total scattering and PDFs using X-ray free-electron lasers: quality data in 30 femtoseconds 143	10
Thermally Stable Binary Two-Dimensional Hybrid Organic-Inorganic Perovskite Glasses 23	11
Structural Fingerprints of Plasticity: Linking the Shear Transformation Zone Size to Pair Distribution Functions in Metallic Glasses 133	11
Phase Sensitive Detection Analysis on Modulation Excitation PDF Data of Ni Based Catalysts 139	11
Single-Crystal Diffuse scattering 118	12
DISCUS: Simulation and refinement of disordered crystal structures 127	12
Whole-nanoparticle-ensemble refinements of compositionally complex systems from X-ray pair distribution function data via the Reverse Monte Carlo method 134	12
Whole-nanoparticle-ensemble refinements of compositionally complex systems from X-ray pair distribution function data via the Reverse Monte Carlo method 36	12
Happy Accidents: Spatially Resolved X-ray Beam Damage Effects in a Lithium-Ion Battery 19	13

Intermediate-range order in glassy oxide materials revealed by topological analysis 132	14
Assessing Short-range order using total scattering and RMC - methods, challenges and strategies 142	14
Spinvert and Spinteract: Magnetic structure refinement for paramagnets 158	14
Exploring magnetic correlation lengths in frustrated systems via single-crystal neutron diffraction 153	14
Structure of Liquid and Amorphous Materials using Pair-Distribution Function Analysis 116	14
Structural evolution of Tungsten Oxide Network during WO ₃ .H ₂ O formation 135	14
Temperature Dependent Diffuse Scattering in Sanidines 77	14
Isolating TEM instrumental function to the ePDF 149	15
Isolating TEM instrumental function to the ePDF 50	15
Dynamic magnetic pair-density function analysis (DymPDF) 150	16
3D-ΔPDF: Pair distribution function analysis for single crystals 128	16
Fast Simulation of Disordered Crystals Using Gaussian Copulas 154	16
Hidden complexity in D ₂ O Ice VII 155	16
Hidden complexity in D ₂ O Ice VII 53	16
RMCProfile: Local structure of crystalline to amorphous materials 123	17
Novel Vacancy Ordering in YbAlO ₃ Under Compression 107	17
Magnetism in metallic glasses - a clear need for PDF 141	18
Magnetism in metallic glasses - a clear need for PDF 32	18
IN SITU AND PDF NEUTRON DIFFRACTION FOR THE ADVANCED STRUCTURAL ANALYSIS OF MOF CATALYSTS FOR CARBON DIOXIDE VALORISATION 40	19
In situ/operando studies for understanding the metal-support interaction of Ni-based catalysts for ammonia decomposition 138	19
EPSR & Dissolve - Data-driven structural modelling of total scattering data 124	20
EPSR & Dissolve - Data-driven structural modelling of total scattering data 126	20
EPSR & Dissolve - Data-driven structural modelling of total scattering data 157	20
Technical Aspects and Practices in Using Neutron Total Scattering for Local Magnetic Ordering Studies 140	20
Temperature-dependent structural evolution of GeO ₂ 102	20
3D-DeltaPDF: From synchrotron to in-house sources 33	21

Exploring local structure in some oxygen deficient perovskite polymorphs by Total Neutron 24	22
Magnesium silicate hydrate-based cement under repository conditions 25	22
Conference welcome 129	23
TOPAS for small box Pair Distribution Function refinements 156	23
Effects of sample preparation and synchrotron beamline instrumentation on total X-ray scattering data and their atomic pair distribution functions 34	24
High-Throughput Orientation Extraction via Symmetry-Adapted Filters 38	24
Role of Fe, Co and Cu addition in the structural and magnetic properties of Ni-Mn-Ga Magnetic Shape Memory Alloys 48	25
A JOINT ACADEMIC-INDUSTRIAL STUDY ON THE ROLE OF FLUORINE IN MOLD CAST- ING FLUORINE-ALUMINOSILICATE GLASSES 52	25
Polymorphism in the metal-organic framework Qc-5-Cu 54	26
Intermediate-range order in glassy oxide materials revealed by topological analyses 69 . .	27
Synthesis, properties and local structure analysis of the mineral strätlingite 64	27
scikit-package - software packaging standards and roadmap for sharing reproducible sci- entific software 56	28
Fast Simulation of Disordered Crystals Using Gaussian Copulas 28	28
Real-time observation of rapid densification and degradation in flash sintered multilayer systems for battery materials 51	29
Short-Range Order in Water and Amorphous Ice 62	30
Structural evolution of Tungsten Oxide Network during WO ₃ .H ₂ O formation 18	30
Nature of short-range incommensurate magnetic order in YBa ₂ Cu ₃ O _{6+x} 110	31
Pair Distribution Function analysis applied to the study of ancient Roman mortars 92 . .	31
Unravelling Nucleation in Pt Atomic Layer Deposition Using Grazing Incidence X-ray Total Scattering, Grazing Incidence Small-Angle X-ray Scattering, and X-ray Fluorescence 103	32
Multi-doped Cu catalysts: How the additional doping changes the exsolution behaviour 108	33
Understanding local structure and dynamics in Prussian blue analogues 45	33
Preparation and characterisation of Fe-based alloys prepared by mechanical alloying 70 .	34
NiAl layered double hydroxides as precursor for Ni/Al ₂ O ₃ catalysts for CO ₂ methanation 81	35

Investigating preferential adsorption of N ₂ from the air in Zeolite 13X using total neutron scattering 66	35
Structure of Liquid and Amorphous Materials using Pair-Distribution Function Analysis 10	36
Electrodeposition: A Synthesis Platform for Experimental Models in Electrocatalysis 112	37
Structural Fingerprints of Plasticity: Linking the Shear Transformation Zone Size to Pair Distribution Functions in Metallic Glasses 59	38
3D- Δ PDF: Pair distribution function analysis for single crystals 13	38
In situ/operando studies for understanding the metal-support interaction of Ni-based catalysts for ammonia decomposition 58	38
Single-Crystal Diffuse scattering 16	39
Assessing Short-range order using total scattering and RMC - methods, challenges and strategies 35	40
Refinement of Magnetic Diffuse Scattering Data 15	41
Phase Sensitive Detection Analysis on Modulation Excitation PDF Data of Ni Based Catalysts 41	41
Challenges in XPDF Analysis of High Pressure-Temperature Metal-Organic Frameworks 21	42
CO-induced dynamic behaviour of Al ₂ O ₃ -supported Pd nanoparticles at room temperature 47	42
Boron Phosphide Nanocrystals by Pair Distribution Function Analysis 17	43
Thermodynamic, kinetic and structural study of Pt _{42.5} Cu _x Ni _{36.5-x} P ₂₁ alloy variations 20	44
DISCUS, Simulation and refinement of disordered crystal structures 11	45
Intermetallic phases and liquid alloys in SCALMS catalysts studied by X-ray PDF analysis 43	45
EPSR & Dissolve - Data-driven structural modelling of total scattering data 7	46
DiffPy-CMI - a software toolbox for real-space structure analysis and Complex Modeling 9	47
Dynamic magnetic pair-density function analysis (DymPDF) 68	48
Technical Aspects and Practices in Using Neutron Total Scattering for Local Magnetic Ordering Studies 27	48
Total scattering and PDFs using X-ray free-electron lasers: quality data in 30 femtoseconds 30	49
Correlated Disorder in Crystals: From Understanding to Control of the Local Structure 44	49
Local structure of Ammonia Borane: how much do we really know? 29	50

Operando investigations of the Electrocatalytic performance of Metal-Organic Frameworks 37	50
Cation substitution and Fe(III) trapping in layered double hydroxides deciphered by PDF, XAS, and DFT 46	51
Eu ₃ Zn ₂ As ₄ - A New Zintl Phase Exhibiting Complex Transport Properties and Magnetic Anisotropy 65	51
Synthesis of Highly Non-Stoichiometric Garnets by Glass Crystallisation 63	52
Revealing the Early Metal–Oxide Phase Transition of Platinum Nanocatalysts under PEMFC-Relevant Conditions 55	53
Operando X-Ray Total Scattering for Electrocatalysis 57	53
Structural Stability of Liquid Bismuth Along the Melting Curve 60	54
Insights into the cubic symmetry of silver nanoparticles prepared by bottom-up mechanochemical synthesis 76	54
Discovering the hidden (dis-)order in A ₂ Se ₂ C ₂ (A = Na–Cs) 71	55
Characterization of Zr-based bulk metallic glasses with high thermal stability for thermoplastic forming 75	56
Investigation of the short-range order and disorder in U ₃ O ₈ using neutron total-scattering PDF analysis 74	56
From 100 keV to MeV: Energy Effects in Ultrafast Electron Diffraction 96	57
Pair distribution functions of cellulose calculated from molecular dynamics 98	58
Atomic-scale investigation of short-range ordering formation in Fe–Mn–Al–C lightweight steels 104	58
Effect of manganese substitution on the local atomic structure of amorphous Fe-based metallic glasses 84	59
Total scattering analysis of Si-thin film anodes for lithium ion batteries 105	60
From 100 keV to MeV: Energy Effects in Ultrafast Electron Diffraction 97	60
PDF data collection at MSPD beamline: past, present and future 95	61
Unveiling Atomic-Level Disorder in Zinc Hydroxy-stannate (ZnSn(OH) ₆) using Three-Dimensional ΔPDF Approach 91	61
How the behavior of cations within the interfacial layer can influence the water structure in nanoconfined electrolyte solutions 85	62
Linking the local structure to reversible O redox and electrochemical performance of Li ₂ MnO ₃ 86	62
In situ reaction monitoring of sulfide solid electrolytes in liquid phase. 94	63
Growth and Characterization of Yb ₂ Si ₂ O ₇ and Yb ₂ SiO ₅ Crystals 83	63

Polymorphism in the metal-organic framework Qc-5-Cu 99	64
Structural Evolution in Metal-Organic Frameworks Melting and Glass Transition via Pair Distribution Function Analysis 109	64
Absorption correction of high-Q electron PDFs: A comparative study on Au and Bi _{1.5} Co _{0.25} Ti ₂ O _{6.5} 87	65
PDF across-the-board in science - the x-ray total scattering portfolio at P07-DESY and P21.1 at PETRA III 89	66
On the Multistage Mechanism of Lithium (De)insertion of Lithium Iron Oxysulfide Disor- dered Antiperovskite Cathodes 106	66
Effects of compression on the local structure of selected active pharmaceutical ingredients in liquid and glass 93	67
Three-dimensional magnetic pair distribution function analysis of TbSb 79	67
Structural and thermal behavior of Cu _{1-x} Bi _x nanowires grown by template-assisted elec- trodeposition 101	68
PDF Investigations of novel ambient temperature reactive hydride composites for hydrogen storage 88	68
2D-PDF data reduction: for fibre textured (thin film) samples 73	69
Fast, interpretable (pre-)processing of large, mixed diffraction datasets with ad-hoc super- pixels and randomized non-negative matrix factorization 111	69
RMCPProfile: Local structure of crystalline to amorphous materials 12	70
Exploring magnetic correlation lengths in frustrated systems via single-crystal neutron diffraction 113	71
Investigating short-range magnetic correlations in real space with magnetic pair distribu- tion function analysis 6	71
Recent and future developments in PDF-land 8	72

Conference sixth session / 147

Short-range atomic ordering in $\text{PbZr}_x\text{Ti}_{1-x}\text{O}_3$ single crystal revealed by diffuse scattering and 3D- Δ PDF modeling

Corresponding Author: anzheyi@xjtu.edu.cn

31

Short-range atomic ordering in $\text{PbZr}_x\text{Ti}_{1-x}\text{O}_3$ single crystal revealed by diffuse scattering and 3D- Δ PDF modeling

Author: Zheyi An¹Co-authors: Arkadiy Simonov²; Marek Paściak³; Nan Zhang¹¹ Xi'an Jiaotong University² ETH Zurich³ Institute of Physics of the Czech Academy of Sciences

Corresponding Author: anzheyi@xjtu.edu.cn

The $\text{PbZr}_x\text{Ti}_{1-x}\text{O}_3$ (PZT) solid solution is one of the most widely applied ferroelectric materials due to its excellent electromechanical properties. However, despite the extensive studies in the past half century, the physical origin of its properties is still not fully understood, which is mainly caused by the complexity of its crystal structure, especially in the local atomic scale [1]. By electron diffraction with ferroelectric PZT [2], it was found that the diffuse scattering (DS) intensity form $\{111\}$ planes, while a complete local-structural model of such DS pattern still lacks.

In this study, we performed x-ray DS experiments with PZT single crystals ($x \sim 0.4$) with average rhombohedral symmetry at room temperature, and reconstructed the three-dimensional distribution of the DS intensity in full reciprocal space (Fig. 1a). To get quantitative information out of this distribution of DS intensity, we constructed a difference-pair-distribution-function (Δ PDF) model with short-range correlation of atomistic displacements, and refined this model against the experimental data using the software Yell [3]. The feature of DS intensity was successfully reproduced with the refined model (Fig. 1b). From the model, it is revealed that there exists various types of short-range displacive correlations between neighboring Pb atoms and they may be the result of the impact of surrounding Zr^{4+} and Ti^{4+} cations. This study provides a more-complete understanding of the local atomic behavior in ferroelectric crystals with long-range ordered cation displacements.

References:

- [1] The missing boundary in the phase diagram of $\text{PbZr}_{1-x}\text{Ti}_x\text{O}_3$, Nat. Commun. 5, 5231 (2014).
- [2] Influence of short-range and long-range order on the evolution of the morphotropic phase boundary in $\text{Pb}(\text{Zr}_{1-x}\text{Ti}_x)\text{O}_3$, Phys. Rev. B 70, 184123 (2004).
- [3] Yell : a computer program for diffuse scattering analysis via three-dimensional delta pair distribution function refinement, J. Appl. Crystallogr. 47, 1146 (2014).

Lectures / 114

School welcome and opening

Corresponding Author: andersen@ill.fr

Conference first session / 131**Amorphous Pharmaceuticals****Corresponding Author:** benmore@anl.gov

26

Amorphous Pharmaceuticals**Author:** Chris Benmore¹**Co-authors:** Jeffery Yarger²; Pamela Smith³; Richard Weber⁴; Stephen Byrn⁵; Stephen Wilke⁴¹ *Argonne National Laboratory*² *Arizona State University*³ *Improved Pharma*⁴ *Materials Development Inc.*⁵ *Purdue University***Corresponding Author:** benmore@anl.gov

Amorphous active pharmaceutical ingredients can possess a range of different intra- and inter-molecular interactions, that can directly enhance medicinal efficacy. Order of magnitude improvements in the solubility and bioavailability of orally taken amorphous drugs can be achieved compared to their crystalline forms. High Energy X-ray Diffraction (HEXRD) studies of amorphous pharmaceuticals is a relatively new application that uses 50-100keV photons to enable high-resolution investigations of organic materials, because x-rays are highly sensitive to the orientation of the molecular backbone in the Ångstrom to nanometer range. Amorphous forms of Indomethacin, Carbamazepine, Posaconazole, Cannabidiol, Nifedipine, Felodipine, water in PVP, as well as the amorphous solid dispersion Ketoprofen-PVP have been studied using HEXRD. The data are modeled using Empirical Potential Structure Refinement (EPSR) with the aid of chemical and molecular constraints provided by NMR and Raman spectroscopy. Our models attempt to establish the optimal intra-molecular rotations, librations and dihedral angles in the amorphous state, together with preferred inter-molecular bonding interactions. Quantitative coordination numbers arising from hydrogen bonding and aromatic ring interactions can be extracted, which in some cases show substantial variations between the liquid and glass. In addition, chain or ring distributions in the amorphous state can lead to new bonding patterns or molecular clusters not present in the crystalline polymorphs. The effects of humidity, temperature or preparation method on drug stability and storage will also be discussed.

Lectures / 117**Recent and future developments in PDF-land****Corresponding Author:** sb2896@columbia.edu**Tutorial introductions / 120****DiffPy-CMI - a software toolbox for real-space structure analysis and Complex Modeling**

Corresponding Author: sb2896@columbia.edu

Conference fifth session / 145

CO-induced dynamic behaviour of Al₂O₃-supported Pd nanoparticles at room temperature

Corresponding Author: daniele.bonavia@esrf.fr

82

The new Debye beamline at SLS2.0: a versatile operando platform for X-ray scattering and X-ray absorption spectroscopy

Authors: Daniele Bonavia¹; Adam Clark¹; Maarten Nachtegaal¹; Stephan Hitz¹

¹ Paul Scherrer Institute

Corresponding Author: daniele.bonavia3@gmail.com

The newly constructed Debye beamline at the upgraded Swiss Light Source (SLS 2.0) is now accepting users. Debye is positioned to provide multimodal X-ray absorption spectroscopy (XAS) and X-ray diffraction (XRD) to investigate the chemical, geometrical and electronic structure of functional materials under operating conditions. The beamline is equipped with a 2.1 T bending magnet source (soon to be upgraded to a tuneable 3.5 - 5 T superbend) and an in-house engineered quick scanning channel-cut monochromator to offer an accessible energy range from 4.5 keV to 60 keV. A cutting-edge motion control system provides a diverse range of control options, facilitating quick-scanning XAS (with sub-second time-resolution), and quasi-simultaneous XRD pattern collection at stationary points in the monochromator oscillation.

The Debye beamline is equipped with a photon-counting Pilatus 6M area detector that allows both independent and quasi-simultaneous XRD collection up to 25 keV. We aim for a second high-Z photon-counting pixel detector to cover the higher energy range available and include time-resolved X-ray total scattering to the beamline capabilities.

A pilot experiment following the in situ Zr-MOF synthesis was recently conducted in quasi-simultaneous mode. XRD patterns were collected with a time resolution of 15 s while fluorescence XAS Zr K-edge spectra were collected every 1 s. The experiment tracked the conversion from initial precursors chemical, the early nucleation of Zr centers through to the crystallisation of the metal organic framework, providing insights on the kinetics and dynamics of the synthesis process. This combined approach enabled to track crystallization kinetics, coherence lengths and degrees of crystallinity, as well as oxidation states and pre-crystalline structure through the pairing of XAS with XRD.

This experiment is a good example of the type of research questions that would benefit from the combination of XRD and XAS. Besides following the synthesis of crystalline materials, this multimodal approach is especially useful for operando characterization studies in heterogeneous catalysis and electrocatalysis, providing time-resolved insights on the electronic and structural properties of these materials.

Tutorial introductions / 119

PDFgui – a small box modelling platform for nanoscale structure analysis

Corresponding Author: emil.bozin@gmail.com

14

PDFgui – a small box modelling platform for nanoscale structure analysis

Corresponding Author: emil.bozin@gmail.com

PDFgui is a user-friendly graphical interface built on the PDFfit2 small box modeling engine to fit neutron and X-ray PDF data and extract nanoscale structure information. The easy to use PDFgui environment organizes fits and simplifies many data analysis tasks, such as configuring and carrying out sequential refinements and plotting multiple fits. PDFfit2 is a program as well as a library for real-space refinement of crystal structures. It is capable of fitting a theoretical three-dimensional (3D) structure to atomic pair distribution function data and is ideal for nanoscale investigations. The fit system accounts for lattice constants, atomic positions and anisotropic atomic displacement parameters, correlated atomic motion, and experimental factors that may affect the data. The atomic positions and thermal coefficients can be constrained to follow the symmetry requirements of an arbitrary space group. PDFfit2 and PDFgui are freely available [1]. In this talk, the PDFgui concept and layout as well as essential capabilities will be presented. To exemplify the small-box analysis as applied to bulk systems featuring nanoscale heterogeneities, a brief illustration of a recent hidden local symmetry breaking detection in a high performance thermoelectric system will be shown [2]. PDFgui functionality and typical use cases, such as co-refinement of multiple datasets, phase analysis, sequential refinements of variable length scales, temperature & composition, will be demonstrated during the followup hands-on tutorial.

[1] “PDFfit2 and PDFgui: computer programs for studying nanostructure in crystals”, C L Farrow et al., *J. Phys.: Condens. Matter* **19** 335219 (2007).

[2] “Hidden local symmetry breaking in silver diamondoid compounds is the root cause of ultralow thermal conductivity”, H. Xie et al., *Adv. Mater.* **34** 2202255 (2022).

72

Using mPDF to probe magnetic exchange interactions

Author: Edison Carlisle¹

Co-authors: Benjamin FRANDSEN¹; Emma Zappala¹

¹ Brigham Young University

Corresponding Author: epicarlisle@gmail.com

Determining magnetic exchange interactions is vital for understanding the magnetic behavior of materials. The standard method for exchange interaction determination involves performing inelastic neutron scattering experiments on single crystals to measure spin wave dispersions from a long-range-ordered magnetic ground state. However, the influence of exchange interactions is not limited exclusively to spin waves in ordered states but also governs the system’s physics in all magnetic states, including the short-range correlations that persist into the paramagnetic regime. Exchange parameters have been successfully recovered in the past from energy-integrated diffuse neutron scattering data from paramagnets, indicating that the diffuse scattering and underlying short-range magnetic correlations are rich in information. Consequently, magnetic pair distribution function (mPDF) analysis, which directly probes short-range magnetic correlations, is expected to be well suited for extracting exchange parameters from correlated paramagnets. Here, we demonstrate two approaches for determination of exchange parameters from mPDF data, including Monte Carlo mPDF simulations and a robust mean-field theory approach. In the latter case, we incorporate the Onsager reaction field to develop an analytical model for exchange interaction determination from the mPDF. We showcase several materials where we use real-space magnetic correlation data to successfully recover exchange interaction values comparable to literature values.

Conference third session / 136

X-ray PDF-analysis applied to energy materials, including in operando studies

Corresponding Author: karena.chapman@stonybrook.edu

Tutorial introductions / 122

Topas

Corresponding Author: philip.chater@diamond.ac.uk

Conference first session / 130

Introduction and information

Corresponding Author: stefano.checcchia@esrf.fr

90

ToScaNA: A Python Module for the Treatment of Total Neutron Scattering Data

Author: Gabriel Julio Cuello¹

¹ *Institut Laue Langevin*

Corresponding Author: cuello@ill.fr

We present ToScaNA (Total Scattering Neutron Analysis), a Python module designed to streamline the reduction and treatment of data from the D4 neutron diffractometer at the ILL. Once the primary reduction stage is completed, the resulting three-column files (angle or Q, intensity, and uncertainty) – whether originating from D4 or from any other total-scattering instrument – can be processed to account for sample-dependent effects and to produce differential cross-sections, structure factors, and real-space correlation functions.

This poster outlines, step by step, a general workflow for reducing and treating total neutron scattering data. Through selected examples, we illustrate how these steps are implemented in practice using ToScaNA together with Jupyter notebooks. The aim is to provide users with an accessible and reproducible path from raw detector counts to physically meaningful quantities.

ToScaNA is fully integrated within the ILL's virtual machine environment (VISA), enabling users to analyse their data without installing additional software on their own computers. The module is also platform-independent and can be run on standard Python distributions (such as Anaconda) under Linux, Windows, or macOS.

Conference sixth session / 148

Investigating preferential adsorption of N₂ from the air in Zeolite 13X using total neutron scattering

Corresponding Author: marta.falkowska@manchester.ac.uk

Lectures / 115

Introduction and information

Corresponding Author: fischer@ill.fr

Tutorial introductions / 125

Information on tutorials

Corresponding Authors: fischer@ill.fr, stefano.checcchia@esrf.fr

Tutorial introductions / 121

diffpy.mpdf - Investigating short-range magnetic correlations in real space with magnetic pair distribution function analysis

Corresponding Author: benfrandsen@byu.edu

Conference fifth session / 144

Real-time observation of rapid densification and degradation in flash sintered multilayer systems for battery materials

Corresponding Author: riku.fukada@neel.cnrs.fr

100

Liquid-liquid phase transition in covalent materials

Author: Jean-Pierre Gaspard¹

Co-authors: Gabriel Julio Cuello ¹; Jean-Yves Raty ²; Françoise Hippert ³

¹ ILL

² University of Liège

³ INPG-UGA

Corresponding Author: gaspard@ill.fr

Almost all materials expand when heated with a few exceptions among which Tellurium-based liquids. $\text{Se}_x\text{Te}_{1-x}$ liquid alloys exhibit uncommon properties. Among them a negative thermal expansion (NTE) is found in a wide range of concentrations for Te-rich compositions ($x \leq 0.5$). These unusual properties result from a covalent bonding with additional Peierls distortion. We measured the structure factors $S(Q)$ and the vibrational densities of states $n(\omega)$ by neutron scattering, as a function of temperature and concentration ($x \leq 0.4$). In a theoretical model we show that NTE arises from competition between electronic and entropic contributions: the NTE is the result of the entropy-induced weakening of the Peierls distortion with temperature. A careful analysis of the diffuse neutron scattering data showed both an increase in coordination numbers and a cancellation of the Peierls distortion as the temperature rises. A discreet pre-peak is observed around 1.2 \AA^{-1} , it is an imprint of the Peierls distortion, its intensity is reduced when heating and it broadens. Its behaviour is linked to the NTE. The Fourier transformation of total-scattering diffraction data into real space produces a Pair-Distribution Function (PDF) that is central for analysing the structure in real space. The first peak position of $g(r)$ shows a shift as a function of temperature that is in agreement with the NTE. Finally we discuss the conditions of the occurrence of this continuous liquid-liquid phase transition.

Furthermore, this analysis shed some light on the specific chemical bond and mechanism of Phase Change Materials (PCM).

22

Total scattering as a tool to understand the incomplete phase transition in sodium-ion battery materials

Authors: Andrea Testino¹; Samuel Gatti^{None}; Sigita Trabesinger²

¹ Paul Scherrer Institut (PSI) / EPFL

² Paul Scherrer Institut (PSI)

Corresponding Author: samuel.gatti@psi.ch

Samuel Franz Gatti, Andrea Testino, Sigita Trabesinger

WAXS is well established technique to understand structural evolution of battery materials during electrochemical charge-discharge-cycles and allows to explain charge-compensation mechanisms. This

allows to understand initial, meta-stable and intermediate structures, as well as the structural changes of cathode materials during cycling.

New materials, such as sidorenkite-type $\text{Na}_3\text{Fe}(\text{PO}_4)(\text{CO}_3)$, with more complex structures are on the rise due to their potential to lead to higher energy densities. Due to their stiff framework, complete long-range structural rearrangements are impeded. Nevertheless, structural rearrangements occur locally. To understand these rearrangements, we combine ex-situ PDF analysis and operando WAXS, which shows that the oxidation of Fe^{3+} to the Jahn-Teller distorted Fe^{4+} incorporates a rotation of the

PO_4 framework. This transition is incomplete due to the stiff framework, which limits the utilization of

this redox couple. Based on these results, we develop the next generation of sidorenkite-type cathode

materials for sodium ion batteries without detrimental Jahn-Teller distorted electron configurations.

61

Structural origin of magnetic softening of annealed 3D-printed and as-cast Co-free Fe-Si-B-based metallic glasses

Author: Amirhossein Ghavimi¹

Co-authors: Purbasha Sharangi ²; Uma Rajput ³; Enzzo Ferrara ²; Paola Tiberto ²; Isabella Gallino ⁴; Ralf Busch ¹

¹ Saarland University

² INRIM

³ INRiM

⁴ Technical University Berlin

Corresponding Author: amirhossein.ghavimi@uni-saarland.de

The fundamental structural origin of magnetism in Fe-based amorphous alloys remains not fully understood. In this work, we obtained soft magnetic properties in newly developed Co-free Fe-Si-B-based compositions (with additions of Nb, Ni, and Cr) in the shapes of ribbon, plate, and printed parts by carefully tailoring the annealing process as part of an EU project (AM2SoftMag, EU-Pathfinder Open Grant No: 101046870). Using synchrotron radiation (SAXS/WAXS) and high-resolution transmission electron microscopy, the changes are revealed in both short-range and medium-range atomic structures as the key to the observed magnetic softness at optimal annealing temperatures and times. These insights offer a promising approach for tuning the magnetic performance of Fe-based amorphous alloys and contribute to a deeper, quantitative understanding of the relationship between atomic structure and magnetic properties in amorphous materials.

Conference third session / 137

Mechanistic Insights into Solvent-Guided Growth of MoO₂ Nanoparticles from in situ Total Scattering Studies

Corresponding Author: lgg@chem.ku.dk

39

Mechanistic Insights into Solvent-Guided Growth of MoO₂ Nanoparticles from in situ Total Scattering Studies

Author: Laura Graversen¹

Co-authors: Andrea Kirsch ; Kirsten Marie Jensen ¹; Maria S. Thomsen ¹; Mikkel Juelsholt ¹; Nicolas P. L. Magnard ; Olivia Aalling-Frederiksen ¹; Rebecca K. Pittkowski ¹; Ulrik Friis-Jensen ¹

¹ University of Copenhagen

Corresponding Author: lgg@chem.ku.dk

Metal oxide nanoparticles continue to show great potential for applications as advanced energy materials.[1] Despite significant progress in synthetic methods, our ability to synthesise metal oxide nanomaterials is limited by an incomplete understanding of the fundamental chemistry occurring during their formation. One highly successful method for producing metal oxide nanoparticles is through non-aqueous sol-gel synthesis, where a metal chloride precursor is suspended in an alcohol and treated solvothermally.[2] Here, we investigate the solvent effects on the structure and crystallite size of MoO₂, and deduce their reaction pathways.

Using *in situ* pair distribution function (PDF) analysis combined with X-ray absorption spectroscopy, we reveal that solvent-dependent ligand exchange dynamics control the atomic structure and crystallite size of the formed materials.[3] A fast ligand exchange occurs between an oxygen supplied from the solvent and chloride from the precursor, leading to the rapid formation of extended [MoO₆]-networks. These networks slowly condense into ~30 nm particles with the conventional MoO₂

distorted rutile structure. Conversely, when Cl/O-ligand exchange is slowed down, a $[\text{Mo}^{\text{IV}}\text{Cl}_x\text{O}_{6-x}]$ complex is formed, which directs the formation of very small (2-3 nm) particles adopting the high-pressure MoO_2 polymorph. These findings establish how the solvent chemistry controls the mechanistic pathways and the intermediates formed prior to crystallisation. Thereby, demonstrating how *in situ* total scattering and PDF analysis can elucidate solvent-controlled reaction routes in metal oxide formation. This understanding provides a direct strategy for tailoring specific nanocrystalline materials through controlled synthesis conditions.

[1] R. Deshmukh et al., *Chem. Eur. J.* 23 (2017), 8542-8570.

[2] J. Buha et al., *PCCP* 12 (2010), 15537.

[3] L. Graversen et al., *Chem. Sci.* 16 (2025), 14350-14365.

Conference seventh session / 151

Understanding local structure and dynamics in Prussian blue analogues

Corresponding Author: elodie.harbourne@hertford.ox.ac.uk

78

In-Situ Observation of an Isosymmetric Superionic Phase Transition in $\text{Li}_7\text{P}_3\text{S}_{11}$

Author: Md Rana Hossain¹

Co-author: Akira Miura²

¹ Hokkaido University, Japan

² Hokkaido University

Corresponding Author: rana@eng.hokudai.ac.jp

Solid-state electrolytes are indispensable for enabling safe and high-performance energy storage technologies due to the liquid-like diffusion of mobile ions through interstitial pathways. Ion conduction is typically a thermally activated process described by an Arrhenius relationship; however, deviations from linearity (non-Arrhenius behavior) are frequently observed when a material undergoes a normal-to-superionic phase transition upon heating. Accordingly, superionic conductors are commonly classified based on the nature of the phase transition: Type-I (abrupt) or Type-II (gradual)—knowledge that is crucial for guiding the design of next-generation solid electrolytes.

In this study, by leveraging high-energy in-situ X-ray diffraction measured at the Spring-8 BL13XU beamline (Hyogo, Japan), temperature-dependent structural evolution has been characterized in both reciprocal (Rietveld refinement) and real space (pair distribution function).

We identify an isosymmetric phase transition occurring above ~310K in $\text{Li}_7\text{P}_3\text{S}_{11}$. This transition is driven by the displacement of P atoms within the corner-sharing P_2S_7 units and the accompanying reduction in their tetrahedral volume. The resulting structural evolution enlarges the percolation channel radius, lowers migration barrier heights, and activates previously inaccessible pathways between adjacent P_2S_7 tetrahedra for Li^+ transport.

Conference seventh session / 152

Grazing Incidence Total Scattering at PETRA III: Extending Local Structure Analysis to Ultrathin Films on Single-Crystal Substrates

Corresponding Author: fernando.igoa@desy.de

42

Grazing Incidence Total Scattering at PETRA III: Extending Local Structure Analysis to Ultrathin Films on Single-Crystal Substrates

Authors: Fernando Igoa¹; Jorden De Bolle²; Simone Mascotto³; Xiao Sun³; Martin von Zimmermann¹; Ann-Christin Dippel⁴

¹ DESY

² Department of Solid State Sciences, Ghent University (Belgium)

³ Institut für Integrierte Naturwissenschaften, Universität Koblenz (Germany)

⁴ Deutsches Elektronen-Synchrotron DESY

Corresponding Author: fernando.igoa@desy.de

Grazing incidence scattering is a technique that takes advantage of the total external reflection of X-ray photons as they shine on a flat surface below the material's critical angle. When this condition is met, the X-ray photons only penetrate the material some 1-10 nm as an evanescent wave. Hence, surface scattering is amplified with respect to the bulk. If combined with high energy photons and high-angle data collection, then surface sensitive grazing incidence total-scattering (GI-TS) and pair distribution function (pdf) analysis can be achieved.

The critical angle depends on the photon energies, such that it lies around (10 - 60) millidegrees, which imposes strict boundary conditions for alignment, sample flatness and roughness. As a matter of fact, empirically, always a certain degree of bulk penetration is observed, which contributes to background scattering. Therefore, well-behaved, i.e. isotropic scattering, substrates have been historically chosen to perform GITS, neglecting the more application relevant options, such as single-crystalline silicon.

Single-crystalline silicon exhibits an anisotropic scattering that combines discrete Bragg reflections and distributed diffuse scattering. Azimuthal averaging is out of question in this case, for which its use in GITS has long been considered a dead-end. We recently optimized a 2D-background correction and subtraction strategy that successfully allows to eliminate the anisotropic background contribution, and hence isolate thin film scattering that can be transformed to pdf. This strategy is based on using the substrate Bragg reflections as a reference to correct and subtract 2D images prior to azimuthal integration.

In this presentation, the grazing incidence total scattering capabilities at P21.1 at PETRA III will be discussed, along with recent advancements that enable the use of anisotropic substrates.

Conference sixth session / 146

3D-DeltaPDF: From synchrotron to in-house sources

Corresponding Author: kjuul@chem.au.dk

Conference fifth session / 143

Total scattering and PDFs using X-ray free-electron lasers: quality data in 30 femtoseconds

Corresponding Author: david.keen@stfc.ac.uk

23

Thermally Stable Binary Two-Dimensional Hybrid Organic-Inorganic Perovskite Glasses

Author: Arad Lang¹¹ Technion - Israel Institute of Technology

Corresponding Author: aradlang@technion.ac.il

Two-dimensional hybrid organic-inorganic perovskites (2D-HOIPs) have recently garnered significant attention for their potential integration into next-generation optoelectronic applications. Their chemical diversity and straightforward synthesis, together with band gap tunability and enhanced stability, make them promising candidates to replace their three-dimensional counterparts as active materials in photovoltaics, light emitters, and photodetectors. Recent studies have revealed that 2D-HOIPs with the chemical formula $(RNH_3)_2MX_4$ (where R is a bulky organic moiety, M is a divalent metal cation, and X is a halide) can undergo melting – a reversible solid-liquid transition – upon heating. Furthermore, by carefully engineering the organic cation, the cooling-induced crystallisation can be suppressed, resulting in a glassy (amorphous) state. However, these so-called “HOIP glasses” exhibit thermal instability, reverting to their thermodynamically stable crystalline form upon mild heating or even at room temperature over a time span of hours to days.

In this work, we address the thermal instability of HOIP glasses through melt alloying, a technique we recently demonstrated to apply to meltable 2D-HOIP systems. Binary HOIP glasses were synthesized by blending powders of two glass-forming 2D-HOIPs: $(S-NEA)_2PbBr_4$ (where S-NEA = (S)-(-)-1-(1-naphthyl)ethylamine) and $(MIPA)_2PbI_4$ (where MIPA = methyl-iodopropylamine). Melt-quenching these blends resulted in the formation of glassy phases. The glass transition temperatures, optical band gap, and mechanical hardness of these glasses were found to depend on the blend composition. Most notably, the binary glasses exhibited complete thermal stability, with no recrystallisation observed even after one month of storage at room temperature.

Conference second session / 133

Structural Fingerprints of Plasticity: Linking the Shear Transformation Zone Size to Pair Distribution Functions in Metallic Glasses

Corresponding Author: v.lemkova@matsci.uni-saarland.de

Conference third session / 139

Phase Sensitive Detection Analysis on Modulation Excitation PDF Data of Ni Based Catalysts

Corresponding Author: manzoni@ifk.rwth-aachen.de

Lectures / 118**Single-Crystal Diffuse scattering****Corresponding Author:** reinhard.neder@fau.de**Tutorial introductions / 127****DISCUS: Simulation and refinement of disordered crystal structures****Corresponding Author:** reinhard.neder@fau.de**Conference second session / 134****Whole-nanoparticle-ensemble refinements of compositionally complex systems from X-ray pair distribution function data via the Reverse Monte Carlo method****Corresponding Author:** tmn@chem.ku.dk

36

Whole-nanoparticle-ensemble refinements of compositionally complex systems from X-ray pair distribution function data via the Reverse Monte Carlo method**Author:** Tobias Molgaard NIELSEN¹**Co-authors:** Kirsten Marie Jensen ¹; Lewis OWEN ²¹ *University of Copenhagen*² *University of Sheffield***Corresponding Author:** tmn@chem.ku.dk

Compositionally complex nanomaterials such as High-Entropy Alloys (HEAs), which consist of five or more elements randomly mixed in a solid solution structure, have continued to attract interest as promising catalyst materials in recent years[1]. While a high-dimensional compositional space makes HEAs prospect catalysts with tuneable properties, their multi-element nature also complicates comprehensive structural analysis through conventionally applied methods such as powder diffraction and X-ray absorption spectroscopy. Total scattering and pair distribution function (PDF) analysis has proven an excellent tool for structural characterisation of compositionally complex and nano-sized materials[2, 3]. Regardless, PDF analysis has not been explored for identification of chemical short-range order and compositional inhomogeneities in nanoparticles. Such structural effects are difficult to describe through commonly employed small-box modelling methods. In contrast, large-box modelling offers a more holistic approach by including thousands of atoms in the structural model, thereby capturing both local and long-range structural effects. Regardless, large-box methods for nanoparticle systems are only just starting to emerge[4].

We present an approach for the investigation of chemical short-range order and elemental inhomogeneities in multimetallic nanoparticle systems through large-box modelling of X-ray PDF data. Specifically, we demonstrate a methodology for atomistic whole-nanoparticle-ensemble refinements

of compositionally complex nanoparticles, with average particle sizes down to just 2.8 nm, through the Reverse Monte Carlo (RMC) method. We analyse a series of supported nanoparticle systems of increasing compositional complexity (Pt, PdPt, PdPtRh, PdPtRuRh and IrPdPtRuRh) to probe the robustness of the technique. The resulting RMC PDF refinements exhibit excellent fit quality, demonstrating that the employed atomic NP configurations accurately describe the experimental data. Refinement results of NP ensembles of different compositional ordering, including core@shell, compositional gradient and fully random structures are compared to determine which model best describes the synthesised particles. Finally, by allowing atom-type swapping in the refinement algorithm, the presence of compositional ordering and CSRO is investigated. This work presents a new approach to the identification of CSRO and compositional inhomogeneities in nanoparticle systems and emphasises the challenge of comprehensive structural analysis of compositionally complex nanomaterials.

[1] T. Löffler, A. Ludwig, J. Rossmeisl and W. Schuhmann, *Angew. Chem. Int. Ed.*, 2021, 60, 26894-26903.

[2] B. Jiang, C. A. Bridges, R. R. Unocic, K. C. Pitike, V. R. Cooper, Y. Zhang, D.-Y. Lin and K. Page, *J. Am. Chem. Soc.*, 2021, 143, 4193-4204.

[3] L. R. Owen, E. J. Pickering, H. Y. Playford, H. J. Stone, M. G. Tucker and N. G. Jones, *Acta Mater.*, 2017, 122, 11-18.

[4] Y. Zhang, M. McDonnell, W. Liu and M. G. Tucker, *J. Appl. Cryst.*, 2019, 52, 1035-1042.

19

Happy Accidents: Spatially Resolved X-ray Beam Damage Effects in a Lithium-Ion Battery

Author: Erlend Tibergh NORTH¹

Co-author: David S. Wragg²

¹ *University of Oslo*

² *University of Oslo / Institute for Energy Technology, Norway*

Corresponding Author: erlend.north@hotmail.com

An operando battery experiment using a multichannel collimator (MCC) was performed at ESRF's ID15A beamline. The technique allowed us to probe the metallic coin cells used in an electrochemical lab and obtain clean diffraction data. Combining this with a micron-sized beam allowed us to extract data from a specific volume within the electrode of interest. This experiment requires both high energy and high brilliance, and to minimize beam damage it is normal to scan across the sample in the beam to avoid severe damage to one area. Unfortunately, an accidental coding error led to one part of the sample being continuously exposed to the beam for 7.5 hours during operation rather than repeated line scans.

While electrochemical cycling data indicated standard lithium intercalation into graphite, the X-ray diffraction data revealed no structural changes in the sample, indicating no lithiation of the graphite in the beam during the experiment.

To look for structural changes outside the area illuminated during the operando experiment, we used the MCC setup for an in situ line scan post-operando. This revealed a gradient of peak positions as a function of distance from the operando irradiated area (OIA), signalling an increase in lithiation and thus in electrochemical function as the distance from the OIA increased. Electrolyte decomposition products were also observed around the OIA.

This presentation will go into the details of those operando and in situ line scan results, comparing them to a simulation of the experimental setup performed in the particle physics Monte Carlo simulation package FLUKA, which reveal that the electrochemistry of the system would have been affected even if the original plan of scanning the sample through the beam had been implemented. The work highlights that mistakes in data collection can sometimes lead to findings with much greater relevance.

Published paper here: <https://pubs.acs.org/doi/10.1021/acsenerylett.5c02442>

Conference second session / 132

Intermediate-range order in glassy oxide materials revealed by topological analysis

Corresponding Author: onodera.yohei@nims.go.jp

Conference fourth session / 142

Assessing Short-range order using total scattering and RMC - methods, challenges and strategies

Corresponding Author: lewis.owen@sheffield.ac.uk

Tutorial introductions / 158

Spinvert and Spinteract: Magnetic structure refinement for paramagnets

Corresponding Author: paddisonja@ornl.gov

Conference eighth session / 153

Exploring magnetic correlation lengths in frustrated systems via single-crystal neutron diffraction

Corresponding Author: o.petrenko@warwick.ac.uk

Lectures / 116

Structure of Liquid and Amorphous Materials using Pair-Distribution Function Analysis

Corresponding Author: p.s.salmon@bath.ac.uk

Conference second session / 135

Structural evolution of Tungsten Oxide Network during WO₃.H₂O formation

Corresponding Author: capucine.sassoye@sorbonne-universite.fr

Temperature Dependent Diffuse Scattering in Sanidines

Author: Ella Mara SCHMIDT¹

Co-authors: Christin Wiggers¹; Daniel Chaney²

¹ *University of Bremen*

² *ESRF*

Corresponding Author: ella.schmidt@uni-bremen.de

Sanidine is the high-temperature, monoclinic polymorph of potassium feldspar. It is typically found in felsic rocks, often incorporating significant amounts of sodium due to rapid cooling. Sanidine's crystal structure has four non-equivalent tetrahedral sites where Al and Si are tetrahedrally coordinated by four oxygen ions, forming a framework of corner-sharing AlO_4 and SiO_4 tetrahedra. In this disordered alkali feldspar, Al^{3+} and Si^{4+} are randomly distributed across all four tetrahedral sites. In the other potassium feldspars, Al and Si are fully ordered in triclinic microcline and partially ordered in monoclinic orthoclase. In this study, we investigate possible differences in local ordering due to different thermal treatments with single crystal diffuse scattering.

In our diffuse scattering studies, we observe changes in the diffuse scattering, for the sample in-situ heated to 1000 °C, quenched to 30 °C and annealed for one week at 1050 °C and slow cooled. We assign the differences in the experimentally observed diffuse scattering to an interplay of potential K/Na and Al/Si ordering processes that vary with cooling rate. In the future, we envision that by comparing the diffuse scattering of sanidines with different compositions and thermal histories we can make the diffuse scattering a potential geospeedometer for cooling rates.

The project is funded through the Cluster of Excellence “The Ocean Floor – Earth’s Uncharted Interface” and supported by GLOMAR – Bremen International Graduate School for Marine Sciences, University of Bremen.

Conference seventh session / 149

Isolating TEM instrumental function to the ePDF

Corresponding Author: seccolemos@gmail.com

Isolating TEM instrumental function to the ePDF

Author: Victor Secco Lemos¹

Co-authors: João Batista Souza Junior²; Ute Kolb³

¹ *JGU Mainz | UNICAMP*

² *Brazilian National Center for Research and Materials*

³ *Johannes Gutenberg Universität Mainz*

Corresponding Author: seccolemos@gmail.com

Solids in the nanometer scale (1–100 nm), known as nanomaterials, present different physical properties compared to their bulk counterparts. The nanomaterials' unusual properties arise mainly from size effects, where surface properties also become increasingly dominant. Probing the structure of

nanomaterials accurately is extremely challenging with either single-crystal or powder X-ray diffraction, since the former cannot sample diffraction information from a single nanocrystallite domain, and the latter presents too much peak broadening and diffuse scattering. Additionally, due to the dominant influence of surface on nanomaterials, crystallographic changes compared to bulk can occur. In this context, structural analysis of nanomaterials with PDF can overpass those forementioned diffraction problems as PDF is a remarkable crystallographic tool to understand diffuse scattering. The usual methods to obtain accurate PDFs involve X-rays or neutrons. Electron PDF (ePDF) methods, while still under development, present advantages for nanomaterials samples due to their capability to selectively probe at the nanometer scale. However, the strong scattering of electrons limits their application due to dynamic scattering, signal loss at high Q , and lack of understanding of the instrument's contribution to the pattern. For this reason, in this work we synthesized monodisperse nanoparticle samples with increasing sizes, which serve as standards for modeling the TEM instrumental contribution to the diffraction pattern and, consequently, to the ePDF. This approach aims to eliminate the need for benchmarking against xPDF or nPDF to isolate the sample contribution from the instrument. By applying precession electron diffraction on self-sustained thin films of nanoparticles, a quasi-kinematical regime was ensured for diffraction acquisition. The patterns were fed to DISCUS's Debye scattering model, and by fixing the nanoparticle diameter as obtained from manual particle picking from TEM images and monochromatic X-Diffraction, an instrumental contribution was obtained.

Conference seventh session / 150

Dynamic magnetic pair-density function analysis (DymPDF)

Corresponding Author: shamoto@outlook.jp

Tutorial introductions / 128

3D- Δ PDF: Pair distribution function analysis for single crystals

Corresponding Author: arkadiy.simonov@mat.ethz.ch

Conference eighth session / 154

Fast Simulation of Disordered Crystals Using Gaussian Copulas

Corresponding Author: arkadiy.simonov@mat.ethz.ch

Conference eighth session / 155

Hidden complexity in D2O Ice VII

Corresponding Author: wslawinski@chem.uw.edu.pl

Hidden complexity in D2O Ice VII

Authors: Krzysztof Wozniak¹; Wojciech Slawinski²

Co-authors: Christopher Ridley³; Craig Bull⁴; Grzegorz Lach¹; Michal Chodkiewicz¹; Mihails Arhangelkis¹; Piotr Rejnhardt¹; Roman Gajda¹

¹ *University of Warsaw*

² *Univeristy of Warsaw, Faculty of Chemistry*

³ *Oak Ridge National Laboratory*

⁴ *Rutherford Appleton Laboratory ISIS Neutron and Muon Source*

Corresponding Author: wslawinski@chem.uw.edu.pl

Ice VII is thought to play a role in the water-rich interiors of Jupiter's moon Europa and Saturn's moon Enceladus and other planetary bodies. From its average cubic structure, ice VII is seemingly simple, however the local structure reveals hidden complexity, namely individual positions of water molecules forming a complex network via hydrogen bonds. Through coupling Pair Distribution Function and Reverse Monte Carlo modelling to high pressure neutron scattering data, we have quantified the atomic and molecular structures of disordered ice VII. The decomposition of the average structure of ice VII into the individual positions of water molecules within the crystal lattice reveals that the D2O molecules are displaced along the direction of the polarization vector of each molecule. By applying this displacement, the structural model more accurately matches the D–O distances and D–O–D angles determined from the other ordered ice structures. Our results are also supported by DFT calculations confirming that deviations of water molecules from their average crystallographic positions energetically stabilize the structure of ice VII. Our studies open new perspectives for structural studies of different forms of ice, their phase transitions treating them as vast clusters of molecules with an average periodic structure but symmetry-free local arrangements.

Tutorial introductions / 123

RMCPProfile: Local structure of crystalline to amorphous materials

Corresponding Authors: tuckermg@ornl.gov, wslawinski@chem.uw.edu.pl

107

Novel Vacancy Ordering in YbAlO₃ Under Compression

Author: James Vazquez¹

Co-authors: Irina Chuvashova¹; Lia Vaquero¹; Olga Barkova¹; Stella Chariton²; Vitali Prakapenka²; Zain Hussein¹

¹ *Florida International University*

² *University of Chicago*

Corresponding Author: jvazq170@fiu.edu

Oxide perovskites exhibit complex defect chemistries that strongly influence their optical, electronic, and structural properties, yet the factors governing vacancy formation and ordering remain poorly understood. Prior work has largely focused on the roles of stoichiometry, octahedral distortion, and tensile strain. Of these factors, both experimental and first-principles studies show that tensile strain lowers equatorial oxygen vacancy formation energies and promotes vacancy clustering. In contrast, compressive strain is consistently predicted to suppress oxygen vacancy formation, but its direct

influence has remained experimentally unexplored. Classical atomistic simulations of $REAlO_3$ compounds further suggest that oxygen vacancies are energetically unfavorable relative to cation-based point defects under ambient conditions. Despite this, recent experimental studies on oxide perovskites show that ordered oxygen vacancies can emerge under non-equilibrium conditions that may stabilize into unique local structures or lattice modulations.

We report localized, crystallographically selective oxygen vacancies in orthorhombic $YbAlO_3$ synthesized at high pressures inside a diamond anvil cell (DAC). Single-crystal synchrotron X-ray diffraction shows that only one of the two axial oxygens of the AlO_6 octahedron undergoes depopulation across multiple lattice points within the same grain, producing a local AlO_5 square-pyramidal environment. Importantly, no ordered vacancies are observed on equatorial O sites, indicating a highly selective and strain-coupled vacancy configuration. We interpret this as a consequence of pressure-enhanced lattice strain anisotropy. Compression reduces octahedral tilt and amplifies energetic differences between the symmetrically non-equivalent axial and equatorial Al-O bonds, making vacancy formation favorable only along the axis that provides the greatest structural relief. This behavior parallels strain-driven vacancy ordering in thin films and the axial vacancy chains reported in $Sr_xFe_xO_{3x-1}$ systems.

These results demonstrate that high-pressure synthesis can stabilize vacancy-ordered states inaccessible at ambient conditions, revealing a new mechanism for tuning the local coordination environment in oxide perovskites. The resulting axial vacancy motif may have significant implications for the ionic, electronic, and dielectric properties of $REAlO_3$ perovskites, and highlights a tunable defect pathway relevant to materials design under extreme conditions.

Conference fourth session / 141

Magnetism in metallic glasses - a clear need for PDF

Corresponding Author: wildes@ill.fr

32

Magnetism in metallic glasses - a clear need for PDF

Author: Andrew Wildes¹

Co-author: Neil Cowlam²

¹ Institut Laue Langevin

² Sheffield University

Corresponding Author: wildes@ill.fr

Neutron diffuse scattering has long been recognised as a means to study complex magnetism in condensed matter, providing deep insight in fields from critical phase transitions to quantum spin liquids. The studies have frequently used cold neutrons to focus on the scattering at relatively small momentum transfers, encompassing the first few Brillouin zones of crystalline materials, where the magnetic scattering for most elements is strongest. Modern methods like Reverse Monte Carlo can usually analyse the data accurately and rapidly for crystalline materials, even if they are non-stoichiometric, as the positions for the atoms can be fixed and a sufficiently large supercell can be defined to allow for the resolution and chemical composition of the sample.

This is not the case for non-crystalline materials where positional disorder exists in addition to magnetic and, possibly, chemical short-range order. Metallic glasses are archetypical examples of these types of materials, featuring non-collinear ferro- and ferrimagnetic structures that must be correlated to a characterisation of their atomic structures. As will be shown in this presentation, neutron scattering with polarisation analysis will provide the data. Structural and magnetic PDF analysis would provide a full characterisation, and the materials present perhaps the most challenging test for the methods.

This presentation will summarise neutron experiments on magnetic metallic glasses and some efforts to characterise their structures, hopefully initiating discussion on the best way to model them.

40

IN SITU AND PDF NEUTRON DIFFRACTION FOR THE ADVANCED STRUCTURAL ANALYSIS OF MOF CATALYSTS FOR CARBON DIOXIDE VALORISATION

Author: Kirstin Wilson¹

Co-authors: Celia Castillo-Blas²; Felipe GANDARA³; Gabriel Julio Cuello⁴; ines puenteoreench³

¹ *ILL*

² *Materials Science Institute of Madrid*

³ *CSIC*

⁴ *Institut Laue Langevin*

Corresponding Author: wilson@ill.fr

This project focuses on the structural analysis of metal-organic frameworks (MOFs) comprising multiple metal elements, and their calcination products using neutron diffraction techniques to unveil their unique structural features and role in catalysing CO₂ reduction through the reverse water-gas shift (RWGS) reaction. The RWGS reaction, which converts CO₂ and H₂ into CO and water requires efficient catalysts that enable high activity and selectivity towards CO.[1]

A series of lanthanide multi-metal MOFs has been investigated.[2],[3] They are made of cerium, partially replaced by lanthanum, neodymium or praseodymium at specific ratios. Neutron diffraction data has been collected for the multi-metal MOFs to investigate the position of the metal elements in the structures, by completing Rietveld refinements as well as with PDF analysis to understand how the doped atoms are arranged. Upon calcination of the MOFs, doped CeO₂ is obtained, which shows excellent activity and selectivity as a catalyst in the RWGS reaction.[4],[5] High-resolution neutron diffraction data was collected to accomplish complete crystallographic characterisation of the MOFs, and the calcined products before and after the catalytic reaction.

The oxides displayed a fluorite-type structure and crystallised in the Fm-3m space group with metal cations sharing equivalent crystallographic positions. The Rietveld refinements indicate that as the doping level increases, so does the number of oxygen vacancies —critical for RWGS reaction mechanism— and decreases the lattice dimensions. The undoped cerium sample shows virtually no defects, suggesting most vacancies arise from metal substitution. Additionally, an in-situ neutron diffraction experiment carried out under a reaction gas mixture investigated any structural changes resulting from the interaction of the gas molecules with the MOF-derived oxides. No phase transitions or significant structural changes were observed.

The study demonstrates the viability of using multi-metal MOFs as precursors for designing advanced catalysts with precisely controlled doping level and intrinsic oxygen vacancy defects. Neutron diffraction provided insights into the structural dynamics of MOF-derived oxides, establishing clear relationships between metal distributions and oxygen vacancies. This research highlights the potential to produce catalysts with precise compositions and enhanced performance, paving the way for sustainable CO₂ valorisation.

[1] C. Ampelli et al., *Philos. Trans. R. Soc. A*, 2015, 373, 1-35

[2] H. Furukawa et al., *Science*, 2013, 341, 974-986

[3] F. Gándara et al., *Cryst. Growth Des.*, 2008, 8, 378-380

[4] R. L. Vasile et al., *Chem. Mater.*, 2022, 34, 7029-7041

[5] C. Castillo-Blas et al. *Nanoresearch*, 2021, 14, 493-500

Conference third session / 138

In situ/operando studies for understanding the metal-support interaction of Ni-based catalysts for ammonia decomposition

Corresponding Author: yanamandram@kofo.mpg.de

Tutorial introductions / 124

EPSR & Dissolve - Data-driven structural modelling of total scattering data

Corresponding Author: tristan.youngs@stfc.ac.uk

Tutorial introductions / 126

EPSR & Dissolve - Data-driven structural modelling of total scattering data

Corresponding Author: tristan.youngs@stfc.ac.uk

Tutorial introductions / 157

EPSR & Dissolve - Data-driven structural modelling of total scattering data

Corresponding Author: tristan.youngs@stfc.ac.uk

Conference fourth session / 140

Technical Aspects and Practices in Using Neutron Total Scattering for Local Magnetic Ordering Studies

Corresponding Author: zyroc1990@gmail.com

102

Temperature-dependent structural evolution of GeO₂

Author: Simone ZIGLIO¹

¹ *Università di Trento*

Corresponding Author: simone.ziglio-1@unitn.it

The physical properties of a material are fundamentally determined by its atomic-scale structure. This relationship is especially important for disordered systems, which are pervasive in modern technology yet remain structurally less well understood than their crystalline counterparts.

In this poster, I will present my ongoing research on the temperature-dependent structural evolution of glassy GeO₂. The study combines isothermal neutron diffraction measurements collected at several temperatures between the glassy state (350 K) and the liquid state (1400 K) with structural modeling using Reverse Monte Carlo (RMC) methods.

The initial configuration at 350 K is generated via Monte Carlo simulations employing the well-established Oeffner–Elliott potential and then refined against the neutron diffraction data. This refined structure is subsequently used as the starting configuration for the next temperature, enabling an iterative refinement procedure up to the liquid.

The resulting temperature-dependent structural models allow us to characterize both the short- and medium-range order at each stage, providing a detailed picture of how the structure of GeO₂ evolves from glass to liquid.

33

3D-DeltaPDF: From synchrotron to in-house sources

Author: Karl Juul¹

Co-authors: Bo Iversen¹; Kristoffer Støckler¹

¹ Aarhus University

The analysis of correlated disorder through diffuse scattering using the three-dimensional difference pair-distribution function (3D- Δ PDF) has received increasing attention due to its intuitive analysis [1]. It has proved useful for understanding the structure of complex thermoelectric materials like Cu_{1.95}Se [2], battery materials [3], metal-organic frameworks [4] and many other disordered materials.

Conventionally, studies of diffuse scattering have been carried out using synchrotron radiation due to their high brilliance and low wavelength which make them ideal to study weak diffuse scattering. Recently, Schmidt *et al.* [5] and Schmidt *et al.* [6] showed that it was possible to utilize in-house X-ray sources and electron diffraction for studies of diffuse scattering.

In this work (ref. [7]), we present a benchmarking study using a Rigaku XtaLab Synergy-S diffractometer with Mo K $_{\alpha}$ radiation aimed at comparing the in-house diffuse scattering measurements against their synchrotron counterpart. We examine three target systems aimed at examining the strengths and weaknesses of 3D- Δ PDF analysis.

We examine Cu_{1.95}Se with strong diffuse scattering well separated from the Bragg peaks, Nb_{1-x}CoSb with weak diffuse scattering separated from the Bragg peaks, and finally, we test the limits of the method with the weak diffuse scattering of InTe which overlaps with the Bragg peaks.

We observe larger noise as the most prominent difference between the in-house and synchrotron 3D- Δ PDFs, but otherwise are able to assign (most of) the same disorder features in the in-house 3D- Δ PDF, albeit some additional argumentation is needed for some of the examined cases.

Yet, this work clearly shows the potential for in-house measurements of diffuse scattering as a highly available source, making it more accessible as a routine tool, but importantly also as a support to the better synchrotron measurements.

[1] Weber, T. & Simonov, A. (2012). *Zeitschrift für Kristallographie*, **227**, 238-247.

[2] Roth, N. & Iversen, B. B. (2019). *Acta Cryst.*, **A75**, 465-473.

[3] Simonov, A. & Goodwin, A. L. (2020). *Nature Rev. Chem.* **4**, 657-673.

[4] Erhling, S., Reynolds, E. M., Bon, V., Senkovska, I., Gorelik, T. E., Evans, J. D., Rauche, M., Mendt, M., Weiss, M. S., Pöppel, A., Brunner, E., Kaiser, U. & Goodwin, A. L. (2021). *Nature Chem.* **13**, 568-574.

[5] Schmidt, E. M., Neder, R. B., Martin, J. D., Minelli, A., Lemée, M.-H. & Goodwin, A. L. (2023). *Acta Cryst.*, **B79**, 138-147.

[6] Schmidt, E. M., Klar, P. B., Krysiak, Y., Svorá, P., Goodwin, A. L. & Palatinus, P. (2023). *Nature comm.*, **14**, 6512.

[7] Juul, K. O. R., Støckler, K. A. H. & Iversen, B. B. (2025). *Acta Cryst.*, **A81**, 254-268.

Exploring local structure in some oxygen deficient perovskite polymorphs by Total Neutron

Authors: Gabriel Julio Cuello¹; Monica Ceretti²; Werner Paulus³

¹ *Institut Laue Langevin*

² *ICGM CNRS*

³ *ICGM UM*

Oxygen-deficient perovskite oxides have attracted significant attention over the past few decades due to their rich chemistry, structural complexity, intriguing properties and applications, such as ionic conductors, oxygen sensors, and electrocatalysts. Various structures can emerge from the basic perovskite framework, showing different oxygen vacancy orderings or structural distortions. As an example, the brownmillerite structure, with the general formula $A_2BB'O_5$, is formed by releasing one-sixth of the oxygen atoms along the [110] direction of the cubic perovskite. This structure thus consists of alternating octahedral (O) and tetrahedral (T) layers and exhibits orthorhombic symmetry due to the formation of empty one-dimensional oxygen vacancy channels along the [100] direction. Space group attribution can be ambiguous due to subtle structural changes, making it challenging to differentiate between various types of tetrahedral chain ordering and space group symmetries (*Pnma*, *Imma*, and *I2mb*). These structural differences are crucial for interpreting their potential for oxygen ion conductivity, as *Pnma* and *I2mb* result in ordered $(BO_4)_\infty$ tetrahedral chains, while *Imma* leads to an average and potentially disordered orientation, which can be static or dynamic.

Recently, we reported on the oxygen diffusion mechanisms in a novel oxygen-deficient perovskite, Sr_2ScGaO_5 . Depending on the synthesis route, Sr_2ScGaO_5 exhibits two polymorphs: a brownmillerite and a cubic perovskite structure [1-3]. For the brownmillerite-type structure, Pair Distribution Function (PDF) analysis and Rietveld refinements of neutron diffraction data provided identical structural descriptions. However, on a local scale, a brownmillerite-type vacancy structure was observed in the oxygen-deficient cubic polymorph, indicating complex short-range ordering and a distinctive microstructure [4].

In the present study, we aimed to investigate through neutron PDF the local structure of several oxygen-deficient perovskites (Ba_2InFeO_5 , Sr_2ScFeO_5 , Sr_2ScCoO_5), that exhibit both brownmillerite and cubic perovskite configurations depending on the heat treatment. Data have been collected on the D4 disordered materials diffractometer at ILL. Despite the average structures being significantly different, it appears that, on a local scale, the cubic structures show a brownmillerite framework. This suggests that the retention of the brownmillerite-like structure influences the formation of short-range correlations of oxygen vacancies along with B cation ordering, indicating the presence of brownmillerite nanodomains within the cubic phase, which appears to be a persistent feature of oxygen deficient perovskites. In this context, neutron scattering has proven to be indispensable, as it allows for the detailed analysis of oxygen ordering, which is challenging to observe with X-ray diffraction.

[1] S. Corallini, M. Ceretti, G. Silly, A. Piovano, S. Singh, J. Stern, . . . W. Paulus, J. Phys. Chem. C, 119 (2015) 11447-11458.

[2] M. Ceretti, S. Corallini, W. Paulus, Crystals, 6 (2016) 146.

[3] S. Corallini, M. Ceretti, A. Cousson, C. Ritter, M. Longhin, P. Papet, W. Paulus, Inorg. Chem., 56 (2017) 2977-2984.

[4] M. Ceretti, G. Agostini, M. Brunelli, S. Corallini, G. Perversi, G. Cuello, . . . W. Paulus, Inorg. Chem., 59 (2020) 9434-9442

Magnesium silicate hydrate-based cement under repository conditions

Author: Maciej Delekt^{None}

Co-authors: Barbara Lothenbach ; John L. Provis ; Bin Ma ; Sergey Churakov

The disposal of radioactive waste is one of the key challenges for global society. It is widely accepted that deep geological disposal is a safe and reliable solution. Engineered and natural barriers are combined to protect the biosphere from radionuclides and other hazardous chemical species. Cement-based matrices are commonly used to immobilize low- and intermediate-level radioactive wastes, aiming to control radionuclide release through interactions with cement phases [1], [2]. Concretes based on Portland cement (PC) exhibit high pH values, and thus are not in equilibrium with host rocks that have neutral pH. They may be prone to alkali-silica reaction and/or sulfate attack [3]. Magnesium-silicate cements present a promising alternative for PC due to their lower pH, good chemical stability, reduced heat of hydration, and enhanced compatibility with natural clay barriers [4]. Depending on raw material sources, they may offer a lower carbon footprint [5]. Interactions with magnesium silicate hydrates (M-S-H) will control the potential release of radionuclides from these cements [6].

An M-S-H synthesis protocol was established. Higher crystallographic ordering of aged samples was observed. An increase of pH by sodium hydroxide during the synthesis led to a more crystalline structure, as also observed by SEM. Zn doped M-S-H was coprecipitated using a mixture of magnesium and zinc nitrate salts with a sodium silicate solution. XRD revealed that a higher dose of zinc nitrate disrupted M-S-H ordering. Raman spectra showed decrease of peak intensities related to vibrations associated with O-H and Si-O bonds.

This study highlights the potential of magnesium-silica cements as a viable alternative to PC for some applications in radioactive waste immobilization. Changes in synthesis conditions, such as pH and zinc concentration, influence the structural and chemical properties of M-S-H phases. These findings contribute to a deeper understanding of M-S-H systems, paving the way for tailored material designs that optimize long-term waste containment in geological repositories.

[1] J. Arayro et al., “Thermodynamics, kinetics, and mechanics of cesium sorption in cement paste: A multiscale assessment,” *Phys. Rev. Mater.*, vol. 2, no. 5, p. 053608, May 2018, doi: 10.1103/PhysRevMaterials.2.053608.

[2] B. Ma, J. L. Provis, D. Wang, and G. Kosakowski, “The essential role of cement-based materials in a radioactive waste repository,” *npj Mater. Sustain.*, vol. 2, no. 1, pp. 1–8, 2024, doi: 10.1038/s44296-024-00025-9.

[3] J. Tits and E. Wieland, “Radionuclide Retention in the Cementitious Near-field of a Repository for Low- and Intermediate-level Waste: Development of the Cement Sorption Database. Nagra Technical Report 23-07,” 2023.

[4] D. Nied, K. Enemark-Rasmussen, E. L’Hopital, J. Skibsted, and B. Lothenbach, “Properties of magnesium silicate hydrates (M-S-H),” *Cem. Concr. Res.*, vol. 79, pp. 323–332, 2016, doi: 10.1016/j.cemconres.2015.10.003.

[5] E. Bernard et al., “MgO-based cements – Current status and opportunities,” *RILEM Tech. Lett.*, vol. 8, pp. 65–78, Nov. 2023, doi: 10.21809/rilemtechlett.2023.177.

[6] M. R. Marsiske, C. Debus, F. Di Lorenzo, E. Bernard, S. V. Churakov, and C. Ruiz-Agudo, “Immobilization of (aqueous) cations in low pH M-S-H cement,” *Appl. Sci.*, vol. 11, no. 7, 2021, doi: 10.3390/app11072968.

Conference first session / 129

Conference welcome

Tutorial introductions / 156

TOPAS for small box Pair Distribution Function refinements

Author: Philip Chater¹

¹ *Diamond Light Source*

TOPAS is a fast and flexible program for non-linear least squares refinement with a focus on crystallographic analysis of diffraction data. Alongside powder and single crystal diffraction data, TOPAS also allows the refinement of pair distribution function (PDF) data. Helpful tools like restraints, constraints, and rigid bodies can be used within PDF refinements to model local structure of disordered materials.

In this tutorial you will be introduced to TOPAS and its use for PDF data. Participants will be able to select from a range of tutorials to match their level and areas of interest, including:

- Modelling instrumental and processing impacts on the PDF
- Comparing ways of modelling thermal motion effects
- Modelling of nanoparticles
- Joint powder diffraction and PDF refinements
- Modelling of small molecules
- Modelling short- and long-range effects in the same model

34

Effects of sample preparation and synchrotron beamline instrumentation on total X-ray scattering data and their atomic pair distribution functions

Author: Martin Aaskov Karlsen¹

Co-authors: Alexander Schökel¹; Martin Etter¹; Morten Johansen¹; Volodymyr Baran¹

¹ P02.1, PETRA III, DESY

We demonstrate various effects related to sample preparation and synchrotron beamline instrumentation on total X-ray scattering (TXS) data and their derived atomic pair distribution functions (PDFs) for data collected at the Powder Diffraction and Total Scattering Beamline P02.1, PETRA III, Deutsches Elektronen-Synchrotron (DESY), Hamburg, Germany.

Sample preparation aspects include inner capillary diameter and the type of amorphous capillary material. Synchrotron beamline instrumentation aspects include area detector configuration, sample-to-detector distance (SDD), X-ray beam dimensions, capillary spinning, exposure time, and dark validity.

For empty capillaries and capillaries with Ni powder, effects on dark-subtracted total X-ray scattering images, azimuthally integrated total scattering patterns, derived atomic pair distribution functions, and the weighted residual values of PDF refinements are considered. The illustrations herein will create or elaborate on the understanding of various experimental effects on TXS data and their derived PDFs, aiding the planning and conduction of future TXS beamtimes.

38

High-Throughput Orientation Extraction via Symmetry-Adapted Filters

Authors: Caden Myers¹; Morten Eskildsen²; Nathan Chalus²; Simon Billinge¹; Tess Smidt³; Yucong Chen¹

¹ Columbia University

² University of Notre Dame

³ *Massachusetts Institute of Technology*

High-throughput small angle diffraction and imaging experiments on ordered systems generate large two-dimensional datasets that often exhibit some degree of rotational symmetry. Analyzing these datasets can require model-dependent approaches or extensive manual effort to track how features evolve across measurements. In this work, we present an algorithm for rapidly determining the orientation angle of symmetric features using a brute-force angular search. The method employs a symmetry-adapted filter (SAF) that leverages the known symmetry of the data. The orientation angle is determined by first centering the SAF, applying a mask to isolate the symmetric signal, and then rotating the SAF to maximize its inner product with the image. This automated process enables scalable analysis of large image datasets. We demonstrate the SAF algorithm in two applications, (1) extracting the angular velocity from small angle neutron scattering (SANS) of a driven skyrmion lattice in Cu_2OSeO_3 , and (2) mapping local lattice orientations in atomically resolved transmission electron microscopy (TEM) images.

48

Role of Fe, Co and Cu addition in the structural and magnetic properties of Ni-Mn-Ga Magnetic Shape Memory Alloys

Authors: Natalia A. Río-López¹; Patricia Lázpita¹; Anabel Pérez-Checa²; Jorge Feuchtwanger¹; J. Alberto Rodríguez-Velamazán³; Inés Zabala¹; Volodymyr Chernenko¹; Fernando Plazaola¹; Concepción Seguí⁴; Jose M. Porro⁵

¹ *Department of Electricity and Electronics, Faculty of Science and Technology, University of the Basque Country, 48080 Bilbao, Spain*

² *TECNALIA, Basque Research and Technology Alliance (BRTA), Mikeletegi pasealekua 2, 20009 Donostia, Spain*

³ *Institut Laue-Langevin - 71 avenue des Martyrs, CS 20156, 38042 GRENOBLE Cedex 9 - France*

⁴ *Departament de Física, Universitat de les Illes Balears, E07122 Palma de Mallorca, Spain*

⁵ *BCMaterials, Basque Center for Materials, Applications & Nanostructures, 48940 Leioa, Spain*

Magnetic Shape Memory Alloys (MSMAs) have been attracting attention owing to their interesting magnetocaloric and magnetostrictive effects, which serves as the mechanism governing their applicability in solid state refrigerators, sensors and actuators. These effects arise from a huge magnetostructural coupling allowing the magnetic-field induced martensitic transformation from a low symmetry phase at low temperature (martensitic phase) to a high symmetry one (austenitic phase). Consequently, both the structural and magnetic properties and their transitions play a critical role in these functional responses.

The strong correlation between composition, structure and magnetic properties in magnetic shape memory Heusler alloys is well established. Doped Ni-Mn-Ga alloys are particularly compelling due to their high compositional tunability. Within this context, the present work explores the role of Co, Fe and Cu substitution on the crystal structure and magnetic behaviour of three series of alloys ($\text{Ni}_{50}\text{Mn}_{29-x}\text{Ga}_{20}\text{Co}_x$, $\text{Ni}_{50}\text{Mn}_{29-x}\text{Ga}_{20}\text{Fe}_x$, $\text{Ni}_{50}\text{Mn}_{25-x}\text{Ga}_{25}\text{Cu}_x$). Via Powder Neutron Diffraction (PND), the symmetry and atomic site occupancies of both the austenitic and martensitic phases were disclosed. The structural differences were linked to the observed evolution of martensitic transformation temperature -which increase with Co and Cu substitution but decreases with Fe- and to the atomic distribution, correlated with a change in the predominant type of magnetic exchange interactions, thereby affecting the magnetic coupling. While Fe and Co doping enhance ferromagnetic interactions, Cu atoms create the opposite effect, promoting antiferromagnetic ones.

In summary, the results established a clear correlation between dopant concentration, transition temperatures and type of magnetic exchange interactions. Moreover, they underscore the distinct effect associated with each dopant, providing valuable insight into the mechanism behind the finetuning of the actuation temperature range via compositional variations.

A JOINT ACADEMIC-INDUSTRIAL STUDY ON THE ROLE OF FLUORINE IN MOLD CASTING FLUORINE-ALUMINOSILICATE GLASSES

Author: Riccardo Bono¹

Co-authors: Marco Alloni²; Monica Dapiaggi; Riccardo Carli²; Tristan YOUNGS³

¹ *Università degli Studi di Milano*

² *Prosimet SpA*

³ *ISIS Neutron and Muon Source*

Fluorine-aluminosilicate glasses are a key component in the steel casting to prevent the solidifying steel to stick to the mould walls by creating a thin lubricant layer between the two. These glasses are obtained from the melting of mould powders for continuous casting once they are poured on the solidifying steel. The standard powders have fluorine as fluidifying agent but, since this is corrosive for machineries [Salvadore and Zimmerman, 1976], efforts are focused on finding an alternative that could replace it. The samples and experimental conditions of this study were set up in collaboration with Prosimet SpA, a private company reference partner for world steel industry, interested in better understanding these systems to ameliorate their industrial applications. To do this, it is important to understand the role of fluorine in combination with the other network formers or modifiers components in the disordered structure of the glasses. Pair Distribution Function is the key method to achieve this aim thanks to its proven feasibility to describe local structure of a disordered material. Given the fact that the composition of these glasses is characterized by a non negligible amount of light elements, PDF calculations were based both on X-rays and neutron diffraction from synchrotron experiments at ESRF (ID11) and ISIS (NIMROD) respectively. These data were elaborated with the software EPSR26 [Soper, 2012] which allowed to create a simulation of a 50000 atoms cell replicating a reliable configuration of atoms comparable to the one present in the glasses. For this reason, all the results concerning the coordination numbers, the bond lengths and the medium range order were ascribable, with a great confidence, to the analysed glasses too. The results showed that, concerning coordination numbers, fluorine seems to interfere with a normal Si-O tetrahedron by likely substituting one oxygen, while calcium (another network modifier) maintained a larger distribution with coordination numbers spacing from 4 to 6. Concerning the bond length, deduced from the peaks of the partials of the PDF function, it was determined that an increase in fluorine percentage causes a stretching of the Si-F and Si-O tetrahedrons. An increase in calcium, on the other hand, can cause a weak modification of Al-F and Si-F bond but a remarkable decrease of its own coordination polyhedrons. Moreover, the presence of secondary peaks in the partial functions, with a smaller order of magnitude than the main ones used to determine the principal bond length, showed the presence of a medium range order. This can be said since they indicate the existence of a second set of bond distances, greater than the ones already discussed, not influenced by the variation of single elements. From these first results, it was also possible to correlate the basicity index (i.e. Ca/Si ratio) to a clustering of the Ca-cations which seems to be the key factor for the crystallization of cuspidine ($\text{Ca}_8(\text{Si}_2\text{O}_7)_2\text{F}_4$) from the amorphous material [Carli et al., 2022]. This phase has a great influence in the heat exchange between the steel and the mould affecting the quality of the final product. In conclusion, the results of this work indicate that fluorine, but also calcium, have an influence especially on the bond length of the network forming elements and of Ca itself, opening the path to find possible alternatives to fluorine allowing an improvement in steel casting industry and in the knowledge of these useful systems.

References:

- Salvadore, E. A., & Zimmerman, P. J. (1976). U.S. Patent 3,937,269.
- Soper, A. K. (2012). Empirical Potential Structure Refinement.
- Carli, R., Alloni, M., Martino, G., & Wunderlich, O. (2022). Triggering crystallization in mold flux slag. *La Metallurgia Italiana*, 6.

Author: Julie Brun¹

¹ *University of Oslo*

We want to study the formation of the polymorphs with XAS and PDF :)

69

Intermediate-range order in glassy oxide materials revealed by topological analyses

Author: Yohei Onodera¹

¹ *National Institute for Materials Science*

The structural analysis of glassy materials remains a challenging topic in materials science, primarily due to the absence of long-range order. However, a combination of quantum beam (X-ray/neutron) diffraction measurements, computer simulations, and advanced topological analyses [1,2] focused on rings, cavities, and homologies, enables the investigation of intermediate-range order [3–6], which exists on a length scale larger than atomic bond lengths in glassy materials.

In this presentation, we focus on the intermediate-range order in glassy oxide materials. In particular, recent research in silica [7] and silicate [8] glasses is highlighted, where it was found that topology is a significant structural feature for understanding structure–property relationships in glassy materials. Furthermore, a recent work on the formation of a zirconium oxide crystal nucleus in the initial nucleation stage in aluminosilicate glass-ceramics investigated by anomalous X-ray scattering is addressed [9].

References

- [1] Y. Onodera *et al.*, *J. Ceram. Soc. Jpn.*, **127**, 853 (2019).
- [2] S. Kohara *et al.*, *J. Ceram. Soc. Jpn.*, **132**, 653 (2024).
- [3] A. C. Wright and A. J. Leadbetter, *Phys. Chem. Glasses*, **17**, 122 (1976).
- [4] J. C. Philips, *J. Non-Cryst. Solids*, **43**, 37 (1981).
- [5] D. L. Price *et al.*, *J. Phys. C. Solid State Phys.*, **21**, L1069 (1988).
- [6] P. S. Salmon *et al.*, *Nature*, **435**, 75 (2005).
- [7] Y. Onodera *et al.*, *NPG Asia Mater.*, **12**, 85 (2020).
- [8] Y. Onodera *et al.*, *NPG Asia Mater.*, **11**, 75 (2020).
- [9] Y. Onodera *et al.*, *NPG Asia Mater.*, **16**, 22 (2024).

64

Synthesis, properties and local structure analysis of the mineral strätlingite

Author: Artem Shevchenko¹

Co-authors: Igor Moudrakovski¹; Maxwell Terban; Robert Dinnebier¹; Sebastian Bette¹

¹ *Max Planck Institute for Solid State Research*

Disordered naturally occurring minerals are not a novelty, and are, in fact, known since the development of conventional crystallography and usually are treated using fractional occupancies and split atomic positions. But when it comes to qualitative and (semi)quantitative phase analysis of the nanosized materials, conventional crystallography fails, and alternative structure-sensitive methods must be employed.

In this work we synthesize and characterize the mineral strätlingite ($\text{Ca}_2\text{Al}_2\text{SiO}_2(\text{OH})_{10} \cdot 2.25\text{H}_2\text{O}$), that, based on the crack propagation analysis, is believed to be a key component, contributing to the long-term mechanical stability of the Roman concrete.¹ Strätlingite could be classified as a phyllosilicate due to its layered structure, composed of positively charged brucite-like layers $[\text{AlCa}_2(\text{OH})_6]^+$, and negatively charged double-tetrahedra (DT) layers $[\text{AlSiO}_2(\text{OH})_4]^-$. It exhibits a well-defined long-range order that is described by the space group, but the occupational Si/Al disorder and around 50% of vacancies within the DT-layer represents a local structure that is not fully captured by the average long-range model.

Here we focused on analysis of the defects correlation in the DT-layer using solid-state NMR spectroscopy data and PDF modelling, employing and evaluating various structural models that agree with complementary analytical methods and are chemically reasonable. Based on that, we have proposed a deformed double six-member Si rings with Q3(3Al) configuration as a representation of the local structure of the DT-layer. The additional deformation along the c-axis accounts for the variation in the interplanar d00l distance, which is reflected in the observed anisotropic diffraction peak broadening and provided more realistic Si-O-Si angle in the DT-layer compared to the one in the average model.

[1] M. D. Jackson, E. N. Landis, P. F. Brune, M. Vitti, H. Chen, Q. Li, M. Kunz, H. R. Wenk, P. J. M. Monteiro and A. R. Ingraffea, Proc. Natl. Acad. Sci. U. S. A., 2014, 111, 18484–18489.

56

scikit-package - software packaging standards and roadmap for sharing reproducible scientific software

Authors: Andrew Yang¹; Caden Myers¹; Sangjoon Lee¹; Simon Billinge¹; Tieqiong Zhang¹

¹ *Columbia University*

Scientific advancement relies on the ability to share and reproduce results. When data analysis or calculations are carried out using software written by scientists there are special challenges around code versions, quality and code sharing. scikit-package provides a roadmap to facilitate code reuse and sharing with minimal effort through tutorials coupled with automated and centralized reusable workflows. The goal of the project is to provide pedagogical and practical tools for scientists who are not professionally trained software engineers to write more reusable and maintainable software code. Code reuse can occur at multiple levels of complexity—from turning a code block into a function within a single script, to publishing a publicly installable, fully tested, and documented software package scikit-package provides a community maintained set of tools, and a roadmap, to help scientists bring their software higher levels of reproducibility and shareability.

28

Fast Simulation of Disordered Crystals Using Gaussian Copulas

Author: Arkadiy Simonov¹

¹ *ETH Zurich*

Substitutional disorder is ubiquitous in crystalline materials, from proteins to metal-organic frameworks, yet generating physically realistic disordered structures remains computationally challenging. We present a novel algorithm that employs Gaussian copulas to rapidly generate realizations of disordered crystal structures consistent with experimentally observed diffuse scattering patterns. The method works by first generating correlated Gaussian random variables with a carefully chosen covariance matrix, then applying thresholding to transform these into discrete site occupancies. For

binary disorder with equal probabilities, the relationship between Gaussian and binary correlations follows the analytical arcsin law, enabling straightforward implementation. The approach directly utilizes pairwise correlations obtained from 3D- Δ PDF refinement of diffuse scattering data, providing and provides both a generation method for the real structure in real space and a simple check whether correlation matrix from 3D- Δ PDF is admissible.

Our algorithm offers significant computational advantages over traditional Monte Carlo and Reverse Monte Carlo simulations, requiring only the generation of Gaussian random variables and a single FFT operation for periodic systems. We demonstrate the method on experimental diffuse scattering from various crystals. The technique naturally extends to non-equal probability distributions and multi-state disorder through modified thresholding schemes. By bridging mathematical techniques from signal processing and statistical modeling with crystallographic applications, this work provides crystallographers with a practical, efficient tool for modeling disordered materials that is implementable in just a few lines of code.

51

Real-time observation of rapid densification and degradation in flash sintered multilayer systems for battery materials

Author: Riku FUKADA¹

Co-authors: Maria DIAZ-LOPEZ²; Marlu César Steil³; Renaud Bouchet³; Timothée Fabre³; Claire Colin⁴

¹ Institut Néel

² Institut Neel

³ LEPMI UMR 5279-Grenoble INP

⁴ Institut Néel, CNRS & Université Grenoble Alpes

With increasing demand for advanced energy storage, cost-effective and efficient production of all-solid-state batteries (ASSBs) is critical for sustainable, low-waste energy solutions. ASSBs offer enhanced safety, higher energy density, and improved durability due to their solid electrolytes. However, conventional fabrication methods are costly, energy-intensive, and often yield poor interfacial contact, limiting commercial scalability. Advanced sintering techniques such as spark plasma sintering (SPS), cold sintering (CS), and flash sintering (FS) have emerged as promising alternatives. Flash sintering, in particular, significantly reduces sintering times from hours to seconds and greatly lowers energy consumption, aligning with circular economy principles.

In this study, we explore the fundamental mechanisms of electrochemical flash sintering (EFS) in model multilayer all-solid-state architectures composed of a $\text{Li}_{1.4}\text{Al}_{0.4}\text{Ti}_{1.6}(\text{PO}_4)_3$ (LATP) electrolyte and $\text{Li}_3\text{V}_2(\text{PO}_4)_3$ (LVP):LATP composite electrodes sandwiching an LATP layer.[1,2] Using total scattering (Bragg + Pair Distribution Function), we spatially mapped structural evolution to capture the formation of hotspots, localized regions of intense Joule heating that drive particle cracking and phase decomposition on sub-second timescales. In-situ total scattering experiments performed with the newly commissioned ARC detector at the i15-1 beamline (Diamond Light Source) achieved millisecond temporal resolution, allowing direct observation of both local and mesoscale structural dynamics. These measurements revealed the rapid formation of a transient amorphous intermediate that crystallizes within seconds, providing new insight into metastable states previously inaccessible to observation. Together, these findings elucidate how localized electrochemical and thermal processes drive densification and interfacial reactions in materials relevant to solid-state batteries, enabling assessment of whether EFS can effectively improve interfacial contact in future ASSSB architectures. Our use of ultra-fast total scattering thus establishes a framework for understanding reaction fronts and transient interfaces in electrochemically driven sintering across broader functional materials systems.

References :

- [1] Lachal, M., El Khal, H., Bouvard, D., Chaix, J.-M., Bouchet, R. & Steil, M. C. (2021). Journal of the American Ceramic Society 104, 3845–3854.
- [2] Fukada, R., Colin, C. V., Fabre, T., Steil, M. C., Bouchet, R. & Diaz-Lopez, M. (2025). Manuscript submitted.

Short-Range Order in Water and Amorphous Ice

Author: Neta Ellert¹

Co-authors: Eyal Yahel²; Guy Makov¹

¹ *Materials Engineering Department, Ben-Gurion University of the Negev, 84105 Beer-Sheva, Israel*

² *Physics Department, Nuclear Research Centre-Negev, 84190 Beer-Sheva, Israel*

While the crystalline structure of solids is well-known, the molecular arrangement in liquids and amorphous solids, often overlooked, presents a fascinating and intricate subject of study. The structural characteristics of these systems shed light on their unique properties and the implications for a variety of scientific disciplines. Our study aims to explore the Short-Range Order (SRO) in water and amorphous ice, throughout the Quasi-Crystalline Model (QCM). This is an approach that aims to reveal the underlying SRO of a given Radial Distribution Function (RDF) by a comparison with a mathematical RDF generated from a reference lattice. To study the structural characteristics of water and amorphous ice systems, classical Molecular Dynamics (MD) simulations were carried out to compare with experimental data from the literature. In the case of the amorphous ice states, it was found that the Low-, High-, and Very High- density amorphous ices are distinct not only in their densities, but also in their SRO with an ice Ih- like, an ice III- like, and an ice II- like structures. In the liquid phase, thermodynamic conditions such as temperature and pressure affect the SRO obtained.

Structural evolution of Tungsten Oxide Network during WO₃.H₂O formation

Author: Capucine Sassoye¹

Co-authors: Charles Sidhoum ; Clara DOISNEAU¹; Clement Sanchez ; Ovidiu Ersen

¹ *Sorbonne Université*

Tungsten Oxides (WO_x) are well known for their versatile structures and properties (photo and electro-catalysis, electrochromism, energy storage...), often enhanced at nano-scale, leading to broad applications (smart windows, pollutant degradation...). [1-2] Tungsten Hydrate WO₃·H₂O is here prepared at room temperature using sol-gel synthesis: The initial Decatungstate W₁₀O₃₂4- evolves to amorphous gels, and within few days, toward crystalline WO₃·H₂O powder. [3]

We focus on the pathway from corner and edge sharing WO₆ octahedra W₁₀O₃₂4- clusters to only corner sharing WO₆ octahedra WO₃·H₂O structure, using X-ray Total scattering diffraction coupled to Pair Distribution Function analysis (ID11, ESRF).

PDF curves show short range organization for the amorphous gels. A Machine Learning-Motif Extractor (ML-MotEx) [4] code was used to determine the structural features of the 2h gel. Indeed, this code allows to extract, from a given model, the atoms contributing positively or negatively on the fit results. For the 24h gel, a clusters approach has enabled us to propose a checkerboard finite features that can be seen as early nucleation of the final hydrate WO₃ structure.

PDF refinement on the final powder clearly shows that the use of the usual crystalline Pnmb WO₃·H₂O structure on the entire distance range (1.4–60Å) is not sufficient. Implementing sequential fit in r series has led to the description of two zones: Short Range Order (SRO) for 1.4-20 Å, and Long Range Order for 20– 60Å. Separate refinements, as it has been proposed by Juelsholt et al. [5], show a distorted P1 SRO structure whereas it remain close to the published Pnmb WO₃·H₂O for LRO.

[1] Y. Li et al., Nat. Commun., 6(1), 8064 (2025) <https://doi.org/10.1038/ncomms9064>.

[2] J. Besnardiere et al., Nat. Commun., 10(1), 327 (2019) <https://doi.org/10.1038/s41467-018-07774-x>

- [3] C. Sidhoum et al., Chem. Mater., 37, 5454 (2025) <https://doi.org/10.1021/acs.chemmater.4c03003>
- [4] A. S. Anker et al. npj Comput. Mater. 8, 213 (2022) <https://doi.org/10.1038/s41524-022-00896-3>
- [5] M. Juelsholt et al. J. Phys. Chem. C, 123, 5110 (2019) <https://doi.org/10.1021/acs.jpcc.8b12395>

110

Nature of short-range incommensurate magnetic order in $\text{YBa}_2\text{Cu}_3\text{O}_{6+x}$

Author: Toshinao Loew¹

¹ Max Planck Institute for Solid State Research, Stuttgart, Germany

High- T_c superconductivity in copper oxides arises from antiferromagnetic Mott-insulating parent compounds upon doping. In the $\text{YBa}_2\text{Cu}_3\text{O}_{6+x}$ system, short-range incommensurate magnetic order is present for $x < \sim 0.5$, below a critical hole doping level for static magnetism, $p_c \sim 0.09$. We present a detailed neutron scattering study of the evolution of static magnetic correlations with hole-doping. Our results indicate the presence of diminishing three-dimensional spin correlations up to p_c . We find that superconducting $\text{YBa}_2\text{Cu}_3\text{O}_{6.4}$ ($p = 0.07$, $T_c = 20$ K) exhibits both commensurate and incommensurate magnetic reflections that are intimately related, corresponding to a three-dimensionally ordered state which evolves with a single temperature dependence. Polarization analysis indicates that the magnetism has a dominant unidirectional component, which can be understood in terms of an amplitude modulated structure. We discuss how this might be related to the stripe ordering phenomenon found in other cuprates such as $\text{La}_{2-x}\text{Ba}_x\text{CuO}_4$.

92

Pair Distribution Function analysis applied to the study of ancient Roman mortars

Author: Laura Calzolari¹

Co-authors: Laura Medeghini²; Silvano Mignardi²; Alejandro Fernandez-Martinez³

¹ Université Grenoble Alpes

² Department of Earth Sciences, Sapienza University of Rome

³ ISTerre, Université Grenoble Alpes, Université Savoie Mont Blanc, CNRS, IRD, Université Gustave Eiffel

Ancient Roman aqueducts are engineering structures that maintained their avantgarde record until the 19th century [1]. The archaeometric characterization of the materials used for their construction helps in unveiling the technological level reached by ancient Romans, investigating the factors that lead to this millenary resistance and experimenting with new approaches for cement production recovering a lost knowledge (which is the aim of DAPHNE, MSCA-PF n. 101209231). Our work focuses on the characterization of hydraulic mortars from inner ducts of aqueducts and cisterns that were built for the ancient city of Rome. The archaeometric investigation of these materials using the most applied techniques in the field, such as optical microscopy (OM), X-ray powder diffraction (XRPD) and scanning electron microscopy (SEM-EDS), revealed the presence of a diffuse amorphous/nanocrystalline binder in some of the samples coming from still working aqueducts (*Aqua Virgo* and *Aqua Traiana*)[2,3], which is anomalous respect to what the literature reports so far concerning hydraulic Roman mortars [4]. To understand the structure and properties of this binder, Pair Distribution Function analysis (PDF) has been chosen, as it exploits diffuse scattering [5]: to our knowledge, this is its first application for the study of ancient Roman mortars. PDF analysis has been calculated from X-ray diffraction patterns of binder fraction ($< 63 \mu\text{m}$) obtained at beamline ID22 of the European Synchrotron Radiation Facility (ESRF). The diffractograms have been interpreted to determine if residual crystalline phases were present. Then, their contribution has been

subtracted from the diffraction pattern, using PDFgui, to isolate the signal from the amorphous and nanocrystalline phases. Final interpretation shows the compatibility of the amorphous phase with amorphous Si and C-A-S-H, a hydraulic compound present also in nowadays cement, and presence of nanocrystalline phillipsite, clinotobermorite and/or strätlingite, as attested in other ancient Roman mortars [6].

References:

1. Wilson, A. I. Hydraulic Engineering and Water Supply. in *The Oxford Handbook of Engineering and Technology in the Classical World* 285–318 (Oxford University Press, Oxford, 2008).
2. Calzolari, L., Amadasi, M. E., Medeghini, L. & Mignardi, S. Insights on the Mortars of Ancient Roman Aqueducts: Aqua Virgo and Aqueduct Y, Rome (Italy). *Buildings* 14, 69 (2024).
3. Medeghini, L. et al. The secret of ancient Roman hydraulic mortar: the lesson learnt from the past for future cements. *Cem. Concr. Compos.* 148, 105484 (2024).
4. Torraca, G. *Lectures on Materials Science for Architectural Conservation*. (Getty Conservation Institute, 2009).
5. Egami, T. & Billinge, S. J. L. *Underneath the Bragg Peaks: Structural Analysis of Complex Materials*. (Newnes, 2012).
6. Elsen, J., Jackson, M. D. & Ruiz-Agudo, E. Historic Concrete Science: Opus Caementicium to “Natural Cements”. *Elements* 18, 301–307 (2022).

103

Unravelling Nucleation in Pt Atomic Layer Deposition Using Grazing Incidence X-ray Total Scattering, Grazing Incidence Small-Angle X-ray Scattering, and X-ray Fluorescence

Author: Kinanti Hantiyana Aliyah¹

Co-authors: Jorden De Bolle¹; Robin Petit¹; Martin Rosenthal²; Stefano Checchia²; Christophe Detavernier¹; Matthias Filez¹; Jolien Dendooven¹

¹ Ghent University

² ESRF

Atomic layer deposition (ALD) of metals is typically nucleation-controlled. Initially, 3D nanoislands/nanoparticles (NPs) form. They grow and eventually coalesce to create a continuous thin film as the number of ALD cycles increases. To achieve a continuous layer at a lower thickness, which is important for applications in the semiconductor industry [1], a higher nucleation density is needed. Existing research predominantly emphasizes NP size and coverage during the later stages of nucleation (where size > 4 nm). However, the current state-of-the-art lacks comprehensive insights into the initial stages of nucleation and the atomic 3D structure of NPs, thereby limiting controllability. This study aims to investigate the early stages of nucleation, within a length scale of < 10 nm, with multi-modal X-ray methods in grazing incidence geometry.

X-ray total scattering, used to derive the pair distribution function (PDF) in grazing incidence geometry (GIPDF), is a recent development for studying the structure of thin films.[2] The main benefit of the total scattering method for this work is its sensitivity to the length scales manifested in the early stages of nucleation, specifically size < 4 nm. Pt NPs deposited on fused silica with conventional/thermal ALD (MeCpPtMe₃-O₂) at varying, relatively low loadings (<5 monolayers equivalent) were fabricated and subjected to grazing incidence X-ray total scattering measurements at ID15A, ESRF. Additionally, Pt NPs on fused silica fabricated with enhancement strategies [3,4], aiming to achieve a higher nucleation density, were also investigated and compared to conventional ALD. Total scattering intensity profiles were transformed into PDFs after subtracting background/substrate contributions, then fitted using the attenuated-crystal (AC) spherical model to determine the NPs' size.

To verify the structural information obtained from the PDFs, grazing incidence small-angle X-ray scattering (GISAXS) patterns were collected at BM26, ESRF, and simulated to determine the width, height, and center-to-center distance of the nanoparticles. Length scales accessible by GISAXS complement GIPDF: GIPDF is ideal for lower Pt loadings, while GISAXS is sensitive at higher loadings

(where size > 4 nm). In conjunction with GISAXS measurement, Pt loadings (# atoms/cm²) were extracted from the Pt fluorescence line obtained via X-ray fluorescence (XRF). Combined, these X-ray techniques provide a window into the early stages of nucleation, advancing our understanding and paving the way for better control of nucleation density.

References:

- [1] George, S. M. et al. Chem. Rev. 110, 1, 111-131 (2009)
- [2] Dippel, A.-C. et al. IUCr, 6, 290-298 (2019)
- [3] de Paula, C. et al. Chem. Mater. 32, 315-325 (2020)
- [4] Juan Santo Domingo Peñaranda. Doctoral Thesis (2024)

108

Multi-doped Cu catalysts: How the additional doping changes the exsolution behaviour

Author: Hedda Drexler¹

Co-authors: C. Rameshan¹; F. Schrenk¹; J. Michalke¹; J. Rollenitz¹; L. Lindenthal¹; M. Groß¹; T. Berger¹; T. Ruh¹

¹ Chair of Physical Chemistry, Technical University of Leoben, Austria

The important role of Copper (Cu) catalysts for the conversion of CO₂ to methanol (MeOH) is already well-known [1,2], but for a viable industrial application further improvement must be done. As literature describes the promoting effect of another element (e.g. Zn) and / or the support [3], bi-metallic and / or multi-phased nanoparticles could be a solution.

Perovskite-type oxides (ABO₃) provide the possibility of doping with multiple elements on the B-site, which can be exsolved in the form of catalytically active, evenly distributed nanoparticles under reducing conditions [4]. With an additional oxygen-rich host which prevents coking, these materials are promising catalysts in CO₂ utilisation reactions [5].

To gain insight into the exsolution behaviour of Cu containing perovskites in the context of methanol synthesis, several multi-doped perovskites oxides (Nd_{0.7}Ca_{0.3}Fe_{0.9}Cu_{0.05}M_{0.05}O_{3-δ}, M = Co, In, Mn, Zn, Zr, named: NC30F-Cu5M5) were synthesised via the modified Pechini-method. Temperature Programmed Reduction (TPR), and (in-situ) powder X-Ray Diffraction (pXRD) experiments (in-house or synchrotron-based) reveal influences on the exsolution temperature, phase purity, and phase transitions of the different materials. Reduction experiments at different temperatures to trigger nanoparticle (NP) formation are compared.

Complementary techniques reveal differences in the oxygen vacancy formation, oxidation states and exsolution temperatures. Phase changes are analysed via Rietveld refinement. Also, the dopant element (M) has an influence on shape and size of the nanoparticles. Understanding the effect of the dopant element M on the exsolution behaviour enables controlled formation of nanoparticles already at lower temperatures, thus making CCU applications, e.g. MeOH synthesis more applicable.

This research was funded by the Austrian Science Fund (FWF) [10.55776/COE5] (Cluster of Excellence MECS). We acknowledge DESY (Hamburg, Germany), a member of the Helmholtz Association HGF, for the provision of experimental facilities. Parts of this research were carried out at PETRA III, and we would like to thank Martin A. Karlsen for his assistance in using P02.1. The beamtime was allocated for proposal I-20240893 EC.

References

- [1] A. Álvarez et al., Chem. Rev. 2017, 117, 9804–9838
- [2] O. Martin et al., Angew.Chem. Int.Ed. 2016, 55,6261–6265
- [3] N. J Azhari, et. al., Results in Engineering 16 (2022) 100711
- [4] D. Neagu et al., Nat Commun., 2015, 6:8120
- [5] L. Lindenthal et al., Appl. Catal. B Environ., 2021, vol. 292, p. 120183

Understanding local structure and dynamics in Prussian blue analogues

Author: Elodie Harbourne¹

Co-authors: Andrew Goodwin¹; David A. Keen²

¹ University of Oxford

² Rutherford Appleton Laboratory

Prussian blue analogues (PBAs) are an important and compositionally diverse class of hybrid frameworks with applications spanning a variety of different fields, including potassium-ion cathode materials and gas storage [1,2]. PBAs can contain a wide variety of different distortions and defect structures, including correlated octahedral tilts, Jahn–Teller (JT) distortions, and hexacyanometallate vacancies [3]. Gaining a better understanding of the interplay of the different distortion mechanisms is therefore important when seeking to optimise the performance of functional PBA materials.

Transition-metal hexacyanoplatinates, $\text{MPt}(\text{CN})_6$, are a compositionally simple subfamily of PBAs that are of interest due to their negative thermal expansion (NTE) behaviour [4]. We used a combination of X-ray pair distribution function (PDF) measurements, lattice dynamical calculations, and ab initio density functional theory (DFT) calculations to study the local structure and dynamics in various $\text{MPt}(\text{CN})_6$ PBAs. In order to link directly the local distortions captured by the PDF with the lattice dynamics of this family, we developed and applied a new Monte Carlo-driven, ‘interaction-space’ PDF refinement approach based on the optimisation of harmonic force constants, from which the (experiment-derived) low-energy phonon dispersion relations could be approximated [5]. Calculation of the corresponding Grüneisen parameters allowed us to identify correlated octahedral tilts as the key modes responsible for NTE in these materials.

Next, we sought to understand what rules might govern cooperative Jahn–Teller (CJT) order in PBAs. A simple model governing CJT order, based on the competition between strain and crystal-field stabilisation that can account for the extent of CJT order, crystallite strain, and stability measured experimentally, was developed [6]. This model shows how PBA compositions might be tuned in order to control the emergence and nature of CJT effects. Access to coarse-grained representations of JT orientations in JT-dilute and/or partially-vacant PBAs then allowed us for the first time to construct atomistic models of the local structure in these systems using the ‘interaction-space’ PDF refinement approach developed previously on the NTE PBAs.

References

- [1] Dhir, S.; Wheeler, S.; Capone, I.; Pasta, M. *Chem.* **2020**, *6*, 2442.
- [2] Kaye, S. S.; Long, J. R. *J. Am. Chem. Soc.* **2005**, *127*, 6506.
- [3] Cattermull, J.; Pasta, M.; Goodwin, A. L. *Mater. Horiz.* **2021**, *8*, 3178.
- [4] Chapman, K. W.; Chupas, P. J.; Kepert, C. J. *J. Am. Chem. Soc.* **2006**, *128*, 7009.
- [5] Harbourne, E. A.; Barker, H.; Guérault, Q.; Cattermull, J.; Nagle-Cocco, L. A. V.; Roth, N.; Evans, J. S. O.; Keen, D. A.; Goodwin, A. L. *Chem. Mater.* **2024**, *36*, 5796.
- [6] Harbourne, E. A.; Cattermull, J.; Boström, H. L. B.; Witte, R.; Roth, N.; Pasta, M.; Keen, D. A.; Goodwin, A. L. arXiv:2408.13169

Preparation and characterisation of Fe-based alloys prepared by mechanical alloying

Author: Ravneet kaur¹

Co-authors: Konrad Kosiba²; Jozef Kovac³; Pavel Diko³; Jozef Bednarčík⁴

¹ P.J. Safarik University in Kosice Slovakia

² *Leibniz Institute for Solid State and Materials Research, Institute of Material Chemistry, Helmholtzstr. 20, 01069 Dresden, Germany*

³ *Institute of Experimental Physics, Slovak Academy of Sciences, Watsonova 45, 040 01 Košice, Slovakia*

⁴ *P.J. Safarik University in Kosice, Faculty of Science, Institute of Physics*

Mechanical alloying (MA) was used to synthesize a series of alloys in powder form with the nominal composition $\text{Fe}_{73.5-x}\text{Mn}_x\text{Cu}_1\text{Nb}_3\text{Si}_{13.5}\text{B}_9$ ($x = 2, 4, 6, 8, 10$ at. X-ray diffraction (XRD) analysis confirmed a transition from

81

NiAl layered double hydroxides as precursor for Ni/Al₂O₃ catalysts for CO₂ methanation

Author: Nisrine Akarai^{None}

Co-authors: Fabio Manzoni ; Felix Egger¹; Mirijam Zobel

¹ *Institute of Crystallography, RWTH-Aachen University*

Ni/ γ -Al₂O₃ catalysts are widely used for CO₂ methanation due to their outstanding activity and stability. Catalysts derived from NiAl-Layered Double Hydroxide (LDH) exhibit well dispersed Ni nanoparticles with a strong metal-support interaction contributing to the activity and stability of the catalyst. [1] To study the correlation of the LDH structure and Ni loading, different samples of Ni_xAl_y(CO₃)-LDH/ γ -Al₂O₃ were synthesized for 10, 15, 20 and 30 wt.% Ni on different commercial alumina supports, following a deposition-precipitation with urea as precipitating agent.[2] From powder X-ray diffraction (PXRD), we identify the formation of the takovite phase Ni₆Al₂(CO₃)(OH)₁₆ · 4H₂O, observing a change in crystallinity and basal spacing for varying nickel loading. This matches our results from N₂ physisorption and thermogravimetric analysis coupled with mass spectrometry (TGA-MS), revealing three major processes during heating: dehydration, dihydroxylation and decarbonation of the LDH. The catalyst formation via calcination and activation was ultimately studied by in-situ PDF experiments at Diamond Light Source (Didcot, UK). The PDF analysis revealed a progressive collapse of the LDH structure, evidenced amongst others via the decrease in both the basal M–M and in-plane M–M peaks characteristic of the Takovite structure, and a shift of the M–O peak toward lower r indicative for the dihydroxylation of the brucite-like layers and the increasing contribution of Al–O associated with the alumina support. Such in-depths studies of the structural evolution of catalyst precursors phases to the final catalyst are important to achieve a better understanding of how Ni nanoparticle dispersion is controlled via phase transformations to prepare methanation catalysts stable under dynamic operation conditions.

[1] H.Schaper, D.J. Amesz, E.B.M. Doesburg, P.H.M. de Korte, J.M.C. Quartel, L.L. van Reijen, *Applied Catalysis* 1985, 16, 417-429

[2] B. Mutz, A.M. Gänzler, M. Nachtegaal, O. Müller, R. Frahm, W. Kleist, J.D. Grunwaldt, *Catalysts* 2017, 7, 279

66

Investigating preferential adsorption of N₂ from the air in Zeolite 13X using total neutron scattering

Author: Marta Falkowska¹

Co-author: Daniel Bowron²

¹ *University of Manchester / ISIS Neutron and Muon Source*

² *ISIS Neutron and Muon Source*

Medical oxygen concentrators (MOCs) utilise pressure swing adsorption to produce oxygen with ~88–92 vol% purity from ambient air. In this process a nitrogen-selective zeolite, most commonly molecular sieve 13X, is first used to adsorb nitrogen from an inlet stream of air at higher pressure (approx. 4 bar), and then subsequent adsorbent regeneration is achieved by passing the air through the sieve at lower pressure (below 1 bar).[1] By operating in fast adsorption-desorption cycles, the machines can produce a continuous stream of oxygen used in oxygen-therapies often prescribed for patients with deprived breathing capabilities.[2]

It has been suggested that the preferential adsorption of nitrogen from the air when compared to oxygen on the 13X molecular sieves is caused by the difference in the quadrupole moment of these two molecules, and the fact that for nitrogen it is three times higher than for oxygen.[3] Consequently, the affinity of nitrogen molecules to the electrostatic field of the zeolite is greater than for oxygen, and results in their enhanced adsorption from the air. Even higher adsorption of nitrogen can be achieved when the Na⁺ ions present in the zeolite 13X framework are exchanged for Ca²⁺ or Li⁺. [1,4]

To gain deeper insights, we conducted total neutron scattering experiments (TNS) to directly probe the molecular arrangement of adsorbates within zeolite 13X under varying pressure conditions. TNS has been proven to be an exceptional experimental tool for gaining insight into the local environment of liquids (e.g. water, benzene)[5,6] and gases (e.g. nitrogen, oxygen, methane) contained within pores of porous media such as MCM-41, and without making crystallographic assumptions.[7,8] Our research contributes to the molecular-level understanding of nitrogen adsorption from synthetic air in zeolite 13X (with Na⁺ and Ca²⁺), a critical step in the conscious design of gas-separating solutions.[9] The focus on TNS provides a novel perspective on the behaviour of gases (N₂, O₂, CO₂ and N₂/O₂ mix) within zeolite 13X pores, offering valuable experimental insights for the enhancement of gas separation processes in healthcare applications.

References:

1. Ackley, *Adsorption* 2019, 25, 1437.
2. Pan et al., *J. Nanomater.* 2017, 7, 195.
3. Buckingham et al., *JACS* 1968, 90, 3104.
4. E.g. Wu et al., *Eng. Ind. Eng. Chem. Res.* 2016, 55, 4676.; Richards et al., *J. Porous Mat.* 1995, 2, 43.
5. Mancinelli et al., *J. Phys. Chem. B* 2009, 113, 50, 16169.
6. Falkowska et al., *Angewandte Chemie International Edition Engl.*, 2018, 57, 4565.
7. Soper et al., *Chem. Phys. Lett.* 2017, 683, 529.
8. Soper et al., *J. Chem. Phys.* 2021, 154, 184503.
9. Falkowska et al., *Adsorption* 2025, 31, 86.

Acknowledgements:

The authors would like to thank Gemma Draper and Mark Kibble for their help in preparing the experimental setup at ISIS. The authors would also like to acknowledge the ISIS neutron and muon source for awarding the beam time RB2200307.

10

Structure of Liquid and Amorphous Materials using Pair-Distribution Function Analysis

Author: Philip Stephen Salmon¹

¹ *University of Bath*

The atomic-scale structure of liquids and glasses is a prerequisite for understanding their material properties. There is an absence, however, of translational periodicity that leads to the Bragg peaks observed in the diffraction pattern for a crystal. Instead, the diffraction pattern is diffuse, and it is a challenge to solve the structure.

In this talk I will outline the theory necessary for understanding the X-ray and neutron diffraction patterns that are measured for structurally disordered materials, and show how these patterns can be used to obtain real-space structural information in the form of partial pair-distribution functions $g_{\alpha\beta}(r)$ [1,2]. Attention will be paid to multi-component systems, where overlap of the pair-correlation functions means that it is not possible to obtain all of the individual $g_{\alpha\beta}(r)$ from a

single diffraction experiment. In favourable cases, however, information can be gained by using multi-pattern techniques that include (i) neutron diffraction with isotope substitution (NDIS), (ii) anomalous X-ray diffraction (AXD), and (iii) a combination of X-ray and neutron diffraction. These methods will be illustrated by case studies taken from recent work at central neutron and X-ray facilities.

Finally, I will introduce the ideas behind structural refinement techniques such as reverse Monte Carlo (RMC) and empirical potential structure refinement (EPSR), where measured diffraction patterns are used to guide in the construction of atomistic models.

[1] H. E. Fischer, A. C. Barnes and P. S. Salmon, *Rep. Prog. Phys.* **69** (2006), 233.

[2] P. S. Salmon and A. Zeidler, *J. Phys.: Condens. Matter* **27** (2015), 133201.

[3] P. S. Salmon and A. Zeidler, *J. Stat. Mech.* (2019), 114006.

112

Electrodeposition: A Synthesis Platform for Experimental Models in Electrocatalysis

Author: Divyansh Gautam¹

Co-authors: Ahmad Trimdzi²; Espen Drath Bøjesen³; Gustav K.H. Wiberg²; Jonathan Quinson³; Matthias Arenz²; Sarvada Shailesh Andhare⁴

¹ University of Bern

² University of Bern, Switzerland

³ Aarhus University, Denmark

⁴ Indian Institute of Bombay, India

The High Entropy Alloys (HEAs) are metastable materials constituting of different principal elements in the same lattice [1,2]. The intrinsic property of chemical diversity in HEAs offer a range of adsorption energies for different molecules. So, tuning the composition can offer optimized adsorption energies is desirable in electrocatalysis. Currently, HEAs are being considered as materials platform to find better sensitivity, selectivity and stability, the three major fronts (3S) in electrocatalysis [3,4]. However, searching better electrocatalysts across all the three fronts for electrochemical reactions is an academic challenge to establish HEA's as a materials platform for catalyst discovery. Therefore, medium throughput experimental screening methods are required which demands faster and controlled synthesis of multielement nanoparticles [5,6]. Current work highlights the synthesis of Au-Ir-Pt-Pd-Rh-Ru nanoparticles using electrodeposition in aqueous media [7]. It uses a pulsed electrodeposition protocol to synthesize one sample within 90 seconds. We introduce an adjustment factor using monometallic depositions bridging the precursor compositions of the synthesis and the mesoscale compositions found using energy dispersive spectroscopy (EDX). Herein, a synthesis model is built using compositional space, particle size and coverage obtained using 250 experiments which allows better prediction of the mesoscale composition expected in the nanoparticles. A Gaussian process regressor is used to train different objectives like compositions found in the nanoparticles, particle size, coverage and synthesis charge during electrodeposition. Compositional analysis at different length scales from different microscopes using EDX, suggests random mixing at mesoscale along with a presence of compositional order at nanoscale.

1. Cantor, B., Chang, I. T. H., Knight, P. & Vincent, A. J. B. Microstructural development in equiatomic multicomponent alloys. *Materials Science and Engineering: A* 375–377, (2004).
2. He, Q. F., Ye, Y. F. & Yang, Y. Formation of Random Solid Solution in Multicomponent Alloys: from Hume-Rothery Rules to Entropic Stabilization. *J Phase Equilibria Diffus* 38, (2017).
3. Xu, W., Diesen, E., He, T., Reuter, K. & Margraf, J. T. Discovering High Entropy Alloy Electrocatalysts in Vast Composition Spaces with Multiobjective Optimization. *J Am Chem Soc* 146, (2024).

4. Banko, L. et al. Unravelling Composition–Activity–Stability Trends in High Entropy Alloy Electrocatalysts by Using a Data-Guided Combinatorial Synthesis Strategy and Computational Modeling. *Adv Energy Mater* 12, (2022).
5. Personick, M. L., Jallow, A. A., Halford, G. C. & Baker, L. A. Nanomaterials Synthesis Discovery via Parallel Electrochemical Deposition. *Chemistry of Materials* 36, (2024).
6. Batchelor, T. A. A. et al. Complex-Solid-Solution Electrocatalyst Discovery by Computational Prediction and High-Throughput Experimentation**. *Angewandte Chemie - International Edition* 60, (2021).
7. Gautam, D. et al. Noble Metal-based High Entropy Alloy Nanoparticles Prepared by Pulsed Electrodeposition: An Approach for Medium Throughput Studies. (2025) doi:10.26434/CHEMRXIV-2025-7WHR2.

59

Structural Fingerprints of Plasticity: Linking the Shear Transformation Zone Size to Pair Distribution Functions in Metallic Glasses

Author: Valeria Lemkova¹

Co-authors: Christian Motz ; Florian Schaefer ; Ralf Busch

¹ *Saarland University*

To understand the interplay between local atomic structure and the plastic deformation process in metallic glasses remains a key challenge in materials science. In this work, we combine nanoindentation experiments with structural analysis based on pair distribution functions (PDFs) to explore how shear transformation zones (STZs) and activation volumes correlate with short- and medium-range order. Using statistical evaluation of so-called pop-in events, we estimate the characteristic size of STZs. Through synchrotron-based PDF measurements the structural fingerprint was assessed. Our results suggest that variations in atomic ordering influence the onset of plasticity, providing a quantitative link between mechanical response and structural motifs. This approach offers new insights into the fundamental mechanisms governing deformation in amorphous alloys and opens pathways for tailoring their properties through structural design.

13

3D- Δ PDF: Pair distribution function analysis for single crystals

Author: Arkadiy Simonov^{None}

This tutorial will be focused on understanding disorder in single crystals using diffuse scattering. In particular I will introduce the Three-Dimensional Difference Pair Distribution Function (3D- Δ PDF) method for analyzing diffuse scattering from single crystals and the program Yell which can perform 3D- Δ PDF refinements.

58

In situ/operando studies for understanding the metal-support interaction of Ni-based catalysts for ammonia decomposition

Author: Nrusimha Teja Yanamandram¹

Co-authors: Christina Scheu²; Claudia Weidenthaler³; Jan Ternieden³; Sebastian Leiting³; Yiqun Jiang²

¹ PhD student, Max Planck Institute for Kohlenforschung

² Max-Planck-Institute for Sustainable Materials

³ Max-Planck-Institut für Kohlenforschung

Ammonia is considered a promising hydrogen carrier due to its high hydrogen content (17.8 wt%) and ease of transportation at room temperature under moderate pressures [1]. Ammonia decomposition into hydrogen and nitrogen is a carbon-free, endothermic reaction that requires suitable catalysts to lower the reaction temperature. Various supported metal catalysts are tested, and understanding metal-support interactions (MSI) during activation and catalysis is crucial for designing effective catalysts [2]. In this work, Ni catalysts supported on CeO₂, TiO₂, MgO, Al₂O₃, and SiO₂ are investigated using a combination of in-situ characterization techniques such as X-ray diffraction (XRD), X-ray absorption spectroscopy (EXAFS), X-ray photoelectron spectroscopy (XPS), and total scattering with pair distribution function (PDF) analysis, complemented by transmission electron microscopy (TEM). Wet impregnation is used for the synthesis of 10 at. % Ni on different supports, among which Ni/CeO₂ showed the highest ammonia conversion, while Ni/TiO₂ showed the lowest. XRD provides insights into the average crystal structures of the catalyst and the support, whereas EXAFS offers element-specific information on the local coordination environment of Ni. Total scattering with PDF analysis, however, provides understanding of both short- and long-range structural order. In the current study, operando PDF analysis was particularly useful for Ni/SiO₂, owing to the amorphous nature of the support, and for Ni/Al₂O₃, which forms NiAl₂O₄. Temperature-dependent operando total scattering experiments were conducted at P02.1 (Petra III, DESY), and the structural evolution was compared during the activation and ammonia decomposition processes. Comparative PDF analysis revealed distinct variations in the local Ni environments across different supports. For Ni/CeO₂, the PDF analysis showed well-defined Ni–Ni pair correlations characteristic of metallic Ni nanoparticles. These correlations remained largely unchanged during both activation and ammonia decomposition. This immobilization type-MSI enhanced catalyst stability and activity, resulting in the highest ammonia conversion. However, subtle changes in the structure of the CeO₂ support were observed, indicating the partial reduction of Ce⁴⁺ to Ce³⁺ also confirmed by in situ XPS. In contrast, the PDF of Ni/TiO₂ showed sharper Ni–Ni correlations, indicating a well-ordered Ni structure. From in situ XRD, larger crystallite sizes and from TEM analysis, larger particle sizes of Ni nanoparticles indicate sintering. This work emphasizes the importance of using characterization techniques across different length scales, from local coordination to long-range order, combined with in situ/operando studies for a complete understanding of complex metal-support interactions in catalytic reactions.

[1] Y. Kojima, M. Yamaguchi, International Journal of Hydrogen Energy, 2022, 47, 22832–22839.

[2] Liu, L., Corma, A., Chemical Reviews, 2018, 118, 4981–5079.

16

Single-Crystal Diffuse scattering

Author: Reinhard Neder¹

¹ Friedrich-Alexander-Universität Erlangen-Nürnberg

Diffuse scattering has been observed for almost as long as any single crystal diffraction, see [1] for a recent review on the subject. Further reviews are found for example in [2–7] and references therein. Diffuse scattering is observed for all classes of crystalline materials, metal alloys, simple inorganic materials, quasicrystals, molecular structures including protein crystals.

The intensity of the Bragg reflections describes the crystal structure very well with one important limitation. To the Bragg reflections all unit cells look alike. The Bragg reflections thus contain information on the average structure only. Any difference between the unit cells manifests itself in additional, usually weak diffuse scattering between the Bragg reflections. The diffuse scattering may be an almost featureless background or show a pattern of intricate complexity and may consist of streaks, layers, broad peaks or even curved distributions.

The origin of the structural deviations may be due to dynamic effects such as the thermal movement of atoms or due to static effects. The first effect is commonly termed thermal diffuse scattering, while the second effect is referred to as disorder diffuse scattering.

The static deviations from the average structure can have many different reasons and may be present at different dimensions within the crystal. The deviations may be something as simple as a distribution of two or more atom types at a single site within the unit cell. Very often these local replacements cause a slight static shift of the surrounding atoms and these may be described as small clusters of slightly different structure. In a molecular structure the simplest defects might be a molecule in a slightly different conformation. From these simple defects one can consider a continuous and gradual change to larger objects such as domains with slightly different order or actual disolutions of a guest phase in the host crystal. Other defect types may disrupt the strict periodicity of the crystal on a larger scale such as stacking faults. Commonly the periodicity is maintained within the layers but the layer sequence deviates from a strictly periodic sequence.

Somewhat independent of the actual defect type, we need to consider the distribution of the defects throughout the host structure. Many times the defects are not randomly distributed and the correlations between neighboring defects introduce structure into the diffuse scattering.

In this lecture an overview of defect types, the arrangement of defects and the corresponding diffuse scattering is given. The lecture will describes current measurement, analysis and modelling techniques.

[1] T.R. Welberry, T. Weber, *Crystallography Reviews* **22**, (2015).

[2] B.T.M. Willis, H. Jagodzinski, F. Frey, J.M. Cowley, J. Gjonnes, P.S. Pershan in *Int. Tables for Crystallography Vol B*, U. Shmueli (Ed.), IUCR (1993), p. 383.

[3] W. Schweika, Springer (1998).

[4] V.M. Nield, D.A. Keen, Oxford University Press (2001).

[5] T.R. Welberry, Oxford University Press (2004).

[6] R.B. Neder, T. Proffen, Oxford University Press (2008).

[7] T.R. Welberry, D.J. Goossens., *IUCrJ.* **1**, 550 (2014).

35

Assessing Short-range order using total scattering and RMC - methods, challenges and strategies

Author: Lewis OWEN¹

¹ *University of Sheffield*

Chemical short-range order (SRO), whereby local atomic arrangements differ from the average structure, has been cited as affecting key physical properties of metallic systems such as strength, electrical resistivity and magnetic properties since as early as the 1950s [1]. However, due largely to the lack of suitable experimental probes, and the complexity of the analysis, studies in this field were largely abandoned. With the advent of the total scattering method, and use of the reverse Monte-Carlo algorithm [2] for analysis of the data, it has become possible to understand and characterise this chemical short-range order.

In this talk, I will describe the methodologies we have developed for assessing and characterising short-range order in metallic systems using total scattering and RMC methods [3-4]. I will discuss common errors that can lead to spurious results if not assessed correctly, and the creation of 'artificial ordering' or chemical clustering within a system. In turn, I will discuss refinement strategies that aid in the mitigation of these effects and the extraction of the order within the system. The framework and numerical quantifiers we have developed to aid in the description and characterisation of the order present will also be presented. Finally, we will discuss how these methods may be generalised and used in other chemical systems where local-ordering may be affecting the properties, including compositionally complex materials, nanoparticles and functional materials [5].

- [1] Cowley, J. M. *Physical Review*, 1950, 77 (5), 669-675. DOI: 10.1103/PhysRev.77.669.
- [2] McGreevy, R. L.; Pusztai, L. *Molecular Simulation*, 1988, 1 (6), 359-367. DOI: 10.1080/08927028808080958.
- [3] Owen, L. R.; Playford, H. Y.; Stone, H. J.; Tucker, M. G. *Acta Materialia*, 2016, 115, 155-166. DOI: 10.1016/j.actamat.2016.05.031.
- [4] Owen, L. R.; Playford, H. Y.; Stone, H. J.; Tucker, M. G. *Acta Materialia*, 2017, 125, 15-26. DOI: 10.1016/j.actamat.2016.11.048.
- [5] Summer, A.; Playford, H. Y.; Owen, L. R.; Fisher, J. M.; Kolpin, A.; Thompsett, D.; Walton, R. I. *APL Materials*, 2023, 11 (3). DOI: 10.1063/5.0139567.

15

Refinement of Magnetic Diffuse Scattering Data

Author: Joe Paddison¹

¹ *Oak Ridge National Laboratory*

I will discuss techniques for refinement of magnetic diffuse scattering data, and the real-space information they can provide about magnetic materials such as spin liquids, spin ices, and skyrmion crystals. I will introduce the computer programs Spinvert and Spinteract, which can be used to estimate the short-range magnetic correlations and the magnetic interactions that drive them, respectively. I present several examples to demonstrate the capabilities of the suite of programs: fitting to powder and single-crystal diffuse-scattering data, predicting single-crystal diffuse-scattering patterns given powder data, and parametrising spin Hamiltonians of magnetic materials using magnetic diffuse scattering data.

41

Phase Sensitive Detection Analysis on Modulation Excitation PDF Data of Ni Based Catalysts

Author: Fabio Manzoni¹

Co-author: Mirijam Zobel

¹ *RWTH Aachen University*

Among catalysts employed for CO₂ methanation, Ni nanoparticles supported on γ -Al₂O₃ are the most widely used. Moreover, the transition from fossil to renewable energies means that an unstable supply of feedstock or energy must be considered when planning industrial processes and designing catalysts. Fluctuations in operating conditions can lead to structural changes and the formation of transient interfacial structures due to surface reconstruction processes. 1

In-situ experiments involving catalytic cycling between catalysis and dropout conditions allow the power of modulation excitation (ME) experiments to be used. 2

In this work, we present the first application of Phase Sensitive Detection (PSD) analysis to X-ray Pair Distribution Function (PDF) data, collected during in-situ catalysis experiments under ME conditions. 3

To demonstrate the power of such ME-PDF analysis, we performed in-situ ME-PDF experiments on two Ni@Al₂O₃ catalysts (an industrial reference and an in-house synthesized one) under CO₂ methanation and full H₂ dropout conditions. In-situ synchrotron total scattering data were acquired at the I15-1 beamline at the Diamond Light Source in Didcot (Oxford, UK).

From the time-dependent PDF data, we were able to identify dynamic changes in the Ni lattice parameter and particle growth. The PSD transformed ME-PDF data revealed additional structural differences between the two catalysts. The PSD data showed that the synthetic route affects the structure of the catalysts. In the synthesised sample, an interaction between the metal and the support involving Al₂O₃ is observed. This interaction stabilises the Ni nanoparticles and prevents their

oxidation. In contrast, the industrial reference catalyst showed no support involvement during the reaction, but exhibited a surface oxidation of the Ni nanoparticle during dropouts. These structural observations were completely silent in the normal PDF analysis and became visible thanks to the application of the ME condition studied with PSD transformation. In conclusion, ME-PDF analysis can have major impact in the field of catalysis in in-situ investigations at brilliant photon sources allowing ME experiments with fast cycling between operating conditions thanks to sub second measurement times of PXRD and PDF datasets in highly brilliant X-ray beams.

References:

- 1 B. Mutz et Al., *Catalysts*, 2017, 7, 279
- 2 A. Urakawa et Al., *Chem. Eng. Sci.*, 2008, 63, 4902–4909.
- 3 F. Manzoni et Al., *Nanoscale*, 2025, 17, 18766

21

Challenges in XPDF Analysis of High Pressure-Temperature Metal-Organic Frameworks

Author: Georgina Robertson¹

¹ ESRF

Real-space total X-ray scattering analysis of metal-organic frameworks (MOFs) under extreme conditions presents unique experimental and interpretive challenges. Many factors hinder reliable data collection and analysis, including the inherently low X-ray scattering power of MOFs, the presence of pressure-transmitting media (PTM) introducing additional background scattering and structural interactions, and changes in the dimensions of the high-pressure chamber during compression and heating. This presentation will discuss strategies to mitigate these issues, and highlight pathways to extract meaningful structural insights into MOF stability and phase behavior under high pressure-temperature conditions.

47

CO-induced dynamic behaviour of Al₂O₃-supported Pd nanoparticles at room temperature

Author: Daniele Bonavia¹

¹ Paul Scherrer Institute

It is known that metal nanoparticles (NPs) can undergo surface and/or structural rearrangements in the presence of adsorbates, and this has relevance both in catalysis and in the field of NPs characterization. A typical example is the structural rearrangement of Pd NPs in the presence of CO, which has been reported to occur mostly at elevated temperature (e.g. during CO oxidation reaction) 1. However, catalysts with small NPs (~2 nm) tend to exhibit high activity under milder reaction conditions. Moreover, CO is commonly used as probe molecule for the characterization of metal NPs close to room temperature (e.g. through pulsed CO chemisorption). Recently, we demonstrated - by coupling gas volumetry, adsorption microcalorimetry and IR spectroscopy - that CO adsorption at room temperature on Al₂O₃-supported Pd NPs (size ~ 2 nm) causes the corrugation of the (100) facet, entailing the creation of new defective sites 2. Herein, we delve deeper into the structural evolution of these supported Pd NPs upon CO adsorption by using operando Pair Distribution Function (PDF) analysis coupled with mass spectrometry (performed at beamline ID15A at ESRF), allied with complementary in situ IR spectroscopy. The catalyst was initially reduced in H₂ at 393 K, and flushed in Ar at the same temperature, to expose metallic Pd. Then, it was exposed to 1% CO in Ar at 298 K and

time-resolved (1s) total scattering data were collected with a Modulated Excitation (ME) approach 3.

To obtain precise information about the sample state in reaction conditions we used model-free PDF fitting over the ME dataset 4 to investigate the relative expansion/contraction of the NPs ($\Delta R/R$) and changes in their coherence (peak area). Specific fitting starting points were prepared for four different regions (around the 1st, 3rd, 7th and 13th shell) based on the knowledge available from PDF patterns of the blank support (Al₂O₃) in the same conditions and on the expected positions of Pd-Pd pairs peaks in the *fcc* structure. The results present a clear expansion of the structure in the presence of adsorbed CO which becomes less and less prominent for higher order shells, and is always reversed during the half-cycle in pure Ar. Concerning the evolution of the peak area, in the presence of CO the area of the Pd-Pd peak decreases for lower order shells, but the trend is progressively inverted going higher in R, up to the 13th shell where the adsorption of CO produced a steep increase in peak area.

To better understand these trends, we coupled them with geometrical considerations, with the aim of evaluating the influence of structural variations in the core shell on all possible atomic pair within a Pd NP of compatible size. The chosen descriptor is the distance *D* between the center of the NP and the midpoint of a Pd-Pd pair. Shorter *D* values mean that the chosen atomic pair is more influenced by structural changes in the core region, longer *D* values are related to atomic pairs that are only marginally affected by those same changes. By computing the distribution of *D* values across the regions in R interested by the various Pd shells, this approach shows how shells of higher order (higher R regions) are more influenced by structural changes in the core region of the NP with respect to those of lower order (lower R regions), which are less affected.

The trends observed with the model-free PDF fitting are interpreted according to these considerations, concluding that CO adsorption induces two reversible effects on these Pd NP:

- An expansion throughout the NP that is more pronounced at the surface with respect to the bulk
- A decrease in coherence (disordering) at the surface (as expected by previous *in situ* characterization 2) and an increase (ordering) in the core of the NP.

This relatively simple but powerful analysis approach allows to extract depth-dependent information from the PDF and, paired with finer analysis approaches, paves the way for a deeper structural understanding of these catalysts in reaction condition.

1 I. Jbir, J. Couble, S. Khaddar-Zine, Z. Ksibi, F. Meunier, D. Bianchi (2016) *ACS Catalysis*, 6, 4, 2545-2558

2 A. Ricchebuono, E. Vottero, D. Bonavia, P. Lazzarini, R. Pellegrini, V. Crocella', N. Porcaro, S. Checchia, D. Ferri, A. Piovano, E. Groppo (2024) *ACS Catalysis*, 14, 18, 13736–13746

3 D. Ferri, M. Newton, M. Di Michiel, G.L. Chiarello, S. Yoon, J. Andrieux (2014) *Angew. Chemie*, 126, 34, 9036-9040

4 D. Bonavia, A. Ricchebuono, P. Lazzarini, E. Vottero, R. Pellegrini, A. Piovano, C. Chizallet, P. Raybaud, C. Dejoie, I. Alxneit, S. Checchia, D. Ferri, E. Groppo (2025), *Nat Commun* 16, 9591.

17

Boron Phosphide Nanocrystals by Pair Distribution Function Analysis

Author: Clara DOISNEAU¹

Co-authors: David Portehault ¹; Amandine SENE ¹; Capucine Sassoye ¹

¹ Sorbonne Université

Cubic boron phosphide is known as a super-hard material, potential photoelectrocatalyst of water splitting and p-type transparent conductor.[1, 2] We recently developed the first synthesis of c-BP nanocrystals with controlled size of ca. 5 nm, using inorganic molten salts as liquid reaction media at 550 °C. These nanocrystals offer new opportunities to tune the properties of c-BP and to process the material.

Although XRD patterns are consistent with the sphalerite structure, further investigations at shorter range show discrepancies. Indeed, XPS indicates an excessive phosphorus ratio at the surface and more than one local environment were detected by ^{31}P and ^{11}B NMR. We have then engaged in an in-depth study using total X-ray scattering coupled to PDF analysis, to identify the nature of local environments, irrespective of the crystalline or amorphous nature of the solid.³

PDF analysis for the as-synthesized powder shows significant deviations to the ideal sphalerite structure. PDF analysis carried out in situ during annealing (ID11 beamline at ESRF) shows that the structure undergoes reorganisation before grain growth at 750 °C. At the 750 °C plateau, the overall structure appears close to ideal sphalerite. Few defects re-appear during cooling. Other experiments (in situ XRD during annealing at 3 GPa – 1200 °C) show a different behaviour, which led us to propose new structural models for the initial powder and two different reorganization pathways.

Finally, PDF analysis during in situ synthesis in molten salts was carried out to grasp the origin of the defects in the pristine nanocrystals, and then identify possible pathways for synthesis optimization. We will discuss PDF data treatment, the nature of the new local environments detected, and the possible origins of these features appearing during the synthesis, with a special focus on the surface states of the nanocrystals.

1 Crovetto et al., *Adv. Mater. Interfaces*, 9, 2200031 (2022)

2 Sugimoto et al., *J. Phys. Chem. C*, 123 (37), 23226–23235, (2019)

3 T. Egami, S.J. Bilinge, *Underneath the Bragg Peaks, Materials Today*, 1369,7021 (2004)

Acknowledgement: the European Research Council (ERC) Consolidator Grant GENESIS (grant agreement n° 864850) funded this project. Experiments were performed at the ID11 beamline (ESRF).

20

Thermodynamic, kinetic and structural study of $\text{Pt}_{42.5}\text{Cu}_x\text{Ni}_{36.5-x}\text{P}_{21}$ alloy variations

Author: Ziyu Ling¹

Co-authors: Amirhossein Ghavimi¹; Andrea Fantin²; Isabella Gallino³; Maryam Rahimi Chegeni¹; Nico Neuber¹; Ralf Busch¹; Sergiy Kasatkov³

¹ *Saarland University*

² *The Federal Institute for Materials Research and Testing*

³ *Technical University Berlin*

The thermodynamic and kinetic properties of $\text{Pt}_{42.5}\text{Cu}_x\text{Ni}_{36.5-x}\text{P}_{21}$ ($x = 36.5, 27, 18.25, 9.5, 0$) glass-forming liquids are studied via differential scanning calorimetry (Perkin Elmer DSC) and Flash DSC (Mettler Toledo). The kinetic fragilities of the alloys are determined by measuring relaxation times in a broad heating rates range (0.025, 0.083, 0.333, 1, 1.33, 2, 3 K/s) using a T_g shift method 1. In addition, the relaxation time of the deeply undercooled liquids is determined by FDSC via a step-response method 2. Furthermore, the specific capacity heat (C_p) as a function of temperature for the glassy, liquid and crystalline state of the chosen alloys are determined. The thermodynamic fragility is assessed from the C_p difference between the liquid and crystalline state at the glass transition temperature and the driving force for crystallization is calculated using fitting parameters of thermodynamic functions derived from C_p data. Moreover, the glass forming ability of the alloy liquids is evaluated based on their critical cooling rates and TTT-diagrams. The interfacial energy of the selected compositions is obtained by JMAK fitting with TTT-diagrams. The ribbon-form specimens were investigated by synchrotron X-ray scattering experiments at DESY for atomic level structural data and by X-ray Photoelectron Spectroscopy and Near-Edge X-ray Absorption Fine Structure at BESSY for energy state changes of each elements.

The aim of this work is to investigate the influence of Cu and Ni substitution on the thermophysical properties of the alloy and explore the key factors behind high GFA of Pt-P based alloys.

- 1Busch, R. (2000). The thermophysical properties of bulk metallic glass-forming liquids. JOM, 52(7), 39–42. <https://doi.org/10.1007/s11837-000-0160-7>
- 2Monnier, X., Cangialosi, D., Ruta, B., Busch, R., & Gallino, I. (2020). Vitrification decoupling from α -relaxation in a metallic glass. Science Advances, 6(17), eaay1454. <https://doi.org/10.1126/sciadv.aay1454>

11

DISCUS, Simulation and refinement of disordered crystal structures

Author: Reinhard Neder^{None}

R. B. Neder

Kristallographie und Strukturphysik, Friedrich-Alexander-Universität Erlangen-Nürnberg, Staudt-str. 3, 91058 Erlangen

DISCUS is a program that can simulate crystal structures and can calculate the corresponding diffraction pattern¹. Its scope includes the possibility to simulate perfect crystal structures, as well as disordered structures. The program includes several toolboxes to introduce defects into the crystal structure. The strength of the program is the nearly unlimited flexibility that it offers to the user. One can use the program to simulate individual atoms, molecules, small clusters, finite-sized nanoparticles or crystals that are essentially infinite in size. Into each of these structures many different defects can be introduced via a set of tools integrated into the program, that still as an average periodic crystal structure, or a complex core/shell nanoparticles as well as a glass like structure without periodicity.

The tools to create disorder include basic options like the manipulation of individual atoms and extended tools to manipulate the crystal at large. These tools include short range order concepts to distribute different atom species or to distribute displacement correlations throughout the crystal. Empirical potential functions allow to introduce local distortions to the structure. Another tool builds stacking faults. These can be created as growth faults or use a short range order mechanism to build faults with more complex layer sequences. A new companion program allows the use of abstract generators to create essentially any stacking fault sequence. DISCUS uses an abstract domain concept to incorporate defects into a host structure. These defects might be anything from an individual atom, a small cluster, a guest crystal with regular or irregular internal host-guest surface or a set of molecules on top of a surface. The domains themselves may be subject to a short-range order distribution. Finally, modulated structures can be simulated with the use of displacement or density waves. To build finite crystals, options exist to create crystals limited by a suitable surface.

DISCUS calculates single crystal diffraction pattern of as well as powder diffraction pattern, the pair distribution function (PDF), and the 3D-PDF. The DISCUS program suite 2 includes two generic optimizer sections to refine disordered crystal structures with respect to experimental data. The DISCUS suite is available for Linux, Mac and Windows. The program includes an MPICH option to allow fast parallel refinement on multiple core architectures or supercomputer frames. A set of interactive teaching pages is available to introduce disorder diffraction concepts³.

1 R.B. Neder, T. Proffen, *Diffuse Scattering and Defect Structure Simulation*, Oxford (2008).

2 DISCUS is available on <https://github.com/tproffen/DiffuseCode>.

3 DISCUS Teaching pages available on <https://www.icsp.nat.fau.eu/neder-group/> (Under revision).

4 K. Page, T.C. Hood, Th. Proffen, R.B. Neder, *J. Appl. Cryst.* **44**, 327 (2011).

Intermetallic phases and liquid alloys in SCALMS catalysts studied by X-ray PDF analysis

Authors: Felix Egger¹; Mirijam Zobel^{None}

Co-authors: Andreas Mölkner²; Julien Steffen²; Marco Haumann³; Narayanan Raman³; Nicola Taccardi³; Peter Wasserscheid³

¹ *Institute of Crystallography, RWTH-Aachen University*

² *Department Chemie und Pharmazie, Lehrstuhl für Theoretische Chemie, Friedrich-Alexander-Universität Erlangen-Nürnberg (FAU)*

³ *Department Chemie- und Bioingenieurwesen, Lehrstuhl für Chemische Reaktionstechnik (CRT), Friedrich-Alexander-Universität Erlangen-Nürnberg (FAU)*

Supported catalytically active liquid metal solutions (SCALMS) offer a promising route to sustainable catalysis by combining single-atom-like dispersion with thermal stability in a dynamic liquid alloy phase. Under reaction conditions, solid alloy particles liquefy on the support surface, enabling efficient high-temperature reactions. To reduce the mobility of the active species, new SiO₂ support materials have been developed, forming small cavities that are meant to trap liquid droplets. Despite the advanced catalyst design and high catalytic activity, selectivity and long-term stability in reactions such as propane dehydrogenation, deactivation processes can still not be completely suppressed. In the case of a Pt-Ga SCALMS catalyst, this type of deactivation is, among other things, linked to the formation of Ga-Pt intermetallic phases or alloys, which form during synthesis or catalysis ¹.

In order to study the liquid and alloy phases including subtle structural changes in a Ga-Pt SCALMS system, we performed pair distribution function (PDF) analysis of high energy X-ray total scattering data collected at PETRA III (DESY Hamburg), beamline P02.1 (59.78 keV, $\lambda = 0.20735$). Samples were measured ex-situ in an as synthesized, as well as post catalysis state, with Ga/Pt ratios ranging from 8 to 144, to investigate the effect of composition on the formation of the intermetallic phase. The unloaded SiO₂ support was measured to calculate difference PDFs. Results of our PDF analysis match the ones of density functional theory studies.

Refinements of the dPDF data using Diffpy-CMI confirmed the formation of an amorphous gallium oxide (β -Ga₂O₃) layer, covering the liquid Ga droplet prior to activation, consistent with previous studies employing Raman spectroscopy ². Additionally, we revealed the formation of Pt fcc nanoparticles for the pristine catalyst, with a size depending on the Pt content, increasing from ~ 2.5 nm up to 4 nm. In the post catalysis samples the Pt nanoparticles had transformed into a Pt₂Ga intermetallic phase. We suggest the formation of this intermetallic phase to happen during the catalysis, therefore explaining the deactivation of the system that can be seen by catalysis data. The formation of this phase was observed for all studied systems with different Ga/Pt ratios, except for the one with the lowest Pt content ³. This observation suggests that the superior performance of SCALMS with low active metal content compared to their high metal content counterparts, might be linked to low intermetallic phase formation for such systems.

1 Carl, S., et al. (2024). Structural Evolution of GaO x-Shell and Intermetallic Phases in Ga-Pt Supported Catalytically Active Liquid Metal Solutions. *The Journal of Physical Chemistry Letters*, 15(17), 4711-4720.

2 Nair, S., et al. (2025). In Situ Raman Spectroscopy of Supported Catalytically Active Liquid Metal Solutions (SCALMS)—Activation and Coking Behavior in Propane Dehydrogenation. *ChemCatChem*, e202500176.

3 Egger, F., et al. (including Zobel, M.) (2025). Supported Catalytically Active Liquid Metal Solutions (SCALMS) for Propane Dehydrogenation—Intermetallic Phases and Liquid Alloys Studied by Pair Distribution Function Analysis and Density Functional Theory. *Advanced Science*, e11498.

Tutorial introductions / 7

EPSR & Dissolve - Data-driven structural modelling of total scattering data

Author: Tristan YOUNGS¹

Co-authors: Daniel Bowron ²; Marta Falkowska ³

¹ *ISIS Neutron and Muon Source*

² *UK Research and Innovation, Science and Technology Facilities Council, ISIS Neutron and Muon Facility*

³ *University of Manchester / ISIS Neutron and Muon Source*

The study of disordered materials such as liquids and glasses through neutron or x-ray techniques presents an interesting challenge since, due to the presence of only local order (< 1 nm) in these materials, only diffuse scattering prevails. Searching for, or generating model analogues that match this “order in disorder” present in the structure of real systems is normally required to make any kind of scientific interrogation. This is the goal of the Empirical Potential Structure Refinement (EPSR) 1 and Dissolve 2 codes.

Both EPSR and Dissolve rely on a full, atomistic simulation (Monte Carlo and/or molecular dynamics) of a target system and its constituent molecules and moieties within the context of a “realistic” force-field describing the interactions between atoms. While simulations utilising off-the-shelf forcefields typically do not reproduce experimentally-measured structure factors, they act as a useful starting point for further refinement. Critically, the provision of experimental scattering data allows both codes to modify the interatomic potentials provided and drive the simulated system towards better agreement with the real-world one. This data-driven approach to the modelling of total-scattering data has successfully been applied to a multitude of disordered systems covering liquids, liquid mixtures, and glasses, and is increasingly being used to study complex disordered materials such as gases and liquids confined in porous materials, polymers in solution, and self-assembled systems such as aqueous micelles.

Here I will give an overview of the techniques and approaches involved, their advantages, limitations and challenges, and discuss some real-world examples.

1 Soper, *Mol. Phys.* **99**, 1503 (2001)

2 Youngs, *Mol. Phys.* **117**, 3464 (2019)

9

DiffPy-CMI - a software toolbox for real-space structure analysis and Complex Modeling

Author: Simon Billinge¹

¹ *Columbia University + Brookhaven National Laboratory*

This presentation and the associated hands-on tutorial will introduce DiffPy-CMI, a software for structure analysis from experimental atomic Pair Distribution Function (PDF) and for Complex Modeling [1, 2]. DiffPy-CMI (Complex Modeling Infrastructure) has been developed to handle ill-posed inverse problems, where diffraction experiments do not provide enough signal to determine complicated structures or nanostructures. To overcome this problem, we use a Complex Modeling approach 3 which allows users to combine additional experimental or theoretical inputs and uses them all together in a common optimization routine. DiffPy-CMI is a flexible and extensible program allowing user to create such models tailored for the specific knowledge about the material under study. DiffPy-CMI runs on Linux and Mac operating systems and is primarily written in Python with computationally intense parts coded in C++. It can also be run on windows using the Windows Linux Subsystem (WSL). In the big picture DiffPy-CMI provides several ways of representing atomic structures, a set of forward calculators (e.g., PDF, bond valence sums, powder and single crystal diffraction), and finally a fit-manager to define and run multi-input refinements. The fits can be conducted with short Python scripts or within the Jupyter Notebook interactive environment. In addition to Complex Modeling, DiffPy-CMI also enables more subtle PDF refinements which are not possible in PDFgui 4 - for example PDF fits of non-periodic small clusters or of molecular crystals

with rigid structure units. The software provides access to internal simulation routines, which can be tweaked or extended, and thus permits rapid implementation of new ideas and more accurate models. We will demonstrate the capabilities of DiffPy-CMI on a series of science cases, starting from simple forward calculations and following up with PDF fitting examples that go beyond PDFgui.

1 P. Juhás, et al., *Acta Crystallogr. A* **71** (2015), 562-568.

2 DiffPy-CMI is available at <https://www.diffpy.org>.

3 S. J. L. Billinge, I. Levin, *Science* **316** (2007), 561-565.

4 C. L. Farrow et al., *J. Phys: Condens. Mat.* **19** (2015), 335219.

68

Dynamic magnetic pair-density function analysis (DymPDF)

Author: Shinichi SHAMOTO¹

¹ *Japan Atomic Energy Agency*

The pair distribution function (PDF) has a long history of use in structural analyses, ranging from liquids to crystals. The energy-resolved pair density function analysis has also been developed for lattice dynamics [1, 2]. Here, we present the dynamic magnetic pair-density function (DymPDF) analysis. The DymPDF, $D_M(r, E)$, is obtained in the “Utsusemi” software 3 by the Fourier transform of the dynamic magnetic structure factor, $S_M(Q, E)$, measured by nonpolarized inelastic neutron scattering. The real-space spin dynamics of the ilmenite FeTiO_3 powder sample exhibit magnon mode transitions in the spin-spin correlation with increasing energy, from θ -phase shift to π -phase shift 4. This transition is well reproduced by simulations using reciprocal space magnon dispersions. This analysis provides a novel opportunity to study the local spin dynamics of various magnetic systems. This talk will introduce the DymPDF capability. This work is supported by Grants-in-Aid for Scientific Research (C) (22K04678 and 25K08263) from the Japan Society for the Promotion of Science.

References

1. A. C. Hannon, M. Arai, et al., *J. Non-Cryst. Solids* **150**, 239 (1992).
2. W. Dmowski et al., *Phys. Rev. Lett.* **100**, 137602 (2021).
3. <https://mlfinfo.jp/groups/comp/en/utsusemi.html>,
4. K. Iida, K. Kodama, Y. Inamura, M. Nakamura, L.-J. Chang, and S. Shamoto, *Sci. Rep.* **12**:20663 (2022).

27

Technical Aspects and Practices in Using Neutron Total Scattering for Local Magnetic Ordering Studies

Author: Yuanpeng Zhang¹

¹ *Oak Ridge National Laboratory*

Spin-lattice coupling is a critical interaction in condensed matter physics that involves the interplay between the magnetic spins of electrons and the lattice structure of a material. This coupling can influence various physical properties, such as magnetization, thermal conductivity, and electronic structure. Understanding spin-lattice coupling is essential for developing advanced materials with tailored magnetic properties, promising advancements in spintronics, via precise control over magnetic and structural phases. Here in this presentation, I will be demonstrating the exploration of several magnetic system to reflect the spin-lattice coupling and its impact on magnetic properties,

including kagome systems and a quantum spin liquid system. Conventionally, the focus for spin lattice coupling studies is more on the average structure, but here through the several cases we present, it is clear that the local structure plays a critical view in understanding the magnetic coupling in various systems. The main technique used here for the local structure studies is neutron total scattering and the main analysis technique is reverse Monte Carlo. Meanwhile, neutrons carry magnetic moments and will be scattered by magnetic moments in materials. Therefore, it can be used for detecting the magnetic ordering and naturally through the magnetic neutron total scattering signal, the local magnetic ordering can be potentially constructed. Here we are going to showcase this type of study with a spin-glass example.

1 Y. P. Zhang, et al. Phys. Rev. B 109, 144407, 2024.

2 T. H. Yang, et al. J. Am. Chem. Soc. 2024, 146, 50, 34374–34382.

3 Q. Zhang, Y. P. Zhang, et al. J. Am. Chem. Soc. 2022, 144, 31, 14339–14350.

4 Y. P. Zhang, et al. Phys. Rev. B 100, 014419, 2019.

30

Total scattering and PDFs using X-ray free-electron lasers: quality data in 30 femtoseconds

Author: David A. Keen¹

¹ *Rutherford Appleton Laboratory*

X-ray free-electron lasers (XFELs) are the pinnacle of X-ray sources with unprecedented intensity concentrated into femtosecond pulses. Despite this they typically will only produce low-quality total scattering data and low-resolution PDFs. A group of us have recently been working to remedy this with a development programme at the European XFEL in Hamburg. This talk will describe how we have set about optimising XFEL total scattering by using the maximum available XFEL X-ray energies and an innovative detector geometry. As a result¹ we can now routinely obtain quantitative total scattering data over a Q -range of $0.35 < Q < 16.6 \text{ \AA}^{-1}$ from a single XFEL X-ray pulse. This is a new opportunity for following ultra-fast structural changes in matter using total scattering/PDF methods.

¹ A F Sapnik *et al*, *IUCr* **12** (2025) 531 (<https://doi.org/10.1107/S205225252500538X>)

44

Correlated Disorder in Crystals: From Understanding to Control of the Local Structure

Author: Yevheniia Kholina¹

Co-authors: Andrew Goodwin¹; Arkadiy Simonov²

¹ *University of Oxford*

² *ETH Zurich*

While disorder is often perceived as random, in crystals it is usually correlated on a local scale and can even enhance material properties. We demonstrate that in framework materials, such correlated disorder can be controlled through crystallization parameters governing growth kinetics 1. Additionally, the crystal growth direction may allow guiding the defects along different growth

directions 2. This anisotropic defect arrangement lowers crystal symmetry, enabling control over directional properties. Importantly, the disorder does not have to remain fixed after the crystallization is completed. Local structure can undergo transformations triggered by post-synthetic treatments. We demonstrate that these modifications can be achieved by treatments like dehydration or loading guest molecules 1. These findings transform correlated disorder from an uncontrolled variable into a design parameter, opening new possibilities for engineering materials with tailored properties.

1 Kholina, Y. Correlated Disorder in Prussian Blue Analogues: From Understanding to Control of the Local Structure. Ph.D. Thesis, ETH Zurich, Zurich, Switzerland, 2025.

2 Kholina, Y., et al. Symmetry breaking in Prussian Blue analogues via growth-guided local ordering of hexacyanometallate vacancies. arXiv 2025, arXiv:2502.05936. <https://doi.org/10.48550/arXiv.2502.05936>

29

Local structure of Ammonia Borane: how much do we really know?

Author: Anna PIEKARA¹

Co-author: Wojciech Slawinski²

¹ *University of Warsaw*

² *Univeristy of Warsaw, Faculty of Chemistry*

Ammonia borane (BH_3NH_3) is a promising hydrogen storage material 1, 2. At room temperature, it crystallizes in the tetragonal space group $I4mm$ ($Z = 2$, $a = b = 5.263 \text{ \AA}$, $c = 5.050 \text{ \AA}$) 1, 2. Its structure has long been debated due to hydrogen disorder, which arises from the mismatch between the molecular symmetry and the crystal symmetry. The B–N bond lies along a fourfold axis, conflicting with the symmetry of the $-\text{BH}_3$ and $-\text{NH}_3$ groups 2, leading to pronounced plasticity in the crystal. To probe the local hydrogen arrangement, we performed synchrotron X-ray total scattering and Pair Distribution Function (PDF) analysis. For deeper insight, we combined PDF with Reverse Monte Carlo (RMC) modelling using the RMCProfile7 program 3. This method refines the average crystal structure against Bragg data while modelling local atomic configurations, fitting both the Pair Distribution Functions $G(r)$, $D(r)$ and the structure factors $F(Q)$, $QF(Q)$.

To clarify these structural features, we performed single-crystal X-ray measurements for both room-temperature and low-temperature phases. The room-temperature phase agrees with previous reports 1, 2, while the low-temperature phase shows a structural modulation, also evident in the powder PDF analysis.

Large-box RMC simulations capture the structural disorder while remaining consistent with the average crystal structure. They also reveal molecular orientations and geometries, matching experimental data without decomposition 4, even at short interatomic distances (B–H, N–H, B–N). Despite strong hydrogen disorder, local molecular symmetry and specific hydrogen positions can still be resolved.

1 M. E. Bowden, G. J. Gainsford, and W. T. Robinson, 'Room-temperature structure of ammonia borane', *Aust J Chem*, vol. 60, no. 3, pp. 149–153, 2007, doi: 10.1071/CH06442.

2 U. B. Demirci, 'Ammonia borane, a material with exceptional properties for chemical hydrogen storage', Apr. 13, 2017, Elsevier Ltd. doi: 10.1016/j.ijhydene.2017.01.154.

3 W. A. Sławiński et al., 'RMCProfile7: reverse Monte Carlo for multiphase systems', *J Appl Crystallogr*, vol. 57, no. Pt 4, pp. 1251–1262, Aug. 2024, doi: 10.1107/S1600576724004175.

4 K. Ikeda et al., 'Temperature Variation of the Local Structure and Dihydrogen Bonds in Ammonia Borane', *J Am Chem Soc*, May 2025, doi: 10.1021/jacs.5c04566.

Operando investigations of the Electrocatalytic performance of Metal-Organic Frameworks

Authors: Maria DIAZ-LOPEZ¹; Vishnu Dhinakaran²

¹ *Institut Neel*

² *Institut Neel CNRS*

Metal-Organic Frameworks (MOFs) have attracted considerable attention in electrocatalysis due to their large number of exposed active sites, which is due to their high specific surface area. However, the structural robustness of these MOFs have been put into question. The weaker nature of the bonds between the metal nodes and organic linkers in MOFs can lead to structural rearrangements under electrochemical environments. This can lead to formation of new phases on the surface of the material, which act as the true catalyst. Thus, it is not clearly understood if the MOF is a stable catalyst, or an unstable precatalyst. In order to track the changes that occur during the Oxygen Evolution Reaction (OER), an operando measurement of the structural evolution of the Zeolitic imidazolate framework – 67 (ZIF-67) by X-ray total scattering was done at the I15-1 beamline at Diamond Light Source (UK). A novel “containerless” electrochemical cell was used to allow the acquisition of high-quality Pair Distribution Function (PDF) data on the catalyst-electrolyte interface. The measurements were made across a range of applied potentials on the ZIF-67, showing the changes in the local structure of ZIF-67, thereby indicating the possibility of the formation of a new catalytic phase that acts as the true catalyst. The results from this experiment would offer critical insights for the design of future OER catalysts.

46

Cation substitution and Fe(III) trapping in layered double hydroxides deciphered by PDF, XAS, and DFT

Author: Jiaxing Ban¹

Co-authors: Barbara Lothenbach²; Bin Ma¹; John Provis¹; Ruotao Yang³; Sergey Churakov¹

¹ *Paul Scherrer Institute*

² *Swiss Federal Laboratories for Materials Science and Technology*

³ *University of Bern*

The incorporation of Fe(III) in layered double hydroxide (LDH) phases is a critical process influencing the corrosion resistance of steel in cementitious environments. Here, we combine synchrotron-based X-ray techniques with density functional theory (DFT) calculations to unravel the atomistic mechanisms governing Fe(III) uptake in Mg-Al LDHs of different Mg/Al ratios. XRD and PDF analyses reveal systematic evolution of both long-range structure and local M-O/M-M distances with increasing Mg/Al ratio. XAS results show that Fe incorporation is suppressed at Mg/Al = 2, with a distinct oscillation pattern indicating incomplete substitution and the presence of ferrihydrite. Higher Mg/Al ratios yield spectra consistent with full incorporation into the LDH phase. DFT calculations support these findings, showing that Fe³⁺ substitutes for Al³⁺ in the main layers, but the details of this behavior are strongly composition dependent. Trends in the calculated substitution energy confirm that Fe(III) incorporation is most unfavorable at a Mg/Al ratio of 2 and becomes progressively more favorable at higher ratios. In Al-rich LDHs, Fe(III) introduces local strain and lowers the mechanical stability by compressing neighboring Al-O bonds, while in Mg-rich LDHs the flexible Mg-O framework accommodates Fe(III) more effectively via variation in the Mg-O environments. Simulated EXAFS spectra align perfectly with experimental trends, validating a model in which Fe(III) is partially excluded and precipitated as ferrihydrite in Al-rich LDHs but fully incorporated in Mg-rich structures. Overall, this study provides mechanistic molecular scale insights into Fe(III)-LDH interactions in cements, offering a new framework for optimizing steel passivation and enhancing the durability of sustainable infrastructure.

65

Eu₃Zn₂As₄ - A New Zintl Phase Exhibiting Complex Transport Properties and Magnetic Anisotropy

Author: Olha Pokhvata^{None}

A new ternary Zintl phase, $\text{Eu}_3\text{Zn}_2\text{As}_4$, was synthesized via a metal flux reaction, and its crystal structure was determined using single-crystal X-ray diffraction. $\text{Eu}_3\text{Zn}_2\text{As}_4$ crystallizes in the monoclinic crystal system with space group $C2/m$ and adopts the $\text{Ba}_3\text{Cd}_2\text{Sb}_4$ - type structure. Notably, $\text{Eu}_3\text{Zn}_2\text{As}_4$ represents the first rare-earth member of this structural family. Electronic structure calculations and electron counting predict metallic behavior for this compound. Resistivity measurements on a single crystal reveal a phenomenon of colossal magnetoresistance, with the highest resistivity observed at 0 Oe: $\rho(40\text{K}) = 1.41\text{ m}\Omega\text{ cm}$ ($\rho(300\text{K}) = 1.19\text{ m}\Omega\text{ cm}$). The Seebeck coefficient at 700 K was found to be $S_{700\text{K}} = 27.59\text{ }\mu\text{V K}^{-1}$. Magnetic studies indicate a complex magnetic structure, as multiple transitions were observed. Single-crystal magnetic measurements were performed with the magnetic field applied both parallel and perpendicular to the b-axis. When the field was aligned along the b-axis, an antiferromagnetic transition occurred at the Néel temperature, $T_N = 38.02\text{ K}$, followed by a ferromagnetic transition at 10.7 K. A Curie-Weiss fit yielded an effective magnetic moment of $7.6\text{ }\mu_B$, slightly lower than the expected value for Eu^{2+} ($7.94\mu_B$). The reduced magnetic moment indicates the coexistence of mixed-valence $\text{Eu}^{2+}/\text{Eu}^{3+}$ species, consistent with the charge balance of $(\text{Eu}^{2+})_{3-x}(\text{Eu}^{3+})_x(\text{Zn}^{2+})_2(\text{As}^{3-})_2[\text{As}_2]^{4-}(\text{e}^-)_x$. When the magnetic field was applied perpendicular to the b-axis, a ferromagnetic transition was observed at 34.6 K, followed by another transition at lower temperatures. The complex magnetic behavior is likely due to Eu chains aligned along the c-axis. The observed physical properties make $\text{Eu}_3\text{Zn}_2\text{As}_4$ a promising platform for exploring the interplay between magnetism and electronic transport.

63

Synthesis of Highly Non-Stoichiometric Garnets by Glass Crystallisation

Author: Michael Pitcher¹

¹ CNRS

The crystallization of glasses and undercooled melts is a relatively under-explored technique for the isolation of new metastable oxides, and when it is coupled to rapid melt-quenching methods it can be applied to a surprisingly wide range of compositions. Here I will present some new families of highly-nonstoichiometric aluminate garnets based on $\text{RE}_3\text{Al}_5\text{O}_{12}$ – well known luminescence hosts that are typically considered as line phases – which can form with up to 20mol% excess of rare-earth cations according to $\text{RE}_{3+x}\text{Al}_5\text{O}_{12}$ ($0 < x < 0.6$; $\text{RE} = \text{Eu}^{3+}$, Gd^{3+} , Tb^{3+} , Y^{3+}) by crystallising glassy precursors.[1-3] The crystal structures of these garnets accommodate excess RE^{3+} by substitution of Al^{3+} at the octahedral sublattice: for example, up to 30% of these crystallographic sites are substituted in $\text{Gd}_{3.6}\text{Al}_{4.4}$ a radical increase upon the defect-level concentrations achievable by solid state reaction methods. The distribution of RE^{3+} over two crystallographic sites has implications for the luminescence properties of these materials, because rare-earth activators are no longer confined to a single sublattice, and this has a strong impact on the chromaticity of up-conversion systems such as $\text{YAG:Yb}^{3+}/\text{Er}^{3+}$. This opens pathways to property tuning in garnets by control of host stoichiometry, and the prospect of improved performance or new applications for other garnet-type materials.

1 Cao et. al., Adv. Funct. Mater., 33, 2213418 (2023) 10.1002/adfm.202213418

2 Fang et. al., Chem. Mater., 36(17), 8555 (2024) 10.1021/acs.chemmater.4c02266

3 Fang et. al., Adv. Opt. Mater. (in press)

Revealing the Early Metal–Oxide Phase Transition of Platinum Nanocatalysts under PEMFC-Relevant Conditions

Authors: Raphaël Chattot¹; Carlos Campos-Roldán¹; Amir Gasmi¹; Meryem Ennaji¹; Jakub Drnec²

¹ CNRS-ICGM

² ESRF

The stability of platinum (Pt) nanocatalysts remains a key limitation for the long-term operation of proton exchange membrane fuel cells (PEMFCs). While Pt oxidation has been extensively investigated under model electrochemical conditions ¹, its behavior under realistic PEMFC operation is far less understood. In this work ², operando high-energy X-ray scattering was employed within a working PEMFC to directly capture the structural dynamics of Pt nanoparticles under potential control. The combined Rietveld and pair distribution function (PDF) analyses reveal a potential-induced transition from the metallic phase to an amorphous oxide state occurring at ~0.80 V vs. RHE—significantly below the commonly accepted onset and even below the cell open-circuit potential. The PDF analysis, although modestly applied, provides critical confirmation of the appearance of a new Pt–Pt interatomic distance around 3.3 Å, consistent with the formation of a disordered oxide layer distinct from the fcc metallic structure. This early metal–oxide phase transition is shown to coincide with a marked loss of surface crystallinity and directly influences both catalytic activity and transient Pt dissolution measured by online ICP-MS. These results challenge the conventional understanding of Pt oxidation limits in PEMFCs and highlight that significant structural reorganization can already occur within the normal operating voltage window. Beyond advancing the mechanistic picture of Pt degradation, this study demonstrates the potential of high-energy X-ray scattering combined with PDF analysis to uncover hidden amorphous states in realistic fuel cell environments, guiding the rational design of more durable catalyst materials and improved testing protocols.

References:

1. Magnussen, O. M. et al. In Situ and Operando X-ray Scattering Methods in Electrochemistry and Electrocatalysis. *Chem. Rev.* 124, 629–721 (2024).
2. Campos-Roldán, C. A. et al. Metal-oxide phase transition of platinum nanocatalyst below fuel cell open-circuit voltage. *Nat. Commun.* 16, 936 (2025).

Operando X-Ray Total Scattering for Electrocatalysis

Author: Meryem Ennaji¹

Co-authors: Alexandr Oshchepkov ²; Amir Gasmi ¹; Frédéric Jaouen ¹; Jakub Drnec ³; Julie GUEHL ⁴; Raphaël Chattot ⁵; Simon Amigues ¹; Tristan Asset ⁴

¹ ICGM, Univ. Montpellier, CNRS, ENSCM, 34095 Montpellier, France

² CBI, ESPCI Paris, Université PSL, CNRS, 75005 Paris, France

³ ESRF

⁴ Institut de Chimie et Procédés pour l'Energie, l'Environnement et la Santé, UMR 7515 CNRS- University of Strasbourg

⁵ CNRS-ICGM

The energy transition stands as one of the greatest challenges of today's society. In this context, electrocatalyst materials at the heart of electrochemical energy conversion devices such as fuel cells and water electrolyzers are expected to play an increasing crucial role in the near future. The urgent bottleneck to be overcome in electrocatalyst materials development to allow the widespread deployment of electrochemical systems is thus reaching combined high activity and long-term stability at low cost. Despite the diversity in electrocatalyst materials, the latter being largely imposed by the various types of electrochemical systems (noble vs. non-noble metals in acidic vs. alkaline media

for example) and the prerequisites of the different electrochemical processes (oxidation or reduction reactions of various species at different electrode potential ranges), most activity and stability properties of electrocatalysts directly derive from their (surface) chemistry and structure.

Advanced X-ray techniques help unlock the complexity of materials and drive innovation in energy applications. In particular, only operando experiments can provide the detailed, real-time understanding necessary to capture these dynamic changes.

Specifically, operando X-ray total scattering combined with atomic pair distribution function (PDF) analysis enables simultaneous probing of both crystalline and amorphous atomic architectures in nanostructured and unsupported Ir-based catalysts used in proton exchange membrane water electrolyzers (PEMWE). Similarly, these techniques allow tracking of Ni nanoparticle (NP) electrodeposition and oxidation states during the hydrogen evolution reaction (HER) for Anion Exchange Membrane Water Electrolyzers (AEMWE), or investigating carbon-capped Ni@C catalysts for the hydrogen oxidation reaction (HOR) at the anode of anion-exchange membrane fuel cells (AEMFCs). Overall, these studies provide insights into the complex, potential-dependent local structural dynamics occurring in electrocatalyst materials during operation, as well as practical examples of methods used to probe such properties.

60

Structural Stability of Liquid Bismuth Along the Melting Curve

Author: Shir Ben Shalom¹

Co-authors: Laura Henry²; Neta Ellert¹; Moran Emuna³; Yuri Kirshon¹; Pierre Pialt²; Andrew King²; Nicolas Guignot²; Yaron Greenberg³; Eyal Yahel³; Guy Makov¹

¹ Ben Gurion University of the Negev

² Synchrotron SOLEIL

³ Nuclear Research Centre Negev

The structure of the liquid phase is characterized by a short-range order, which is described by the structure factor, $S(Q)$, and the pair distribution function, $g(r)$. High pressure can induce notable structural changes in the liquid state, including changes in $S(Q)$ and $g(r)$, or in the coordination number. At extreme pressures and temperatures, liquids may undergo structural transformations as their atomic structures rearrange. Elemental metal liquids often retain the structural characteristics of their corresponding solid phases, exhibiting locally favored arrangements similar to their solid-state order. Bismuth exhibits remarkable structural and thermodynamic behavior under pressure, characterized by an anomalous melting curve, transitions between multiple low-symmetry solid allotropes, and several reported liquid transitions. Despite extensive research at ambient pressure, the structure of liquid Bi under high pressure remains poorly characterized, limiting our understanding of its phase behavior. In this study 1, we investigate the structure of liquid Bi in the 1-4 GPa pressure range, just above the melting line, across multiple solid phase transitions. Energy-dispersive X-ray diffraction (EDXRD) measurements were performed at the PSICHE beamline of the SOLEIL synchrotron. The collected data were used to derive $S(Q)$ and $g(r)$ at each pressure point. The first peak in the $g(r)$ shifts ~ 0.004 nm to higher r values ($\sim 1\%$), despite increasing density, while the second peak moves ~ 0.01 nm to lower r values ($\sim 1.5\%$). Coordination numbers of the first and second shells increase with density. Structural analysis using the Quasi-Crystalline Model reveals a persistent Bi-I rhombohedral-like short-range order, with only a minor variation in the α angle. Despite melting from different solid phases, these results indicate a surprising structural persistence in liquid Bi. Our findings show that the solid-liquid structural correlation observed in some elemental metals does not hold for bismuth.

1 Shir Ben Shalom, Neta Ellert, Laura Henry, Moran Emuna, Yuri Kirshon, Pierre Pialt, Andrew King, Nicolas Guignot, Yaron Greenberg, Eyal Yahel, and Guy Makov. Invariance of Liquid Bismuth Structure Along the Melting Curve. *Communication Materials*. (2025). Accepted.

76

Insights into the cubic symmetry of silver nanoparticles prepared by bottom-up mechanochemical synthesis

Authors: Ismael Pinheiro Lucas Xavier¹; Paulo Filho Marques de Oliveira¹

¹ *Institute of Chemistry*

Studies on the application of silver nanoparticles (AgNPs) in various fields such as catalysis have increased, and their efficiency is directly related to structural variations. Bottom-Up Mechanochemical Synthesis (BUMS) has attracted growing attention due to its simple and solvent-free synthesis approach. However, it still remains unclear how nanoparticles are organized at the local and intermediate structural levels. The present work aims to shed light on how continuous mechanical action can influence the structure of metallic nanoparticles.

The mechanochemical synthesis of silver nanoparticles (AgNPs) revealed, through Rietveld refinement, a lattice expansion of 0.20% after one hour of milling. However, the analysis of thermal parameters did not show a clear trend. Total X-ray scattering (TS) measurements combined with PDF modeling indicated a progressive increase in the agreement factor R_{wp} with increasing milling time (from 5.73% at 5 min to 10.50% at 60 min). The model employed for the PDF analysis was the face-centered cubic (fcc) structure with space group Fm-3m (No. 225 in the International Tables for Crystallography).

The MAXSUB tool from the Bilbao Crystallographic Server was used to identify lower-symmetry space groups compatible with the fcc model. Two progressively distorted structures — body-centered tetragonal (I4/mmm, No. 139) and orthorhombic (Fmmm, No. 69) — were tested, and their lattice and thermal parameters were compared. The PDF analysis, performed over the 1.5–30 Å range, used progressively larger fitting windows, starting from 2–6 Å and increasing in 2 Å steps up to 30 Å.

The results showed that up to the second coordination shell (~12 Å), the fcc (225) and orthorhombic (69) models become indistinguishable, i.e., between the less and more strained configurations. However, due to the stochastic nature of the mechanochemical process, involving random impacts, an anisotropic distortion is more likely, as also supported by the slightly lower R_{wp} values for the orthorhombic phase. Beyond 12 Å, the cubic arrangement provides a noticeably better fit to the AgNP structure, strongly indicating the presence of high local strain in the ball-milled AgNPs. This behavior may also represent a structural remnant of the early stages of nanoparticle formation, as it is well known that rapid nucleation is preceded by the formation of large, highly disordered aggregates.

71

Discovering the hidden (dis-)order in $A_2Se_2C_2$ ($A = Na-Cs$)

Authors: Tim Mattick¹; Uwe Ruschewitz¹

¹ *University of Cologne*

Heating A_2SeC_2H ($A = Na-Cs$) results in the formation of new compounds that can be indexed in small ($a = 3.899$ Å– 4.560 Å) cubic unit cells.¹ Additional spectroscopic data confirmed the presence of the $Se-C\equiv C-Se^-$ anion. This led to the postulation of the formula $A_2Se_2C_2$ and the proposed structure of a primitive cubic cell, in which the alkaline metal cations occupy the 0,0,0 position while the Se atoms are positioned on $\frac{1}{2}, \frac{1}{2}, \frac{1}{2}$.²

Although this simple model matches the XRPD patterns reasonably well, it indicates that the covalently bound $Se-C\equiv C-Se^-$ anion is stretched or compressed across the different alkaline metal cations.

Performing a simultaneous Rietveld and PDF fit of a $4\times 4\times 4$ supercell of the original cell using *TOPAS-Academic*[3,4] proved that the anion remains intact across all alkaline metal cations and that its orientation along the crystallographic a , b or c axes is random and uncorrelated. This arrangement maximizes the distance between neighboring Se^- anions, which can be seen as the driving force behind this configuration.

DFT calculations further proved that models with these randomly disordered anions are more stable than other models.

Bibliography

- 1 M. Hetzert, M. Werker, U. Ruschewitz, *Angew. Chem. Int. Ed.* **2018**, 57, 16475–16479.
- 2 M. Hetzert, PhD thesis, University of Cologne, **2021**.
- 3 A. A. Coelho, *J. Appl. Crystallogr.* **2018**, 51, 210–218.
- 4 A. A. Coelho, P. A. Chater, A. Kern, *J. Appl. Crystallogr.* **2015**, 48, 869–875.

75

Characterization of Zr-based bulk metallic glasses with high thermal stability for thermoplastic forming

Author: Lucas Eisenhut¹

Co-authors: Bastian Adam ; Lucas Ruschel ; Oliver Gross ; Ralf Busch

¹ *Universität des Saarlandes, Lehrstuhl für metallische Werkstoffe*

Bulk metallic glasses (BMGs) with high thermal stability are becoming increasingly important for manufacturing and processing due to their very slow crystallization kinetics in the low-temperature supercooled liquid region close to T_g . This is particularly important for the thermoplastic forming (TPF) process, as it determines the available processing window. In general, a higher thermal stability broadens the process window for TPF, enabling lower viscosities and higher deformations. Therefore, the alloys Zr₆₅Cu₁₅Ni₁₀Al₁₀ and Zr_{62.5}Cu_{22.5}Al₁₀Fe₅, known for their high thermal stability up to $\Delta T_x=110$ K, were examined with regard to their thermodynamic, kinetic and mechanical properties. The deformation behaviour during thermoplastic forming is presented in time-temperature-deformation (TTD) diagrams, which depict the material's response as a function of both temperature and time. Additionally, structural analysis using the reduced Pair-Distribution Function was carried out to investigate the short- and medium-range order, which is known to correlate with the mechanical performance. The results of this work show that the alloys are particularly well suited for industrial applications due to their excellent combination of high thermal stability, slow crystallization kinetics, and favourable deformation behaviour, enabling a wide processing window during TPF while maintaining reliable mechanical properties.

74

Investigation of the short-range order and disorder in U₃O₈ using neutron total-scattering PDF analysis

Authors: Alejandro Vieyra Huerta¹; Dirk Lamoen²; Gianguido Baldinozzi³; Gregory Leinders⁴; Henry Fischer⁵; Marc Verwerft⁴

¹ *Belgian Nuclear Research Center (SCK CEN)*

² *EMAT, University of Antwerp*

³ *Université Paris-Saclay, CentraleSupélec, CNRS, SPMS*

⁴ *Belgian Nuclear Research Centre (SCK CEN)*

⁵ *Institut Laue-Langevin*

Uranium dioxide (UO₂) is the most used nuclear fuel in power reactors. Understanding the uranium–oxygen (U–O) system is essential for managing nuclear waste as UO₂ can undergo oxidation even at room temperature, forming U₃O₈, the most thermodynamically stable oxide 1. While the U₃O₈ long-range crystallographic structure appears well-established [2,3], understanding its local atomic arrangement and potential disorder in the nanoscale is essential for predicting its structural properties and transformations in case of an accident and/or to ensure safety during interim storage or final disposal. In this poster, we present a comprehensive neutron total scattering investigation of

U₃O₈, where the pair distribution function (PDF) analysis was used to probe its short-range order. The determination of the U₃O₈ crystal structure presents a significant complexity due to its inherent nature, as crystallographic, spectroscopic, electronic and computational studies have shown [4-7]; this complexity is reflected in the PDF analysis refinement of U₃O₈, which has been equally challenging, and several strategies have been used to improve the fitting. PDF analysis reveals subtle deviations from the reported long-range orthorhombic lattice to a lower symmetry, suggesting the presence of local distortions, particularly in the uranium-oxygen polyhedra. These findings provide new insights into the structural complexity of U₃O₈ and its implications for fundamental and applied research.

In this work, the neutron scattering data were collected from room temperature to cryogenic temperature at the Institute Laue-Langevin (ILL).

Our results demonstrate the potential of neutron total scattering techniques in resolving hidden structural features in actinide oxides, contributing to a deeper understanding of their behavior under operational and environmental conditions.

1 P. Taylor, D.D. Wood, A.M. Duclos, D.G. Owen, J. Nucl. Mater., 168 (1989) 70.

2 B. Loopstra, Acta Crystallogr., 17 (1964) 651.

3 R.J. Ackermann, A.T. Chang, C.A. Sorrell, J. Inorg. Nucl. Chem., 39 (1977) 75.

4 A. Miskowiec, T. Spano, Z.E. Brubaker, J.L. Niedziela, D.L. Abernathy, R.D. Hunt, S. Finkeldei, Phys. Rev. B, 103 (2021) 205101.

5 A. Miskowiec, T. Spano, R. Hunt, A.E. Shields, J.L. Niedziela, S. Finkeldei, Phys. Rev. Mater., 4 (2020) 093610.

[6] R. Saniz, G. Baldinozzi, I. Arts, D. Lamoën, G. Leinders, M. Verwerft, Phys. Rev. Mater., 7 (2023) 054410.

[7] G. Leinders, R. Bes, K.O. Kvashnina, M. Verwerft, Inorganic Chemistry, 59 (2020) 4576.

96

From 100 keV to MeV: Energy Effects in Ultrafast Electron Diffraction

Author: Till Willershausen¹

¹ University Duisburg-Essen

Ultrafast electron diffraction (UED) captures atomic-scale structural dynamics with sub-picosecond time resolution by probing transient changes in both Bragg peaks and diffuse (inelastic) scattering [1,4]. Bragg scattering reports changes in average lattice order (e.g., transient lattice constants), while diffuse scattering encodes momentum-resolved phonon and quasiparticle populations [1-3].

This poster surveys energy dependence of the electron probe energy. Increasing the energy from the ≈ 100 –200 keV range into the multi-MeV regime substantially increases sample penetration, expands the accessible momentum transfer, and strongly suppresses multiple scattering, thereby simplifying the kinematic interpretation of Bragg intensities [1,2].

The reduced multiple scattering at higher energies improves the fidelity of diffuse signals—making momentum-resolved phonon mapping more robust. Additionally, the nearly flat Ewald sphere and the extended q-range at MeV energies enable quantitative analysis across a significantly larger portion of reciprocal space. Practical considerations at MeV include lower elastic scattering cross sections per atom (affecting signal levels and detector requirements) and higher facility and beam-conditioning demands compared with compact keV-scale setups [2,4]. In this poster, we discuss the suitability and specific advantages of different electron-energy regimes for UED applications.

1 D. Filippetto and H. van der Weide, “Ultrafast electron diffraction: Visualizing dynamic states of matter,” Rev. Mod. Phys. 94, 045004 (2022).

2 S. P. Weathersby et al., “Mega-electron-volt ultrafast electron diffraction at SLAC National Accelerator Laboratory,” Rev. Sci. Instrum. 86, 073702 (2015).

3 M. J. Stern et al., “Mapping momentum-dependent electron-phonon coupling and non-equilibrium phonon dynamics with ultrafast electron diffuse scattering,” Phys. Rev. B (2018).

4 F. Qi et al., “Breaking 50 femtosecond resolution barrier in MeV ultrafast electron diffraction,” *Phys. Rev. Lett.* 124, 134803 (2020).

98

Pair distribution functions of cellulose calculated from molecular dynamics

Author: Nil Tabudlong Jonasson¹

Co-authors: Andreas Fall ²; Malin Wohlerl ³; Maria Bånkestad ²; Michael Reid ²; Shun Yu ²

¹ *KTH Royal Institute of Technology*

² *RISE Research Institute of Sweden*

³ *Uppsala University*

Cellulose is the most abundant biopolymer on Earth, found mainly in the cell wall of plants. Structurally, the existence of different crystal allomorphs of cellulose are known 1. However, non-crystalline parts are believed to be more accesible to sorbed water moisture which can impact the mechanical properties 2.

The current study utilizes molecular dynamics simulations to generate different cellulose-water structures. From this, X-ray pair distrubtion functions (xPDF) are calculated to highlight how different structural features affects the function, such as disorder, surface chain arrangement, etc.

Future work of experimental xPDF are planned to capture changes of non-crystallinity in cellulosic systems with varying relative humidty. The molecular modelling together with machine learning is intended to help interpret the results.

1 Z. Peter, Order in cellulosics: Historical review of crystal structure research on cellulose, *Carbohydr Polym* 254 (2021). <https://doi.org/10.1016/j.carbpol.2020.117417>.

2 L. Solhi, V. Guccini, K. Heise, I. Solala, E. Niinivaara, W. Xu, K. Mihhels, M. Kröger, Z. Meng, J. Wohlerl, H. Tao, E.D. Cranston, E. Kontturi, Understanding Nanocellulose-Water Interactions: Turning a Detriment into an Asset, *Chem Rev* 123 (2023) 1925–2015. <https://doi.org/10.1021/acs.chemrev.2c00611>.

104

Atomic-scale investigation of short-range ordering formation in Fe–Mn–Al–C lightweight steels

Author: Wenwen Song¹

¹ *University of Kassel*

The newly developed alloys, Fe-Mn-Al-C lightweight steels, are designed with heavy alloying to fulfil the specific property requirements driven by their applications in transportation, energy and infrastructure sectors. The strategic engineering of short-range ordering (SRO) in Fe-Mn-Al-C steels for automotive and hydrogen energy applications poses significant advancement in material science and engineering targeted at enhancing strength-ductility balance, and resistance to hydrogen embrittlement. The essence of SRO engineering lies in manipulating the SRO and its atomic structures within the steel matrix. The synchrotron pair distribution function (PDF) analysis stands out as a vital technique for investigating the atomic structure of short-range ordered phases. The local atomic configurations associated with SRO formation influence the subsequent κ -phase precipitation and the overall deformation behaviour. However, the quantitative understanding of the atomic-scale SRO formation in these complex multi-element systems remains largely unclear due to the limited sensitivity of conventional diffraction methods to local order.

In this study, we employed in-situ/ex-situ high-energy synchrotron total-scattering experiments at beamline P02.1 (PETRA III, DESY, Germany) to investigate the evolution of local atomic correlations during the early ageing stages of Fe–Mn–Al–C steels. The scattering vector ranges up to $Q \approx 25 \text{ \AA}^{-1}$. Three representative alloy, Fe–30Mn–8Al–1.2C, Fe–30Mn–6.5Al–1.2C, and Fe–30Mn–8Al–0.8C (wt.%), were studied under controlled isothermal conditions of 600 °C to capture the transition from a chemically disordered solid solution to partially ordered local structures. These synchrotron PDF results are complemented by near-atomic characterization using atom probe tomography (APT) and positron lifetime annihilation spectrum (PLAS) techniques, which together provide complementary insights into the evolution of local chemical ordering and vacancy-related phenomena, establishing a link between atomic-scale clustering and the early stages of SRO formation.

84

Effect of manganese substitution on the local atomic structure of amorphous Fe-based metallic glasses

Author: Daria Yudina^{None}

Co-authors: Ravneet kaur¹; Jozef Kovac²; Pavol Sovak³; Jozef Bednarčík⁴

¹ *P.J. Safarik University in Kosice Slovakia*

² *Institute of Experimental Physics, Slovak Academy of Sciences, Watsonova 45, 040 01 Košice, Slovakia*

³ *Institute of Physics, Faculty of Science, P.J. Šafárik University in Košice, Park Angelinum 9, 041 54 Košice, Slovakia*

⁴ *P.J. Safarik University in Kosice, Faculty of Science, Institute of Physics*

Fe-based metallic glasses are known for their excellent soft magnetic properties, which are mainly due to the disordered structure, inherent to the glassy state. In this work, special emphasis is placed on the study of partial substitution of Fe by Mn and its impact on the local atomic structure and magnetic properties. The single-roller melt-spinning technique was used to prepare a series of alloys in the form of thin ribbons with the nominal composition Fe(73.5–x)MnxSi13.5Cu1Nb3B9 (x = 1–15 at.%). The atomic structure of all materials in the as-quenched state was investigated by high-energy synchrotron radiation at the P21.2 beamline of PETRA III at DESY, Hamburg, Germany. X-ray scattering experiments were performed in transmission mode using a monochromatic beam with energy of 100 keV ($\lambda=0.012398 \text{ nm}$). Scattered photons were recorded using a two-dimensional (2D) detector. The 2D patterns were corrected for background air scattering, and azimuthal integration was performed using the pyFAI program 1. The obtained intensity profiles, $I(q)$, were converted to the structure factors, $S(q)$, which were subsequently Fourier transformed into the pair distribution function (PDF), $G(r)$, using the pdfgetX2 program 2.

Structure factors, $S(q)$, for all samples reveal a distinct first diffuse sharp peak located at around $q=30 \text{ nm}^{-1}$, with gradually decaying oscillations visible up to $q_{\text{max}} = 170 \text{ nm}^{-1}$. Corresponding pair distribution functions, $G(r)$, show asymmetric maximum located between 0.21 and 0.34 nm (first coordination shell), which corresponds to the nearest atomic neighborhood. Considering the concentration of the given atoms and their atomic radii, the shape of the first coordination shell is mostly determined by three components: Fe(Mn)–Fe(Mn), Fe(Mn)–Si, and Fe(Mn)–Nb atomic pairs. Assuming a Gaussian distribution for all three components, excellent fits to the first coordination shell were achieved. Despite the pronounced changes in magnetic properties caused by Mn substitution, as reported in our previous work 3, the PDF analysis showed that the local atomic structure remains stable within experimental uncertainties.

References

- 1 J. Kieffer et al., “Application of signal separation to diffraction image compression and serial crystallography,” *J. Appl. Crystallogr.*, vol. 58, no. 1, pp. 138–153, Feb. 2025, doi: 10.1107/s1600576724011038.
- 2 X. Qiu, J. W. Thompson, and S. J. L. Billinge, “PDFgetX2: a GUI-driven program to obtain the pair distribution function from X-ray powder diffraction data,” *J. Appl. Crystallogr.*, vol. 37, no. 4, pp. 678–678, July 2004, doi: 10.1107/s0021889804011744.
- 3 S. Michalik, J. Bednarčík, J. Kovac, H. Franz and P. Sovak, *J. Phys. D: Appl. Phys.* 45, 455302, (2012)

Contact: daria.yudina@upjs.sk

105

Total scattering analysis of Si-thin film anodes for lithium ion batteries

Authors: Andre ten Elshof¹; Giuseppe Portale²; Harshan Madeshwaran²; Ivan Trefilov¹; marco di michiel³

¹ *University of Twente*

² *University of Groningen*

³ *ESRF*

Si is a promising material candidate for the next-generation of lithium ion batteries. Compared to commercially available graphite electrodes, Si electrodes provide significantly higher gravimetric capacity (3579 mAh/g for Si vs 370 mAh/g for graphite), owing to the alloying mechanism through which Li⁺ is stored as Li_xSi ($x \leq 3.75$) [1,2]. Thus, the commercialization of Si in LIBs will pave the way for high-energy density batteries. However, despite the promising properties of Si electrodes, their utilization is hindered by the 300% volume change that occurs during cycling. This severe volume change generates stress within the electrode, leading to cracking of the electrode and formation of the passivating solid electrolyte interface (SEI). Additionally, the amorphization of the silicon during the first cycle makes XRD unsuitable to investigate the structure of the electrodes. In this regard, total scattering is a unique technique to shed light on the local atomic structure of Si electrode at different states of cycling. PDF analysis can provide information on the local atomic structure (Si-Si and Li-Si correlations) of the cycled model electrode of amorphous nature [4,5], especially for low crystallinity or amorphous electrodes. So far, no reports exist in literature on the investigation of binder free thin-film model systems. To fill this gap of knowledge, we investigated pristine and cycled low crystalline and amorphized Si thin films electrodes deposited by chemical vapour deposition using XRD and PDF analysis

97

From 100 keV to MeV: Energy Effects in Ultrafast Electron Diffraction

Author: Till Willershausen¹

¹ *University Duisburg-Essen*

Ultrafast electron diffraction (UED) captures atomic-scale structural dynamics with sub-picosecond resolution by tracking transient changes in both Bragg peaks and diffuse (inelastic) scattering [1–4]. While Bragg intensities reflect modifications of the average lattice structure, diffuse scattering provides momentum-resolved access to phonon and quasiparticle populations [1–3].

This poster discusses how key aspects of UED performance depend on the electron probe energy. Raising the energy from the ≈ 100 –200 keV range to the multi-MeV regime increases sample penetration, extends the accessible momentum transfer, and strongly suppresses multiple scattering—thereby enabling more kinematic Bragg analysis and reducing interpretational ambiguities [1,2]. The reduction of multiple scattering at higher energies also enhances the clarity and quantitative reliability of diffuse-scattering signals, improving the robustness of momentum-resolved phonon mapping. Moreover, the nearly flat Ewald sphere at MeV energies, together with the expanded q-range, allows analysis over a substantially larger portion of reciprocal space.

1 D. Filippetto and H. van der Weide, “Ultrafast electron diffraction: Visualizing dynamic states of matter,” *Rev. Mod. Phys.* 94, 045004 (2022).

- 2 S. P. Weathersby et al., “Mega-electron-volt ultrafast electron diffraction at SLAC National Accelerator Laboratory,” *Rev. Sci. Instrum.* 86, 073702 (2015).
- 3 M. J. Stern et al., “Mapping momentum-dependent electron-phonon coupling and non-equilibrium phonon dynamics with ultrafast electron diffuse scattering,” *Phys. Rev. B* (2018).
- 4 F. Qi et al., “Breaking 50 femtosecond resolution barrier in MeV ultrafast electron diffraction,” *Phys. Rev. Lett.* 124, 134803 (2020).

95

PDF data collection at MSPD beamline: past, present and future

Authors: Alexander Missyul¹; Catalin Popescu¹; Francois Fauth¹

¹ *ALBA synchrotron light source*

MSPD beamline at ALBA synchrotron is a powder diffraction beamline operating at the energy range from 8 to 50 keV. In order to achieve Q-range suitable for PDF analysis using such energies, diffraction data must be collected up to relatively high 2θ values which is done using linear MYTHEN detector. While this configuration is relatively time-consuming, it has the benefit that the data are collected with high angular resolution and the same dataset can be used both for real-space and inverse-space analysis.

MYTHEN1 detector initially installed at MSPD was limited to 30 keV energy. It was recently upgraded to MYTHEN2 model capable to operate up to 40 keV, which provided access to higher Q-values. Effects of this upgrade are discussed comparing the data from real samples collected in both configurations.

As ALBA is approaching its upgrade to 4th generation, MSPD will be significantly upgraded as well. Expected effects of this upgrade to PDF data collection, including possibility of fast measurements using large-area 2D PILATUS detector are presented.

91

Unveiling Atomic-Level Disorder in Zinc Hydroxy-stannate ($\text{ZnSn}(\text{OH})_6$) using Three-Dimensional Δ PDF Approach

Author: Hassan Murtaza¹

¹ *University of Warsaw*

Zinc hydroxy-stannate ($\text{ZnSn}(\text{OH})_6$, ZHS) has emerged as a distinctive material owing to its adaptable morphology, structural integrity, and potential for an extensive range of applications. Recent investigations have identified two distinct synthesis strategies designed for controlling the crystallinity and shape of ZHS. Study (i) demonstrated the hydrothermal growth of single-crystalline ZHS microcubes on indium tin oxide (ITO) substrates via a dissolution-precipitation mechanism, resulting in highly uniform cubes exhibiting a preferential [200] orientation. Approach (ii) reported low-temperature (10–70 °C) wet-chemical synthesis that produced size-tunable nano-cubes and octahedra, with precursor concentration and reaction temperature having a direct impact on morphology and lattice parameters. Advanced structural characterizations utilizing synchrotron XRD and HR-TEM have validated subtle lattice variations and facet-dependent electrical behavior, with [111]-terminated octahedra demonstrating superior conductivity in comparison to [100]-terminated cubes. However, Prior research didn't sufficiently investigate the local structural disorder of the ZHS lattice.

The goal is to apply 3D- Δ PDF analysis to clarify the short and medium-range atomic distortions of ZHS. This approach will provide significant insights into the structure-property relationship, establishing a robust foundation for the systematic advancement of next-generation hybrid and high-entropy oxide nanostructures.

How the behavior of cations within the interfacial layer can influence the water structure in nanoconfined electrolyte solutions

Author: Hassan Khoder¹

Co-authors: Guilhem Quintard¹; Gavin Vaughan²; Diane Rebiscoul¹

¹ *Institut de Chimie Séparative de Marcoule*

² *European Synchrotron Radiation Facility*

Understanding the processes taking place at solid/aqueous interfaces under nanoconfinement is essential for predicting the behavior of nanoporous materials such as cementitious materials, biominerals, clays, and related materials. The structure and dynamics of confined water in the presence of ions strongly influence these interfacial processes, as we have previously shown in the alteration of mesoporous silica materials [1-2] and glass 3, mainly through ion adsorption at the interface that modifies water structuring [4-5].

Our recent quasi-elastic neutron scattering study [6] shows that water dynamics in MCM-41 with 2.6 nm pores are primarily governed by confinement and by the chaotropic/kosmotropic nature of monovalent cations, whereas divalent cations induce a stronger slowdown of water mobility due to their enhanced interactions with the silica surface.

Building on these insights, this project targets the structural signature of confined water and ions to highlight how chaotropic/kosmotropic properties of ions and their valency manifest within the hydrogen-bond network of water. We performed total X-ray scattering measurements at the ID15-A beamline on water confined with various ions in the same MCM-41 samples. The pair distribution functions (PDFs) were extracted and combined with empirical simulations to obtain partial PDFs within the interfacial layer, following the approach described in [7]. Ongoing analyses show ion-specific effects that depend on their interfacial distribution.

This structural investigation will provide a detailed description of ion organization and its impact on confined water, ultimately enabling the establishment of a structure–dynamics relationship.

1 M. Baum, *et al.*, *J. Phys. Chem. C* **124**, 14531-14540 (2020). 2 M. Baum, *et al.*, *Langmuir* **35**, 10780-10794 (2019). 3 D. Rébiscoul, *et al.*, *J. Phys. Chem. C* **119**, 15982-15993 (2015).

4 K. Wang, *et al.*, *J. Phys. Chem. C* **125**, 20551-20569 (2021). 5 D. Rébiscoul, *et al.*, *Journal of Colloid and Interface Science* **614**, 396-404 (2022).

[6] H. Khoder, *et al.*, *J. Phys. Chem. C* **128**, 12558–12565 (2024).

[7] H. Khoder, *et al.*, *Acta Cryst. A* **76**, 589–599 (2020).

Linking the local structure to reversible O redox and electrochemical performance of Li₂MnO₃

Author: Przemysław Bańkowski¹

Co-authors: Wojciech Olszewski¹; Konstantin Koster²; Payam Kaghazchi³; Jon Serrano⁴; Lakshmi Priya Musuvathi Babual⁴; Marine Reynaud⁴; Oleg Usoltsev⁵; María Jáuregui⁴; Pierluigi Gargiani⁵; Andrea Sorrentino⁵; Vlad Martin Diaconescu⁵; Pol Pérez Quer⁵; Laura Simonelli⁵

¹ *Faculty of Physics, University of Białystok, 1L K. Ciołkowskiego Str., 15-245 Białystok, Poland*

² *Institute of Energy and Climate Research, Forschungszentrum Jülich GmbH, D-52425 Jülich, Germany*

³ *Institute of Energy and Climate Research, Forschungszentrum Jülich GmbH, D-52425 Jülich, Germany; MESA+ Institute for Nanotechnology, University of Twente, 7500 AE Enschede, The Netherlands*

⁴ *CIC EnergiGUNE Parque Tecnológico de Álava, Albert Einstein Kalea, 48, 01510 Vitoria-Gasteiz, Álava*

⁵ *ALBA Synchrotron Light Facility, Carrer de la Llum 2-26, 08290 Cerdanyola del Vallés, Barcelona, Spain*

Li- and Mn-rich transition metal (TM) oxides are the subject of intensive investigation as next-generation cathode materials, offering high capacities (>250 mAh/g) through a joint cationic and

anionic redox activity 1. However, despite their potential to outperform commercial materials like LiCoO_2 , a deeper understanding of the link between their microstructure and the charge compensation mechanism is still missing.

In LiTMO_2 layered structures, Li and TM layers are alternately stacked following an O3 sequence (ABCABC) 2. Because of that layered structure, Li-rich layered oxides possess a high density of stacking faults that significantly impedes accurate microstructural characterization 3. In particular, structural descriptors related to the activation of oxygen have not been identified so far.

In this work, a series of Li_2MnO_3 samples differing in the amount of stacking faults, with similar morphology and substantial difference cycle properties have been prepared and thoroughly characterized by means of temperature dependent X-ray Absorption Spectroscopy and X-ray Spectromicroscopy. Analysis of obtained data allowed to study the concurrent microstructural features on the electrochemical performances of Li_2MnO_3 and to identify the Mn-O local force constant as the key structural descriptor related to the activation of oxygen.

1 G. Assat et al., Nat. Energy. 3 (2018): 373-386.

2 C. Delmas et al., Phys. B+C 99 (1980): 81-85.

3 J. Serrano-Sevillano et al., Phys. Chem. Chem. Phys. 20 (2018): 23112.

94

In situ reaction monitoring of sulfide solid electrolytes in liquid phase.

Author: Zachary Warren¹

¹ *Instituto de Cerámica y Vidrio - Consejo Superior de Investigaciones Científicas*

Understanding how sulfide solid electrolytes form in solution is critical for controlling phase purity, ionic conductivity, and reproducibility in liquid-phase synthesis routes. Here, we employ in situ Raman spectroscopy to directly monitor the reaction pathways governing the formation of thiophosphate-based sulfide solid electrolytes during liquid-phase synthesis. Using a temperature-controlled Raman cell, we track the temporal evolution of key molecular species—ranging from PS_4^{3-} , $\text{P}_2\text{S}_6^{4-}$, and higher-order thiophosphate intermediates to the final solid phases—under realistic reaction conditions. Time-resolved spectra reveal rapid solubilization steps, ligand-exchange processes, and the emergence of reactive molecular clusters that precede precipitation. Kinetic analysis indicates that the reaction follows a nucleation-controlled growth mechanism consistent with a Finke-Watzky two-step model, enabling quantification of rate constants and activation behavior. The combination of molecular-level insight and operando monitoring provides a mechanistic framework that connects early solution chemistry to the structure and performance of the resulting solid electrolyte. This work demonstrates that in situ spectroscopic tracking is essential for rational design, accelerated optimization, and scale-up of liquid-phase synthesis strategies for next-generation all-solid-state batteries.

83

Growth and Characterization of $\text{Yb}_2\text{Si}_2\text{O}_7$ and Yb_2SiO_5 Crystals

Author: Andrius PAKALNISKIS¹

Co-authors: Monica Ciomaga Hatnean ¹; Romain Sibille ²

¹ *Paul Scherrer Institute*

² *Paul Scherrer Institut*

The family of rare earth (RE) based silicate materials is quite vast, not only in terms of possible chemical compositions, but also in terms of the available crystal structures. In particular, the RE_2SiO_5 (monosilicate), $\text{RE}_2\text{Si}_2\text{O}_7$ (disilicate) families have attracted a lot of attention, mainly due to their polymorphic behavior as well as their peculiar physical and chemical properties. For example, the disilicate phase has at least seven known polymorphs that can be obtained based on the composition and temperature 1. Meanwhile, the monosilicate system has two possible polymorphs referred in the literature as either X1 or X2. The X1 polymorph is always obtained with larger RE ions (La – Gd), however, in the case of smaller RE ions (Tb – Lu) X2 can be stabilized by using a relatively low calcination temperature between 900 and 1100 °C 2. The natural abundance of the crystal structures as well as broad chemical composition ranges of rare-earth silicates led to an investigation of potential applications as either host materials for luminescence or for their scintillation properties. More recently, the silicates are being investigated as thermal barrier coating due to their thermal conductivity 3. At the same time, their magnetic properties largely remain unexplored. However, while promising the RE based silicates suffer significantly due to the lack high-quality single phase samples. The main reason for this is that the different phases, be it RE_2SiO_5 , $\text{RE}_2\text{Si}_2\text{O}_7$ or even the apatite ones are quite close in stability. As such, when preparing bulk samples, one often obtains a mixture of all or some of the phases. To further and unambiguously investigate the fundamental properties of the RE silicate materials, high-quality crystal samples are required. In this work we present the synthesis and crystal growth of Yb_2SiO_5 and $\text{Yb}_2\text{Si}_2\text{O}_7$ using a laser diode optical floating zone furnace. We also investigate their crystal structure and quality by means of powder and single crystal X-ray diffraction as well as Laue diffraction.

1 J. Felsche, The crystal chemistry of the rare-earth silicates, in: 1973: pp. 99–197.

2 J. Wang, S. Tian, G. Li, F. Liao, X. Jing, Mater. Res. Bull. 2001, 36, 1855–1861.

3 H.S. Nair, T. DeLazzer, T. Reeder, A. Sikorski, G. Hester, K.A. Ross, Crystals, 2019, 9, 196.

99

Polymorphism in the metal-organic framework Qc-5-Cu

Authors: Julie Brun¹; Petra Agota Szilagyi¹

¹ University of Oslo

The metal-organic framework (MOF) Qc-5-Cu has at least two possible polymorphs. Metal-organic frameworks are built up of organic linkers bridging between inorganic secondary building units (SBUs) and are of interest for catalysis and gas separation. The structures of Qc-5-Cu are either square-layered (Qc-5-Cu-sql) or diamondoid (Qc-5-Cu-dia), with different coordination environments around the copper ion, which is the SBU.

Both the long-range order of the crystal, and within it the pores, and the short-range order of the Cu coordination, the hypothesised catalytic site, are essential for a functioning MOF catalyst.

We want to study the coordination of the Cu ion with PDF, XRD and EXAFS, to first understand the driving force behind the crystallization of the different polymorphs and further investigate the relationship between the catalytic properties and structure.

109

Structural Evolution in Metal-Organic Frameworks Melting and Glass Transition via Pair Distribution Function Analysis

Author: Minhyuk Kim¹

Co-author: Hoi Ri Moon

¹ Ewha womans university

Metal-organic frameworks (MOFs) are a class of materials characterized by infinite networks formed through coordination bonds, offering versatile properties and functions. While traditionally regarded as strictly crystalline solids, the accessibility of liquid and glass states in these materials was experimentally demonstrated in 2015¹. Expanding on this frontier, we recently investigated melting and glass formation in MOFs composed of aliphatic dicarboxylate linkers containing alkane moieties. We observed that the phase transition behavior, specifically the presence of crystallization, glass transition, and melting, is critically dependent on the organic linker length, where longer chains facilitated glass transition and melting. To elucidate the local structural features of the glass and liquid phases, we employed both laboratory and synchrotron X-ray Pair Distribution Function analyses. This approach allowed for a direct structural comparison between the crystalline and amorphous phases. Furthermore, small-box modeling using PDFgui based on the initial crystalline structures enabled us to assign the structural origins of specific PDF peaks. By analyzing structural discrepancies between the glass (ex-situ) and liquid (in-situ) states, we established a plausible hypothesis regarding the glass transition mechanism in aliphatic-based MOF systems. This work highlights the utility of PDF analysis in the field of MOF glasses, demonstrating that comparative data analysis provides strong structural insights and paves the way for future validation through computational modeling.

[Ref. 1] Hybrid glasses from strong and fragile metal-organic framework liquids, T. D. Bennett et al. Nat. Commun. 2015, 6, 807.

[Ref. 2] Melt-quenched carboxylate metal-organic framework glasses, M. Kim et al. Nat. Commun. 2024, 15, 1174.

87

Absorption correction of high-Q electron PDFs: A comparative study on Au and Bi_{1.5}Co_{0.25}Ti₂O_{6.5}

Author: Roman Paul¹

Co-authors: Jefferson Bettini²; João Batista Souza Junior²; Lars Robben¹; Thorsten M. Gesing¹

¹ University of Bremen

² Laboratório Nacional de Nanotecnologia

The accurate determination of electron pair-distribution functions (ePDF) for nano-crystalline materials is strongly affected by absorption, and multiple as well as inelastic scattering contributions. These effects become increasingly significant at high Q, where they lead to systematic reduction of the measured intensity, compared to the ideal elastic scattering intensity. As a result, conventional ePDF processing tools may favor effective atomic scattering factors that are smaller than the true ones, particularly in materials containing heavy elements, a behavior also noted in existing eRDF implementations¹. We have investigated this behavior using gold nanoparticles as a well-defined reference system and applied the resulting corrections to the pyrochlore-type oxide Bi_{1.5}Co_{0.25}Ti₂O_{6.5}. Using the electron scattering factors provided by Lobato and van Dyck² to define the ideal elastic high-Q behavior, we derive a high-Q absorption correction providing a more physically consistent high-Q decay of the elastic scattering intensities. To further validate the corrected structure functions, complementary xPDF data using Ag K α radiation are collected. After correction, the ePDF shows an improvement in relative peak intensities and overall peak broadening. This approach provides a practical route to reduce absorption-related changes in TEM electron diffraction and demonstrates how corrected high-Q intensities enable more accurate local-structure analysis in complex oxides.

We financially acknowledge support by DAAD within the DAAD-CAPES-PPP program under project ID 57750309. We are additionally grateful to LNNano/CNPEM for supporting the project with possibilities using their facilities, especially for TEM measurements.

¹ Shanmugam et al. SoftwareX 6, 2017, 185-192.

² Lobato et al. Found. Crystallogr. 70, 2014, 636-649.

PDF across-the-board in science - the x-ray total scattering portfolio at P07-DESY and P21.1 at PETRA III

Author: Ann-Christin Dippel¹

Co-authors: Olof Gutowski²; Fernando Igoa³; Jiayu Liu³; Philipp Glaeveccke²; Martin v. Zimmermann²

¹ *Deutsches Elektronen-Synchrotron DESY*

² *Deutsches Elektronen-Synchrotron*

³ *DESY*

At the high-brilliance storage ring PETRA III at DESY, Hamburg, the two stations P07-DESY and P21.1 specialize in advanced x-ray total scattering (TS) techniques to study local disorder in a variety of sample types. Fast TS measurements on powdered, liquid or solid bulk samples is routinely available for traditional PDF analysis assuming fully random distribution of the scattering coherent domains. For in situ experiments, the beamlines offer spacious heavy-load sample stages for user-specific setups and access to standard sample environments e.g. for heating and cooling. The stations are equipped to apply the more recent 3d- Δ PDF method on single crystals as well as epitaxial thin films under ambient and non-ambient conditions. All thin film samples exhibiting a film thickness in the nanometer range are measured in grazing incidence to obtain high-quality PDFs on amorphous, nano- and polycrystalline layers as well as single-crystalline films. Owing to the high flux microfocused beams, the surface sensitivity reaches down to just a few nanometers in film thickness when using either amorphous or single-crystalline substrates. In addition, high-performance x-ray diffraction computed tomography (XRD-CT) scans are carried out in TS mode when PDF contrast is required. This presentation outlines the TS capabilities of the P21.1 and P07-DESY instruments to illustrate the wide range of opportunities for PDF-based structural studies at our facilities.

On the Multistage Mechanism of Lithium (De)insertion of Lithium Iron Oxysulfide Disordered Antiperovskite Cathodes

Authors: Xavier Kouoi¹; Marine Reynaud²; Marnix Wagemaker³; Theodosios FAMPRIKIS^{None}

¹ *TU Delft // CIC energiGUNE*

² *CIC EnergiGUNE Parque Tecnológico de Álava, Albert Einstein Kalea, 48, 01510 Vitoria-Gasteiz, Álava*

³ *TU Delft*

Global needs for electrochemical energy storage solutions are increasing, yet the lithium-ion battery market still relies on the same few cathode active materials. The disordered antiperovskite Li_2FeSO promises a cheap iron-based, and high-capacity cathode material with potential for safer solid-state batteries, but the exact reaction is still poorly understood.

This study seeks to understand the structural and chemical changes of the multi-stage (de)lithiation mechanism of positive electrodes through electrochemical cycling, x-ray diffraction, Mossbauer spectroscopy and x-ray absorption spectroscopy (Fe and S k-edges).

We have identified a reversible delithiation (charge) range involving the oxidation of Fe+II to Fe+III, separated into two reversible processes: a phase transition then a solid solution process. The observed peak broadening indicates a lithium-content-dependent crystallinity and the existence of a distorted structure that is reversible into a highly crystalline antiperovskite upon lithiation (discharge).

Further charge increases the energy storage but leads to a third and irreversible delithiation process involving the oxidation of sulfur from S-II to an unidentified sulfur species. Understanding and stabilizing this process may allow increase the capacity from about 200 to 300 mAh/g.

The coordination of redox-active Fe and S causes intricate evolutions in bulk spectroscopy, which require local characterization such as EXAFS and PDF to fully deconvolute the reactivity of each redox center.

These findings may guide future research, design and application of the material in the efforts of diversifying available Li-ion technologies.

93

Effects of compression on the local structure of selected active pharmaceutical ingredients in liquid and glass

Author: Anna Janowska¹

Co-authors: Ewa Kamińska ; Kamil Kamiński ; Karolina Jurkiewicz ; Paulina Jesionek ; Taoufik Lamrani

¹ *University of Silesia in Katowice*

Vitrification is a method commonly used to improve solubility and bioavailability of poorly water-soluble active pharmaceutical ingredients (APIs). It should be mentioned that high-pressure can be applied during the vitrification process, resulting in obtaining pressure-densified glass (PGD), which may differ in properties from glass prepared in conventional way – ordinary glass (OG). However, little is known about the effect of compression on the local structure of different types of glasses and liquids of APIs, in particular, on their intermolecular structure, bonding pattern, molecular conformations, and tendency of molecules to aggregate. Furthermore, it is unknown how these properties affect macroscopic characteristics. This issue is especially important in the case of tableting process, which can result in changes of the structure of amorphous APIs, which in turn can affect pharmacokinetic processes. Therefore, in the present study, we explore the impact of elevated pressure on the structure of two APIs – probucol and loratadine – in liquid and glassy forms. We conducted X-ray diffraction experiments at ambient as well as elevated pressure (using ID15B beamline, ESRF, Grenoble). Because it is impossible to capture subtle structural differences based solely on experimental results, molecular dynamics (MD) simulations were performed. The agreement of MD models with experimental results was validated and detailed structural analysis, including total and partial structure factors and pair distribution functions, was conducted based on them. These studies contribute to gain a better understanding of the atomic-scale structure and properties of pharmaceuticals produced in amorphous forms at various thermodynamic conditions.

79

Three-dimensional magnetic pair distribution function analysis of TbSb

Author: Sabrina Hatt¹

Co-author: Benjamin Frandsen ¹

¹ *Brigham Young University*

Magnetic pair distribution function (mPDF) analysis has been established as an effective means of probing short-range magnetic correlations in both powders and single crystals. For the latter, however, three-dimensional (3D) mPDF analysis of single crystals is somewhat less developed and remains comparatively under-utilized. Here, we present a detailed 3D-mPDF study of antiferromagnetic TbSb, which crystallizes in the NaCl structure. The fcc lattice of Tb atoms results in frustration of the antiferromagnetic interactions, leading to rich behavior including robust short-range magnetic correlations and critical scattering above the ordering temperature. Using TbSb as an example case, we discuss effective methods for extracting and modeling 3D-mPDF patterns from the magnetic diffuse scattering. The data reveal unexpectedly rich features stemming from the short-range magnetic correlations and magnetic domain structure in TbSb, providing insight into the influence of local magnetic correlations in TbSb and highlighting the power of 3D-mPDF analysis. Ultimately, our approach allows us to directly visualize the magnetic structure of the material and determine the nature of its short-range magnetic correlations.

Structural and thermal behavior of Cu_{1-x}Bi_x nanowires grown by template-assisted electrodeposition

Authors: Alejandra Guedeja-Marrón¹; Alok Ranjan²; Catherine Dejoie³; Eva Olsson²; François Fauth⁴; Gabriel Sánchez-Santolino¹; Henrik Lyder Andersen⁵; Inés García-Manuz⁶; Lucas Pérez¹; Lunjie Zeng²; Maria Varela¹; Matilde Saura Muzquiz¹; Paolo Perna⁶

¹ Universidad Complutense de Madrid

² Chalmers University of Technology

³ European Synchrotron Radiation Facility (ESRF)

⁴ CELLS-ALBA Synchrotron

⁵ Instituto de Ciencia de Materiales de Madrid (ICMM-CSIC)

⁶ Instituto Madrileño de Estudios Avanzados – IMDEA Nanociencia

Bismuth (Bi), known for its strong spin-orbit interaction (SOI), has been investigated in semiconductor heterostructures for efficient spin control.[1, 2] In particular, *ab initio* studies identified Bi-doped Cu alloys as promising candidates for all-metallic spin-current generation,³ a prediction later confirmed experimentally by Niimi *et al.*, who reported a large spin Hall angle (SHA \approx -0.24) in CuBi alloys with \sim 0.5% Bi doping.⁴ While skew scattering has been proposed as the main driving force behind the spin Hall effect in CuBi alloys,⁵ there are still unresolved questions regarding the underlying origin of this behaviour. Structural characteristics including composition, crystallinity, Bi distribution, the presence of impurities, and defects like grain boundaries, are expected to play a key role. Moreover, Bi segregation under elevated temperatures or applied electric fields may critically affect the performance of future CuBi based devices.

In this work, we present a synthesis protocol for electrodeposited Cu(1-x)Bi(x) nanowires (NWs), enabling control over both alloy composition and crystalline domain size. Using 4D-STEM, EELS, in situ variable-temperature synchrotron PXRD, and total scattering with pair distribution function (PDF) analysis, we reveal that smaller crystallite domains (\sim 200 nm) promote Bi segregation at grain boundaries, whereas larger domains ($>$ 500 nm) facilitate uniform Bi incorporation into the Cu lattice. PDF analysis suggests local Bi ordering that avoids nearest-neighbour positions. Thermal stability studies show Bi begins diffusing out of the Cu lattice between 100°C and 300°C, but a 1-2 at.% Bi remains stable after heating up to 1000 °C. These results underline the critical influence of synthesis conditions on microstructure and thermal stability, providing valuable guidelines for optimizing CuBi nanowires for next-generation spintronic applications.

References

- 1 Kunihashi, Y., Y. Shinohara, S. Hasegawa, et al., Applied Physics Letters. 122 (2023)
- 2 Fluegel, B., S. Francoeur, A. Mascarenhas, et al., Physical Review Letters. 97, 067205 (2006)
- 3 Gradhand, M., D.V. Fedorov, P. Zahn, et al., Physical Review B. 81, 067205 (2010)
- 4 Niimi, Y., Y. Kawanishi, D.H. Wei, et al., Physical Review Letters. 109, 156602 (2012)
- 5 Levy, P.M., H.X. Yang, M. Chshiev, et al., Physical Review B. 88, 214432 (2013)

PDF Investigations of novel ambient temperature reactive hydride composites for hydrogen storage

Author: Nicholas HALL¹

Co-authors: David Grant¹; Jamie RAMSHAW¹; Luke Woodliffe¹; Martin Dornheim¹; Stefano Checchia²

¹ University of Nottingham

² ESRF

Since the 1970s, considerable research efforts have focused on developing solid-state hydrogen storage materials as viable alternatives to compressed hydrogen gas (700 bar). Ideal materials must exhibit high volumetric and gravimetric hydrogen storage capacities, favourable thermodynamics, rapid kinetics at moderate or ambient temperatures, and good reversibility to enable scalable, practical hydrogen storage solutions. Such advancements would significantly contribute to the growth of the hydrogen economy and support the decarbonization of the energy and transport sectors.

Hydrides such as MgH_2 , $\text{Mg}(\text{BH}_4)_2$, LiBH_4 and LiAlH_4 have attracted attention due to their high hydrogen content (6–18 wt.% H_2). However, their practical application is limited by elevated desorption temperatures, sluggish kinetics or reversibility issues. One promising strategy to overcome these limitations is the development of tuneable Reactive Hydride Composites (RHCs), which combine multiple hydrides to enable synergistic improvements in both kinetics and thermodynamics via interphase reactions. Systems based on $\text{Mg}(\text{NH}_2)_2$ – LiH – LiBH_4 , in ratios such as 2:3:4 (6:9:12) 2 and 6:9:1 3, have demonstrated reversible hydrogen release of 2–3 wt.% at around 170 °C.

Through experimental studies conducted at ILL and ESRF, we have investigated the effect of varying LiBH_4 content (x) in the $6\text{Mg}(\text{NH}_2)_2$ – 9LiH – $x\text{LiBH}_4$ system to better understand the underlying reaction mechanisms. We present our latest results exploring compositions within this system that demonstrate enhanced reversibility, increased hydrogen capacity, faster kinetics, and hydrogen release temperatures as low as 70 °C without any ammonia release. Using temperature-ramped synchrotron PXRD and PDF measurements (ESRF), neutron diffraction experiments (ILL), TGA-DSC-MS, we reveal new insights into the reaction pathways, phase evolution, and overall behaviour of these RHCs - offering fresh perspectives for further optimization and application of these materials in hydrogen storage technologies.

References

- 1 E. Dematteis et al, Prog. Energy, 4.3 (2022), 032009
- 2 H. Wang et al, Adv.Energy.Mat, 7.13 (2017), 1602456.
- 3 G. Gizer, I. Puzkiel, H. Cao, C. Pistidda, T.T. Lee, M. Dornheim, and T. Klassen, Int. J. Hydrogen Energy, 44 (2019), 11920–11929.

73

2D-PDF data reduction: for fibre textured (thin film) samples

Author: Jiayu Liu¹

Co-authors: Ann-Christin Dippel²; Martin von Zimmerman¹

¹ DESY

² Deutsches Elektronen-Synchrotron DESY

Between 1D and 3D PDF analysis, there is an unexplored area called 2D PDF analysis, i.e. for samples that exhibit fiber-texture and their scattering signals are cylindrically symmetric in reciprocal space. To measure such kind of samples, the preferred method is to collect a series of diffractograms with densely spaced incidence/tilting angles, before reconstructing into 3D reciprocal space data. The measurement takes time in the same order of magnitude as what is needed for a 3D-PDF on a single crystal. In a typical in situ experiment, tilting the sample to large incidence angles is not even possible. On the other hand, taking one image at a fixed sample tilting angle leads to the so-called missing-wedge problem. Significant artifacts appear in real-space after Fourier transform of the scattering data with missing-wedge, making it impossible to recognize any useful feature for real-space analysis. No effective way has been reported to address such an issue. Here, we developed an algorithm to minimize the artifact at a cost of negligible loss of real-space resolution. This method makes it possible to extract reliable real-space information for fiber-textured sample with one-shot measurement. A thin film platinum sample is employed to validate the method.

111

Fast, interpretable (pre-)processing of large, mixed diffraction datasets with ad-hoc superpixels and randomized non-negative matrix factorization

Author: Andreas Werbrouck¹

Co-authors: Andrew C. Meng²; Matthias J. Young²; Nikhila C. Paranamana²; Xiaoqing He²

¹ Ghent University

² University of Missouri

The sheer volume of 2D diffraction data from in-situ synchrotron measurements and 4D-scanning transmission electron microscopy (4D-STEM) presents a significant data processing bottleneck. Typical workflows often employ data reduction steps like cropping, binning, or azimuthal integration, which can lead to information loss. Here, we present two strategies that can be combined or used separately to quickly (pre)process large amorphous, crystalline and mixed 2D diffraction datasets with minimal loss of information: automated, optimal superpixel construction and randomized non-negative matrix factorization (RNMF).

Custom superpixel construction: the diffraction space can be compressed by automatically dividing the detector into optimal superpixels of various size, informed by the specific dataset. High-information regions are sampled densely, while low-information areas are aggregated into larger superpixels. In the process, symmetries are captured and exploited to compress the data with a factor 4/8/16 without sacrificing resolution in reciprocal space.

Randomized non-negative matrix factorization: Non-negative matrix factorization (NMF) separates large datasets into non-negative components. In the case of 2D diffraction data, this results in a set of fingerprint 2D diffraction reference patterns (either crystalline or amorphous) and their corresponding spatial maps. The non-negativity constraint makes NMF significantly more interpretable than, for example, principal component analysis. However, this comes at a price: NMF is a non-convex optimization problem and reaching the required convergence can be computationally very expensive for large datasets. Here, we accelerate the process by projecting the entire dataset onto a much smaller subspace before performing NMF and projecting it back into the measurement space (RNMF).

We demonstrate and combine these methods on a diverse set of 4D-STEM datasets, spanning thin films, battery interfaces, and chiral ferroelectrics. We quantify the speedups and reconstruction errors associated with each strategy, showing that over 100-fold performance increases can be achieved with minimal impact on result quality. By combining these strategies, an interpretable analysis of a full 4D-STEM dataset (32x32 scan positions with a 256x256 pixel detector) can be performed in under a minute, compared to several hours using conventional methods. Adoption of these strategies will impact analysis of diffraction data in real, as well as in reciprocal space.

12

RMCPProfile: Local structure of crystalline to amorphous materials

Author: Matt Tucker¹

Co-authors: Helen PLAYFORD²; Wojciech Slawinski³

¹ ORNL

² ISIS Neutron and Muon Source

³ Univeristy of Warsaw, Faculty of Chemistry

Many of the useful materials that make modern life possible are crystalline. Quartz keeps our watches on time, perovskites are widely used in consumer electronics and solid oxide fuel cells may help to power the future.

The importance of local structure and disorder in crystalline materials is being recognised more and more as a key property of many functional materials. From negative thermal expansion to solid state amorphisation and the 'nanoscale' problem to improved fuel cell technology, a clear picture of

the local atomic structure is essential to understanding these phenomena and solving the associated problems.

Total scattering, an extension of the powder diffraction method, is increasingly being used to study crystalline materials. The unique combination of Bragg and diffuse scattering can be used to determine both the average structure and the short-range fluctuations from this average within a single experiment. To maximise the structural information from such data, three-dimensional atomic models consistent with all aspects of the data are required.

RMCPProfile 1 expands the reverse Monte Carlo (RMC) modelling technique 2 to take explicit account of the Bragg intensity profile from crystalline materials. Analysis of the RMCPProfile-generated atomic models gives more detailed information than is available directly from the data alone. We will give examples where RMCPProfile has been used to discover how different the local structure of the material can be in comparison to the limited information provided by its average picture.

¹ see www.rmcpfile.org; M G Tucker, D A Keen, M T Dove, A L Goodwin and Q Hui, *J. Phys. Condens. Matter* **19**, 335218 (2007).

² R L McGreevy and L Pusztai, *Mol. Simul.* **1**, 359 (1988).

113

Exploring magnetic correlation lengths in frustrated systems via single-crystal neutron diffraction

Author: Oleg Petrenko¹

¹ *University of Warwick*

Magnetic systems with frustrated interactions—where competing interactions cannot be simultaneously satisfied—often exhibit “fragile” ground states that are highly sensitive to even weak perturbations. In such systems, magnetic order is frequently incomplete and characterized by a limited correlation length, appearing in neutron diffraction experiments as diffuse scattering. In this presentation, I will discuss the properties of several families of rare-earth-based magnetically frustrated compounds in which we observed a pronounced diffuse scattering component during single-crystal neutron diffraction experiments using both polarized and unpolarized neutrons. Particular emphasis will be placed on the behaviour of these materials under applied magnetic fields, which in some cases induce long-range order, in others suppress it, and in certain instances even lead to the coexistence of both ordered and disordered states.

¹ D.D. Khalyavin et. al., PRB 109, L220411 (2024).

² M. Islam et. al., PRB 109, 094420 (2024).

³ N. Qureshi et. al., SciPost Phys. 11, 007 (2021).

⁴ D.D. Khalyavin et. al., PRB 103, 134434 (2021).

⁵ D. Lancon et. al., PRB 102, 060407(R) (2020).

[6] O. Young et. al., Crystals 9, 488 (2019).

[7] D. Brunt et. al., PRB 95, 024410 (2017).

[8] O.A. Petrenko, et. al., PRB 95, 104442 (2017).

[9] O. Young et. al., PRB 88, 024411 (2013).

[10] T.J. Hayes et. al., PRB 84, 174435 (2011).

Tutorial introductions / 6

Investigating short-range magnetic correlations in real space with magnetic pair distribution function analysis

Author: Benjamin FRANDSEN¹

¹ *Brigham Young University*

Short-range magnetic correlations play a key role in a wide variety of material systems, ranging from quantum materials, such as geometrically frustrated magnets, to technologically applied materials, such as magnetocalorics. Quantitatively characterizing these correlations is necessary to gain a complete understanding of these types of materials, but conventional techniques based on magnetic diffraction fail due to the short-range nature of the correlations of interest. Magnetic pair distribution function (mPDF) analysis is an effective method for studying short-range magnetic correlations by Fourier transforming the magnetic scattering into real space, similar to the more familiar atomic pair distribution function method. mPDF analysis has been applied successfully to numerous magnetic materials, including geometrically frustrated magnets, strongly correlated electrons systems, magnetic thermoelectrics, multiferroics, and more. In this talk, I will introduce the mPDF method, discuss its application to representative materials, and provide an overview of the software tools available for mPDF analysis.

Tutorial introductions / 8

Recent and future developments in PDF-land

Author: Simon Billinge¹

¹ *Columbia University + Brookhaven National Laboratory*

There are recently emerging powerful experimental developments related to atomic pair distribution function (PDF) method and total-scattering studies. At this workshop you will learn in detail about carrying out and applying PDF to your own scientific research, and there will be excellent tutorial talks on this. Therefore, in this talk I will focus on recent technological and methodological developments, and some that are in the pipeline, that are allowing ever richer science to be done. Examples include new spatial and time resolved capabilities and novel approaches to modeling. I will also talk about recent applications of PDF to scientific problems enabled by the new developments. I will also describe recent and upcoming developments in PDF analysis and modeling software that are under development in the group.